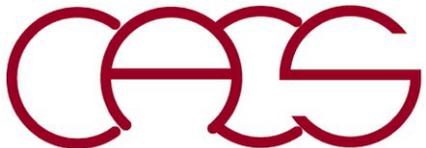# Nonadiabatic Quantum Molecular Dynamics

Aiichiro Nakano

Collaboratory for Advanced Computing & Simulations
Depts. of Computer Science, Physics & Astronomy, Chemical
Engineering & Materials Science, and Biological Sciences
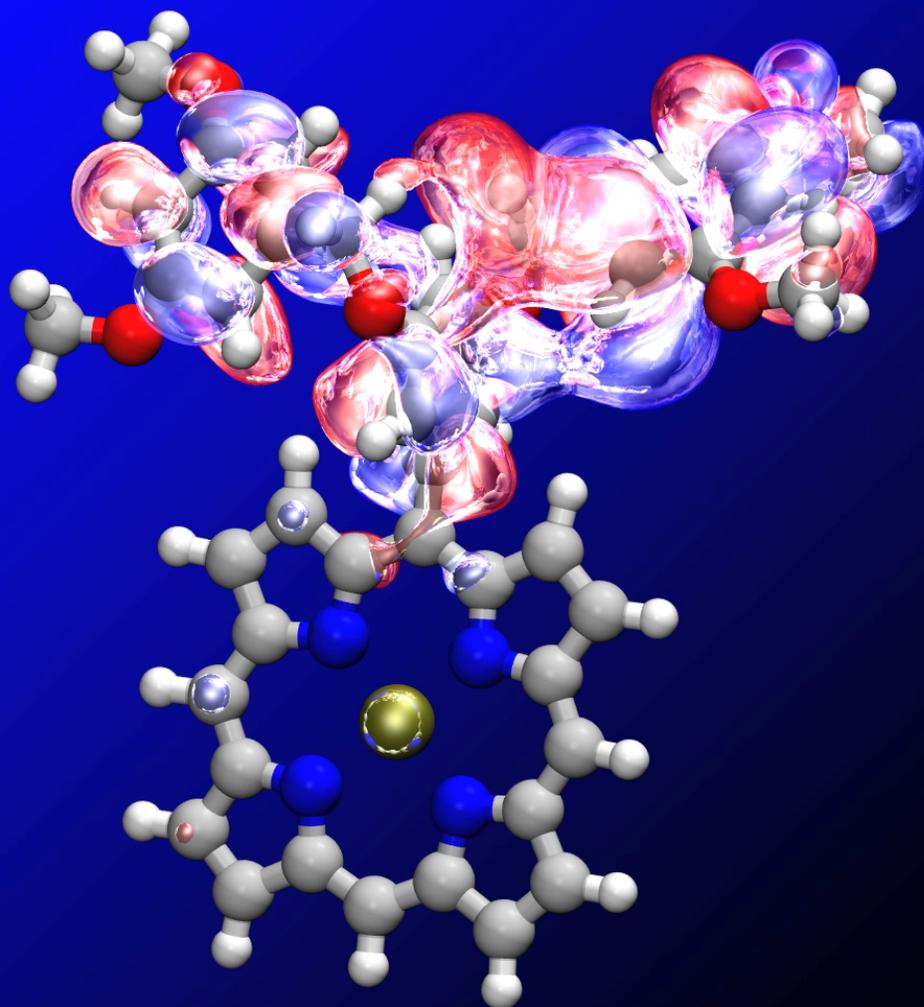*University of Southern California*
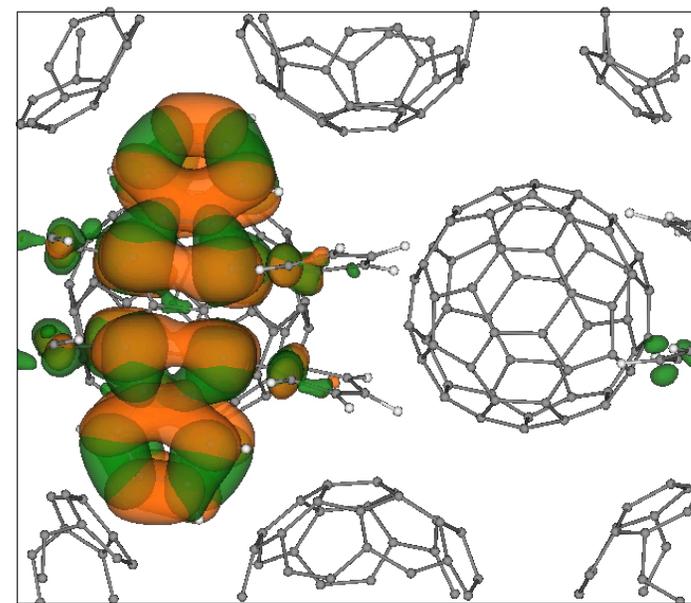
Email: anakano@usc.edu

Nonadiabatic Quantum Molecular Dynamics

W. Mou *et al.*, *Appl. Phys. Lett.* **98**, 113301 ('11); *ibid.* **100**, 203306 ('12); *J. Chem. Phys.* **136**, 184705 ('12); *Comput. Phys. Commun.* **184**, 1 ('13); *Appl. Phys. Lett.* **102**, 093302 ('13); *ibid.* **102**, 173301 ('13); *J. Chem. Phys.* **140**, 18A529 ('14); *IEEE Computer* **48(11)**, 33 ('15); *Sci. Rep.* **5**, 19599 ('16); *Nature Commun.* **8**, 1745 ('17)

Zn porphyrin

Rubrene/C$_{60}$

quasi-electron; **quasi-hole**

- **Excited states: Linear-response time-dependent density functional theory** [Casida, '95]
- **Interstate transitions: Surface hopping** [Tully, '90; Jaeger, Fisher & Prezhdo, '12]

Time-Dependent Density Functional Theory

- **Invertibility theorem**

  The mapping $G: \{v(\mathbf{r}, t) + c(t)\} \mapsto n(\mathbf{r}, t)$ is one-to-one & therefore is invertible

  external potential   time-dependent constant   electron density

- **Time-dependent density-functional theory (TDDFT) theorem:**

  Every physical quantity is a functional of $n(\mathbf{r}, t)$

- **Action principle:**

  Action integral is stationary at the exact density:

  $\delta A_v / \delta n(\mathbf{r}, t) = 0$ at $n(\mathbf{r}, t) = G[v(\mathbf{r}, t)]$, where

  $A_v[n(\mathbf{r}, t)] = \int dt \langle \psi(t) | i\hbar\, \partial/\partial t - T - U | \psi(t) \rangle - \int dt \int d\mathbf{r}\, n(\mathbf{r}, t) v(\mathbf{r}, t)$

  kinetic energy operator   electron-electron interaction

Runge & Gross, *Phys. Rev. Lett.* **52**, 997 ('84); Ng. & Singwi, *ibid*. **59**, 2627 ('87)

Time-Dependent Kohn-Sham Scheme

- **Time-dependent many-body problem is equivalent to solving time-dependent Kohn-Sham (TDKS) equations**

Hartree (mean-field) potential

$$\begin{cases} \left[i\hbar \, \partial/\partial t + \hbar^2 \nabla^2/2m - v(\mathbf{r}, t) - \int d\mathbf{r}' \, \frac{e^2 n(\mathbf{r}', t)}{|\mathbf{r} - \mathbf{r}'|} - v_{\mathrm{xc}}(\mathbf{r}, t) \right] \psi_i(\mathbf{r}, t) = 0 \\ n(\mathbf{r}, t) = \sum_{i=1}^{N} |\psi_i(\mathbf{r}, t)|^2 \end{cases}$$

where the exchange-correlation (xc) potential is given by

$$v_{\mathrm{xc}}(\mathbf{r}, t) = \delta A_{\mathrm{xc}}/\delta n(\mathbf{r}, t)$$

$$A_{\mathrm{xc}}[n(\mathbf{r}, t)] = - \int dt \langle \psi(t) | i\hbar \, \partial/\partial t - T - U | \psi(t) \rangle$$

non-interacting electrons action

$$+ \int dt \langle \psi(t) | i\hbar \, \partial/\partial t - T | \psi(t) \rangle_{e=0}$$

Hartree (mean-field) action

$$- \frac{1}{2} \int dt \int d\mathbf{r} \int d\mathbf{r}' \, \frac{e^2}{|\boldsymbol{r} - \mathbf{r}'|} n(\mathbf{r}, t) n(\mathbf{r}', t)$$

Runge & Gross, *Phys. Rev. Lett.* **52**, 997 ('84)

See notes on (1) TDDFT summary, (2) TDDFT fundamentals

TDDFT & Many-Body Theory

- **TDKS orbitals are used as a basis set to calculate physical properties with the help of many-body theory,** *e.g.,* **GW approximation for one-body** [Hybertsen & Louie, *Phys. Rev. Lett.* **55**, 1418 ('85)] **& Bethe-Salpeter equation (BSE)** [Rohlfing & Louie, *Phys. Rev. Lett.* **81**, 2312 ('98)] **for two-body properties**

- **Many-body theory provides a systematic way to approximate TDKS exchange-correlation (xc) potential** $(1 = (\mathbf{r}_1, t_1),$ *etc.*):

$$v_{\text{xc}}(1) = -2i \int d2 \int d3 \int d4 \, \pi^{-1}(1,2) G_0(2,3) \Sigma_{\text{xc}}(3,4) G(4,2)$$

where (p denotes a closed-time path & $\bar{1}$ denotes integration over 1)

$$G(1,1') = -(i/2) \sum_\sigma \langle T_{\text{p}}[\psi_\sigma(1)\psi_\sigma^\dagger(1')]\rangle$$

$$\Sigma_{\text{xc}}(1,1') = -2^{-1} U(1,\bar{2}) \chi^{(2)}(\bar{3},1';\bar{2}^+,\bar{2}) G^{-1}(\bar{3},1')$$

$$U(1,2) = \frac{e^2}{|\mathbf{r}_1 - \mathbf{r}_2|} \delta_{\text{p}}(t_1 - t_2)$$

$$\chi^{(\nu)}(1,1';\dots;\nu,\nu') = \frac{\delta^{\nu-1}}{\delta\phi(1,1')\cdots\delta\phi(\nu,\nu')} \sum_\sigma \langle T_{\text{p}}[\psi_\sigma(1)\psi_\sigma^\dagger(1')]\rangle$$
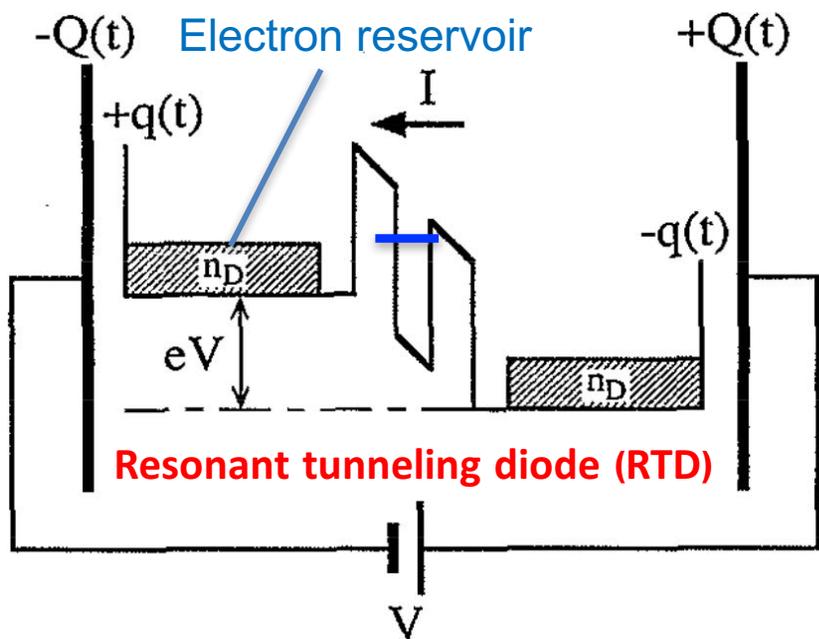
$$G_0^{\text{r}|\text{a}}(1,1') = \mp i[\theta(t_1 - t_1')|\theta(t_1' - t_1)] \sum_i \psi_i(1)\psi_i^*(1') \,;\, G_0^{\text{c}}(1,1') = -i\sum_i \psi_i(1)\psi_i^*(1')$$

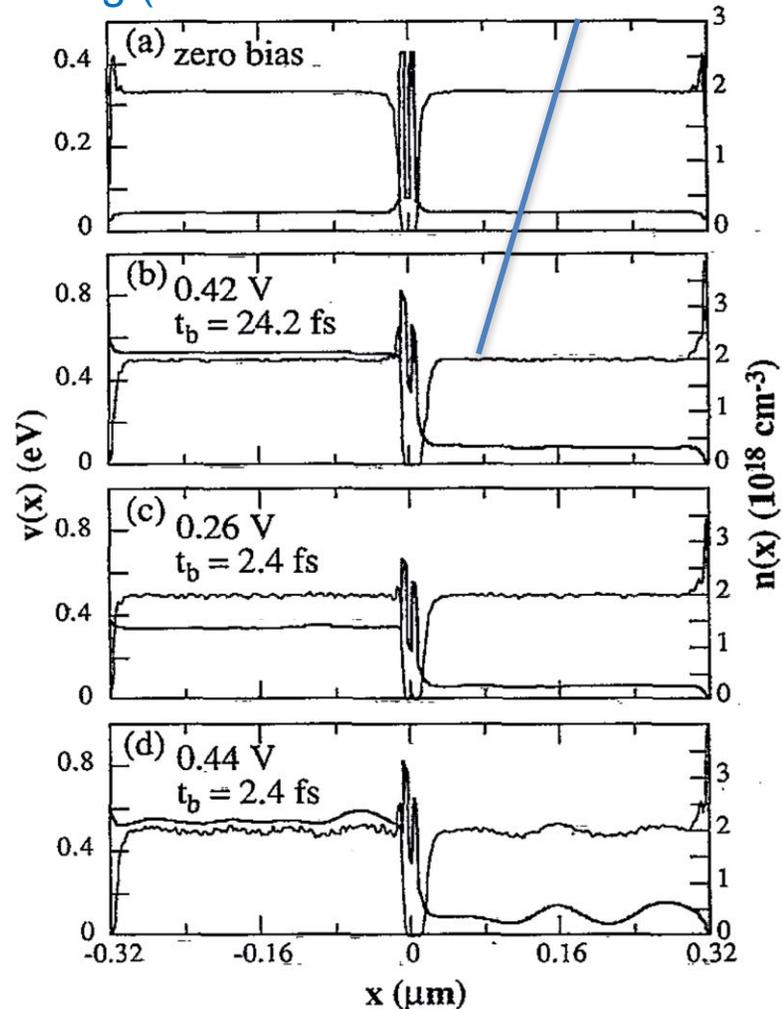$$\pi_{\text{r}}(1,2) = -2i\hbar^{-1}[G_0^{\text{r}}(1,2)G^{\text{c}}(2,1) + G_0^{\text{c}}(1,2)G^{\text{a}}(2,1)]$$

See note on field-theory of xc potential

TDDFT & Physics

- **TDKS equations, even within the random phase approximation (RPA, $v_{xc} = 0$) or static v_{xc}, describe collective effects like screening & plasma oscillation**

Nakano *et al.*, *Phys. Rev. B* **43**, 9066 ('91); *Appl. Phys. Lett.* **64**, 2569 ('94)
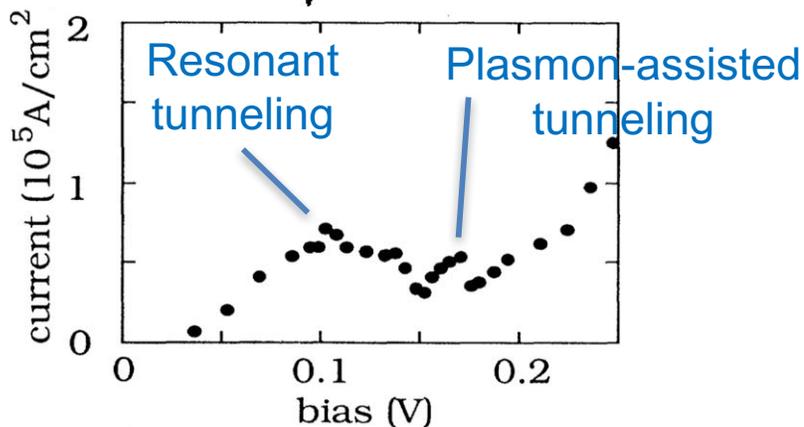
Collective Effects

- **Screening: In electrons with average number density n, along with uniform positive charge that neutralizes the total electronic charge, the electrostatic potential $\phi(\mathbf{r})$ due to an external point charge Q is obtained (within large n & linearized approximations) as**

$$\phi(\mathbf{r}) = \frac{Q}{r}\exp(-k_{\text{TF}}r)\,;\ k_{\text{TF}} = \left(\frac{6\pi n e^2}{E_{\text{F}}}\right)^{1/2};\ E_{\text{F}} = \frac{\hbar^2}{2m}(3\pi^2 n)^{2/3}$$

Fermi energy

Thomas-Fermi wave number

- **Plasma oscillation: A slab of uniform electron/positive-background can sustain an oscillation with plasma frequency**

$$\omega_{\text{p}} = \left(\frac{4\pi n e^2}{m}\right)^{1/2}$$
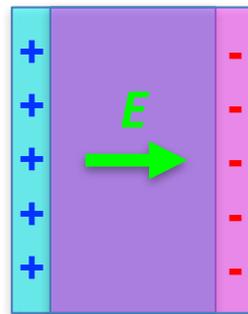
Surface-Hopping NAQMD

- **Incorporate electron transitions with the time-dependent density-functional theory (TDDFT) & surface-hopping method**

Tully, *J. Chem. Phys.* **93**, 1061 ('90), *ibid.* **129**, 044104 ('08) ; Duncan *et al.*, *J. Am. Chem. Soc.* **129**, 8528 ('07)
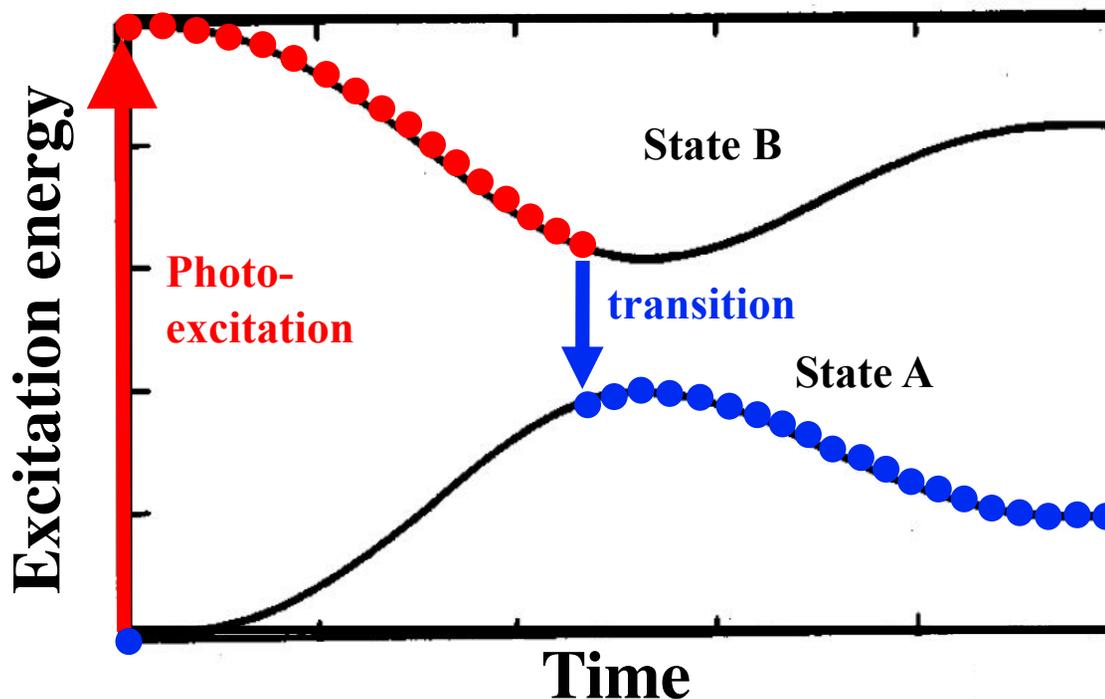
- **Electronic transitions from the current state to another occur stochastically based on the switching probability obtained by solving TDDFT equations**

K-th excitation frequency

J-th adiabatic excited state

Electronic transition assisted by nuclei motion

$$\Psi(\mathbf{r},t) = \sum_J C_J^{(I)}(t)\Phi_J(\mathbf{r};\mathbf{R}(t)) \quad C_I^{(I)}(0) = \delta_{I,J}$$

$$\frac{d}{dt}C_J^{(I)}(t) = -\sum_k C_k^{(I)}(t)\left(i\omega_K\delta_{JK} + \left\langle\Phi_J\left|\frac{\partial}{\partial t}\right|\Phi_K\right\rangle\right)$$

Surface-Hopping Procedure

- **Density matrix $a_{kl}(t)$ & state probability $p_k(t)$**

$$a_{kl}(t) \equiv c_k(t)c_l^*(t); \; p_k(t) \equiv a_{kk}(t) = |c_k(t)|^2$$

- **Probability dynamics**

$$\frac{d}{dt} p_k(t) = \sum_{k'(\neq k)} b_{kk'}$$

Nonadiabatic coupling

$$b_{kk'} = 2\frac{d\mathbf{R}}{dt} \bullet \mathrm{Re}(\mathbf{d}_{kk'} \bullet a_{k'k}); \; \mathbf{d}_{kk'} = \left\langle \psi_k \left| \frac{\partial}{\partial \mathbf{R}} \right| \psi_l \right\rangle$$

- **Fewest-switches surface hopping (FSSH) algorithm**
  During one NAQMD step (Δt), stochastically choose a state transition according to the transition probability matrix

$$\pi_{k' \leftarrow k} = \frac{\Delta t b_{k'k}}{p_k} = 2\Delta t \frac{d\mathbf{R}}{dt} \bullet \frac{\mathrm{Re}(\mathbf{d}_{kk'} \bullet a_{k'k})}{a_{kk}}$$

- **From a swarm of independent classical trajectories toward a quantum-mechanical description of nuclei motion**

  DISH: Jaeger *et al.*, *J. Chem. Phys.* **137**, 22A545 ('12) — implemented in QXMD; SQUASH: Akimov & Prezhdo, *Phys. Rev. Lett.* **113**, 153003 ('14): Liouville space hopping: Wang et al., *J. Phys. Chem. Lett.* **6**, 3827 ('15)

See note on fewest-switch surface hopping

Example: Light Harvesting Dendrimers

Electron-hole pairs photoexcited at peripheral antennas travel to the core
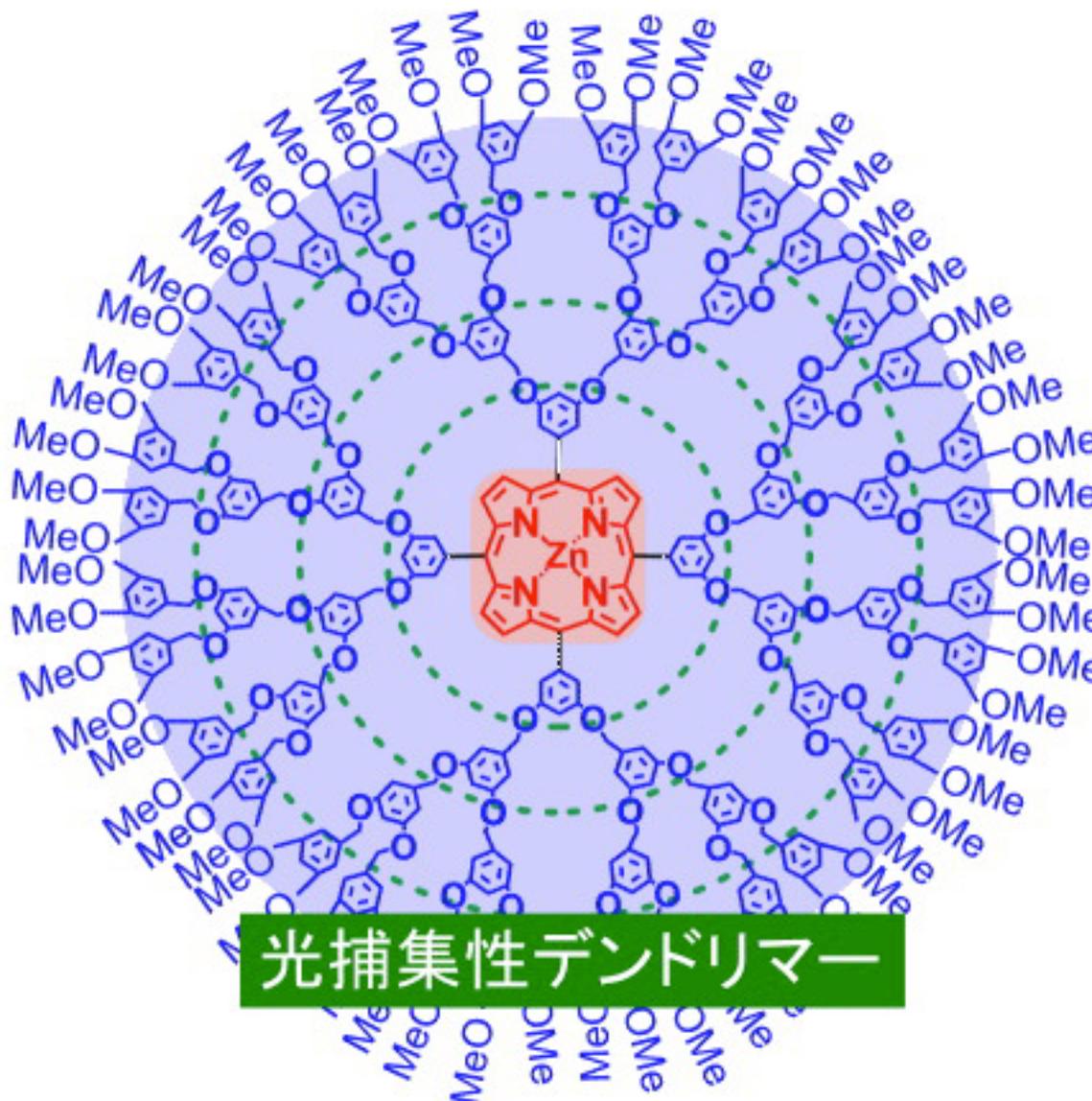
Prof. I. Akai
Kumamoto Univ.

光捕集性デンドリマー

Key: Rapid electron transfer for solar-energy applications

Electron Transfer in a Dendrimer

Nonadiabatic quantum molecular dynamics simulation with fewest-switches surface hopping [Tully, '90] **& time-dependent density functional theory**

peri

O

inter

H

C

N

Zn

core
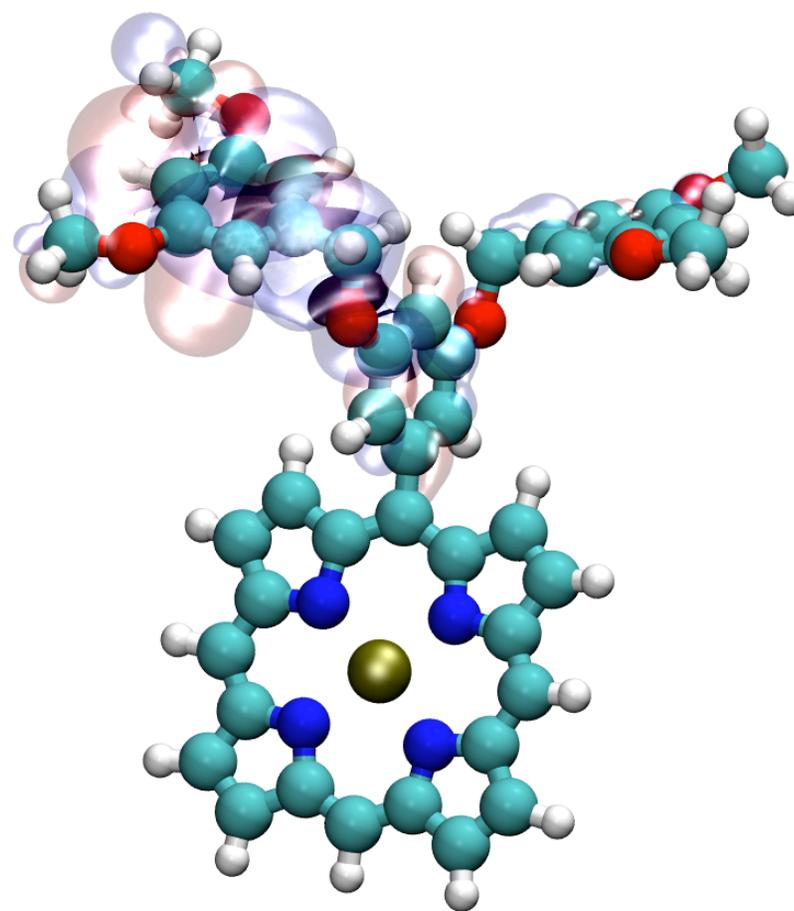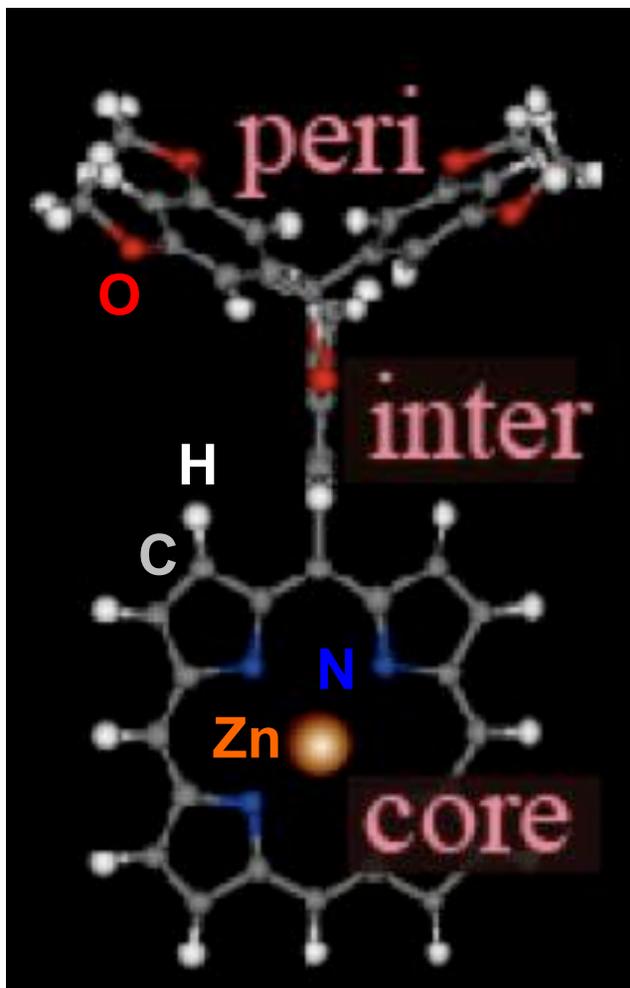
Ohmura *et al.*, *Appl. Phys. Lett*. **98**, 113302 ('11)

Photoexcitation Simulation
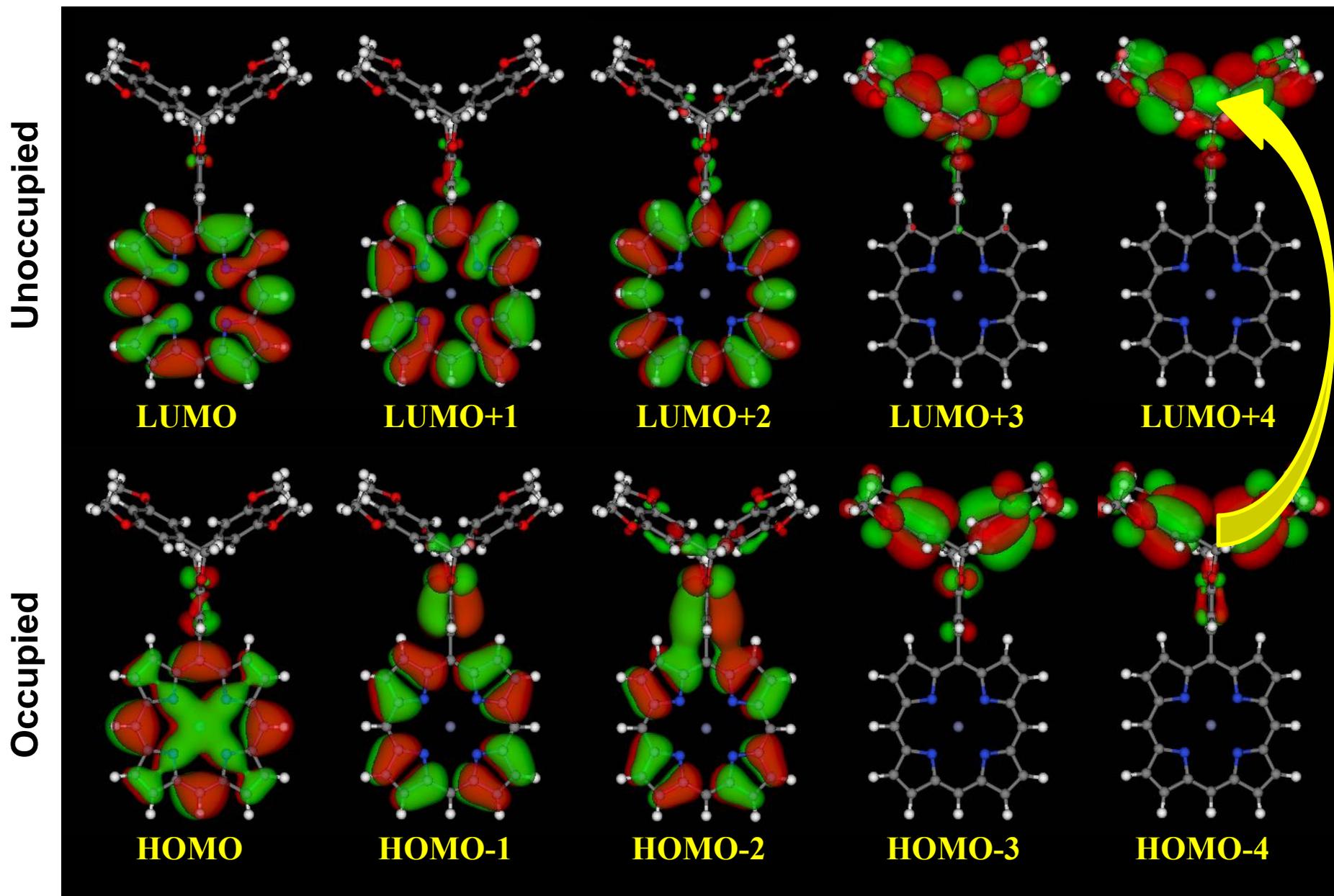
An electron in HOMO-4 is excited to LUMO+4

Optical Absorption Spectrum

- **Oscillator strength calculated by the linear-response TDDFT**
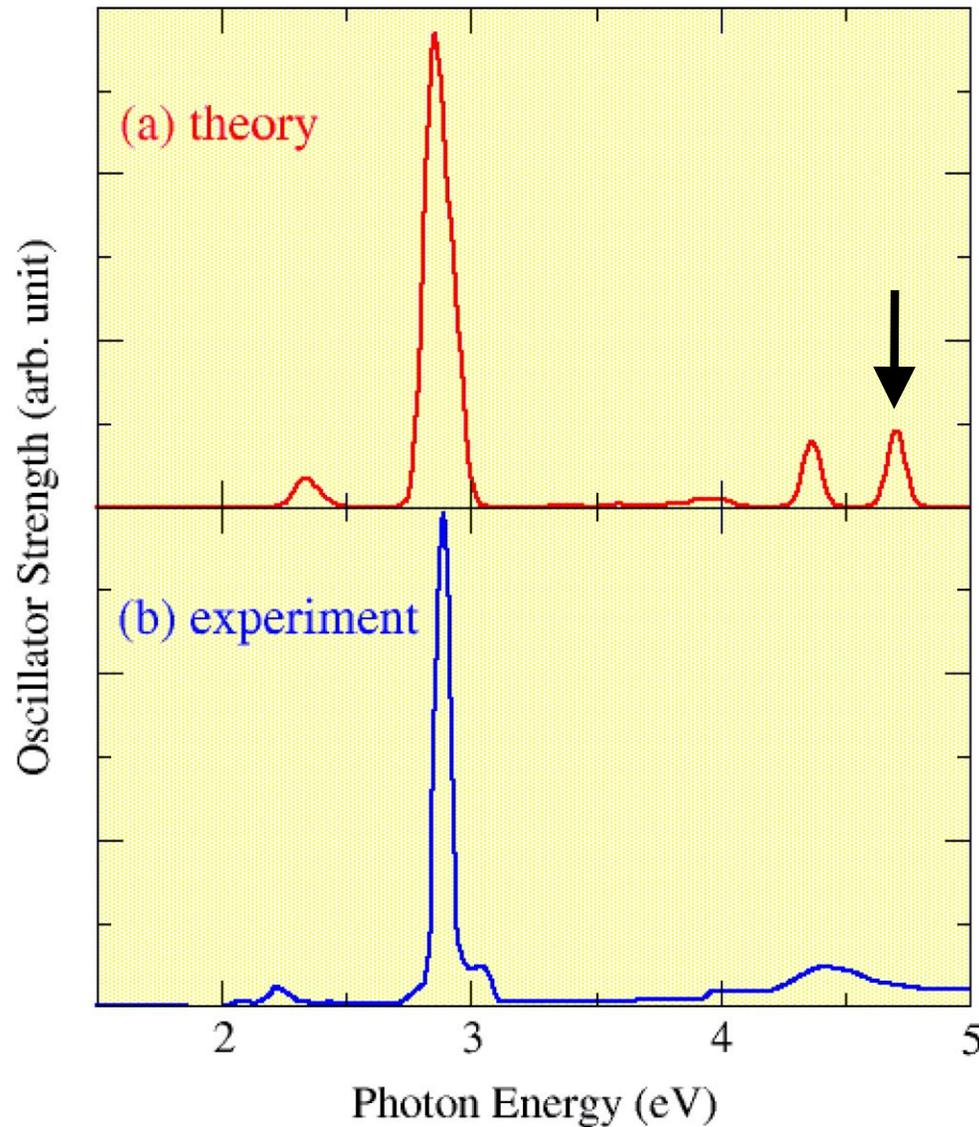
- **Excellent agreement with experimental data** [Akai *et al.*, '06]

Effect of Exchange-Correlation Functional

- **Oscillator strength calculated by the linear-response TDDFT**

$$K_{ia\sigma,jb\tau} = \left[\psi_{i\sigma}\psi_{a\sigma}^* \middle| \psi_{j\tau}\psi_{b\tau}^*\right] - C_{\mathrm{HF}}\delta_{\sigma\tau}\left[\psi_{i\sigma}\psi_{j\sigma}^* \middle| \psi_{a\tau}\psi_{b\tau}^*\right] + (1-C_{\mathrm{HF}})f_{ia\sigma,jb\tau}^{\mathrm{x}} + f_{ia\sigma,jb\tau}^{\mathrm{c}}$$

$$\left[g\middle|h\right] = \int d\mathbf{r}\int d\mathbf{r}' \frac{g(\mathbf{r})h(\mathbf{r}')}{|\mathbf{r}-\mathbf{r}'|}$$

$C_{\mathrm{HF}} = 0.0$
$C_{\mathrm{HF}} = 0.1$
$C_{\mathrm{HF}} = 0.2$
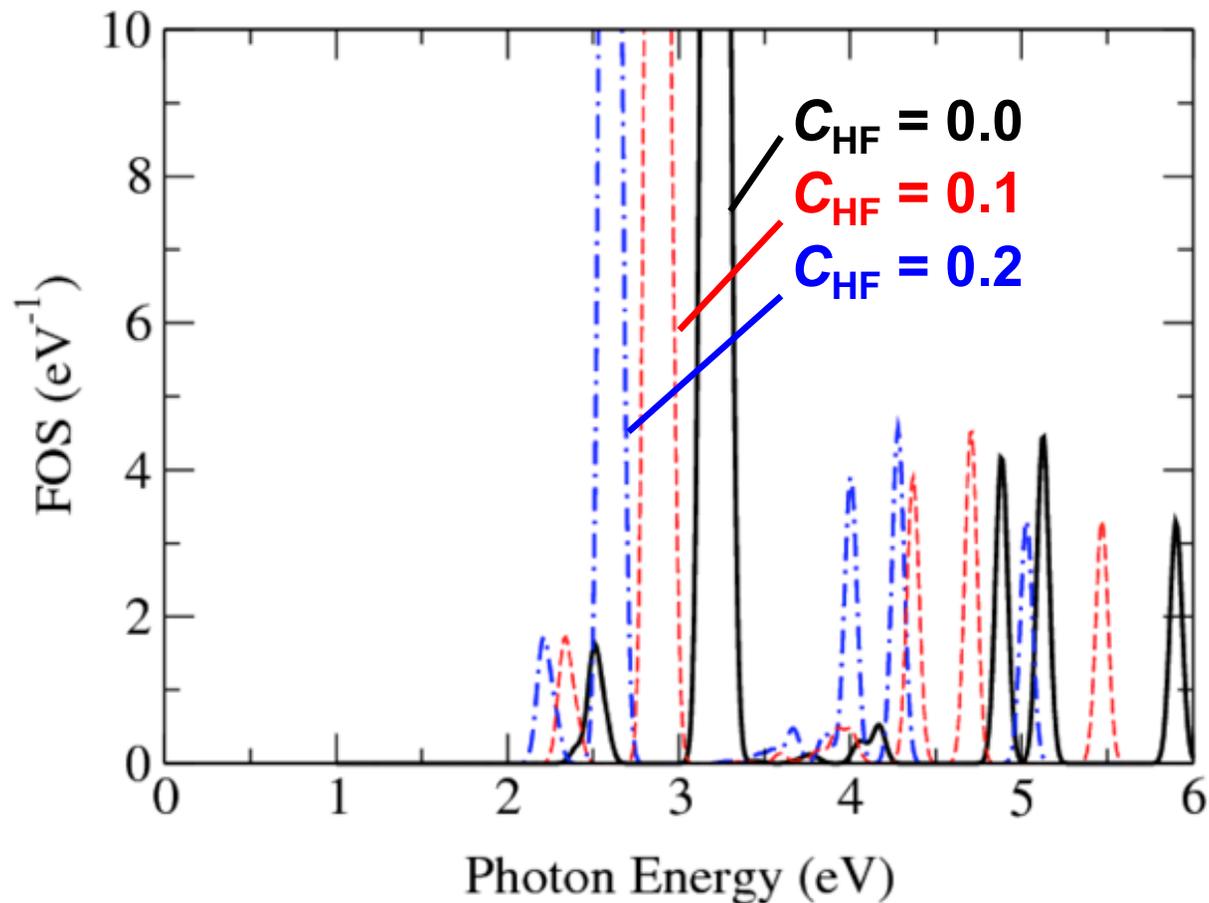
- **At most 20% difference in excitation energies by different approximations**

Electron Transfer in a Dendrimer
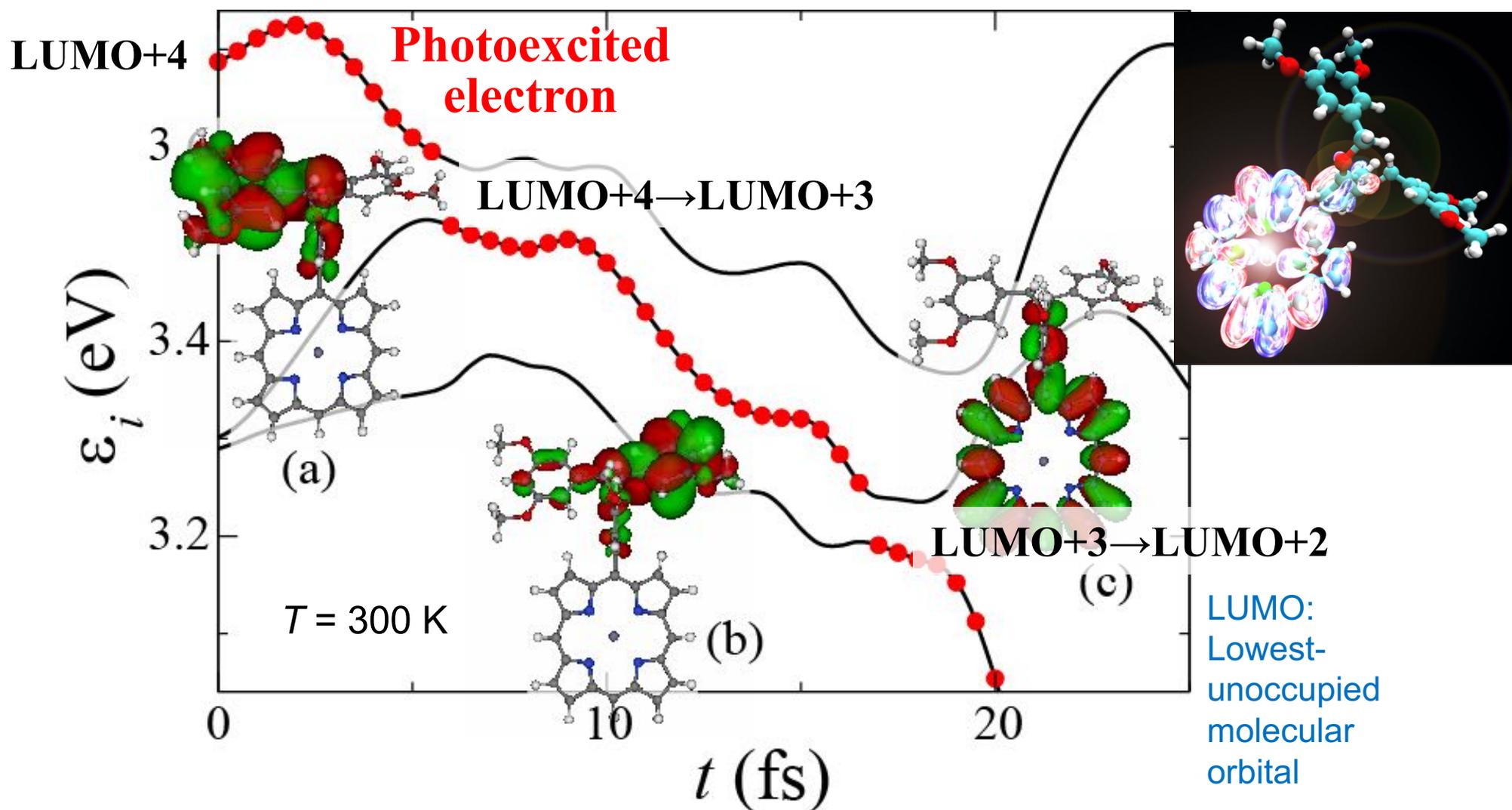
LUMO+4

Photoexcited electron

LUMO+4→LUMO+3

LUMO+3→LUMO+2

T = 300 K

ε_i (eV)

t (fs)

(a)

(b)

(c)

LUMO: Lowest-unoccupied molecular orbital

- **The photoexcited electron at the peripheral antenna is transferred to the core due to the energy-crossing & overlapping of orbitals assisted by thermal molecular motions**

Electron Transfer in a Light-Harvesting Dendrimer
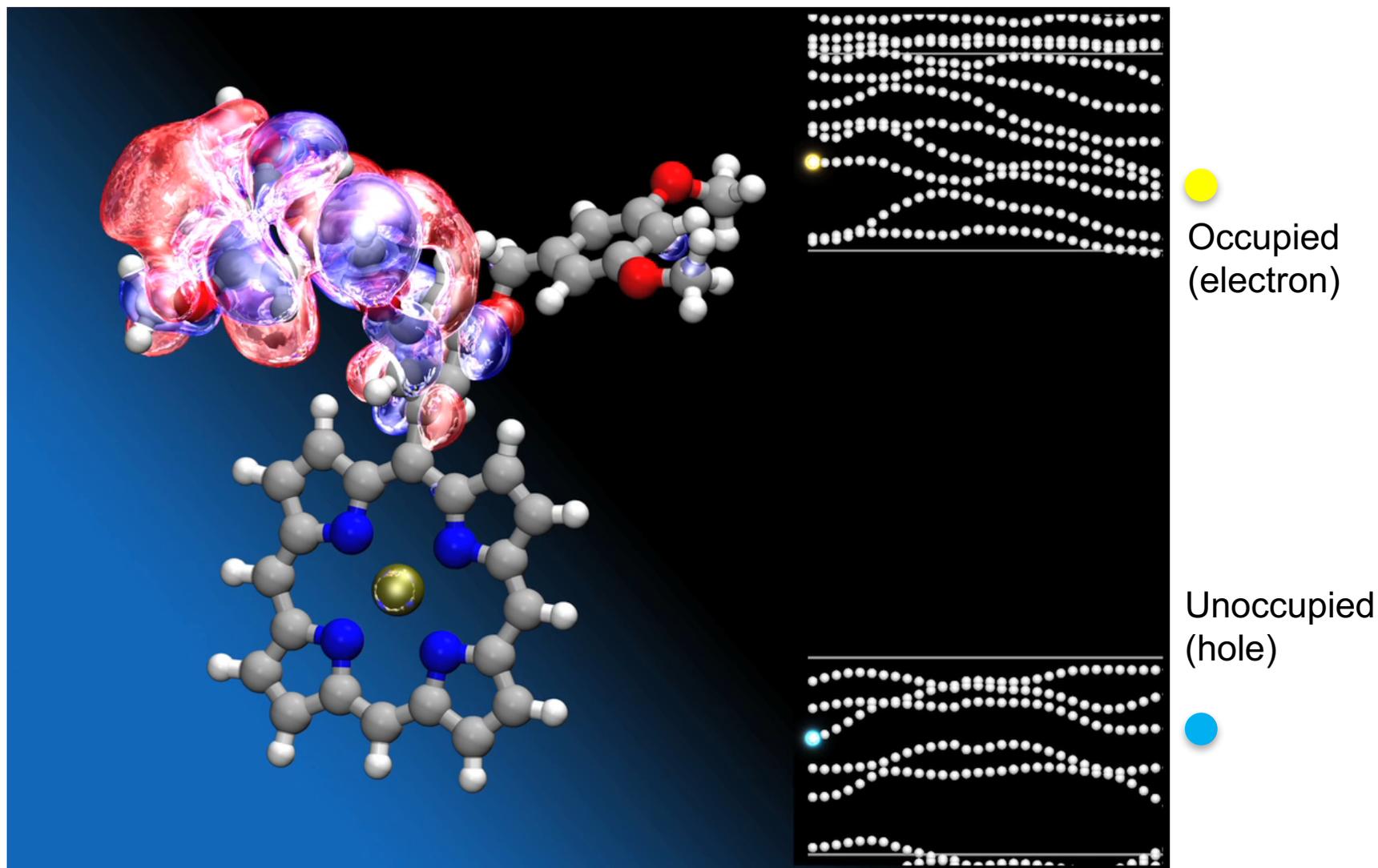
Occupied (electron)

Unoccupied (hole)

- **The photoexcited electron at the peripheral antenna is transferred to the core due to the energy-crossing & overlapping of orbitals assisted by thermal molecular motions**

Electron Transfer Mechanism

- **Probability in the antenna & core regions (averaged over 15 trajectories)**
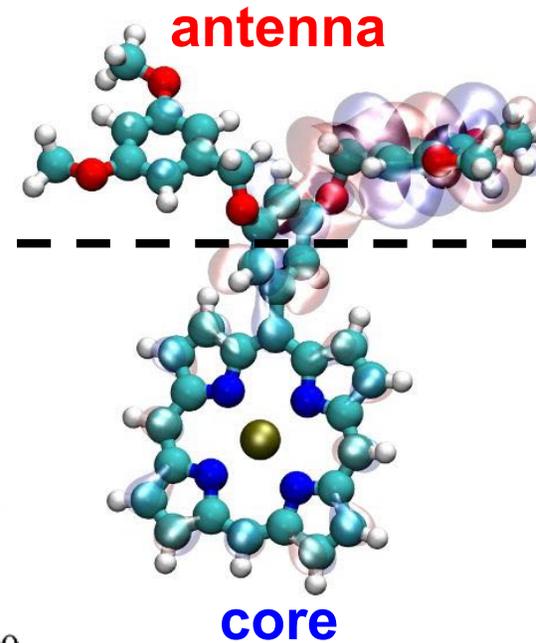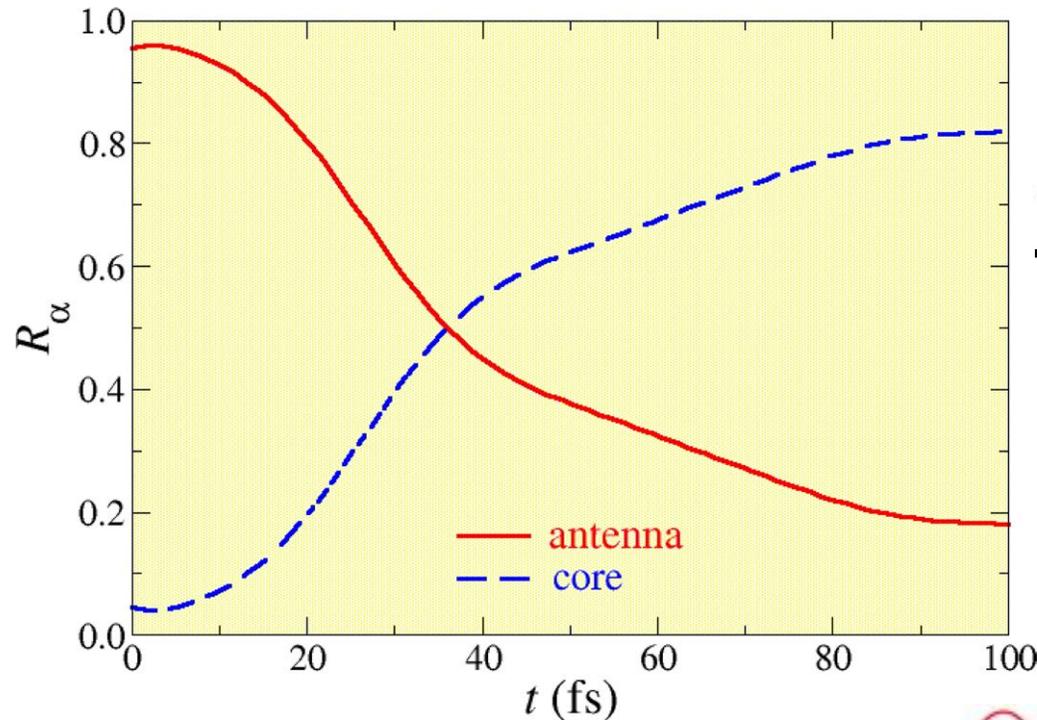
- **The resulting electron transfer rate due to the *Dexter* mechanism is much larger than that due to the *Förster* mechanism**
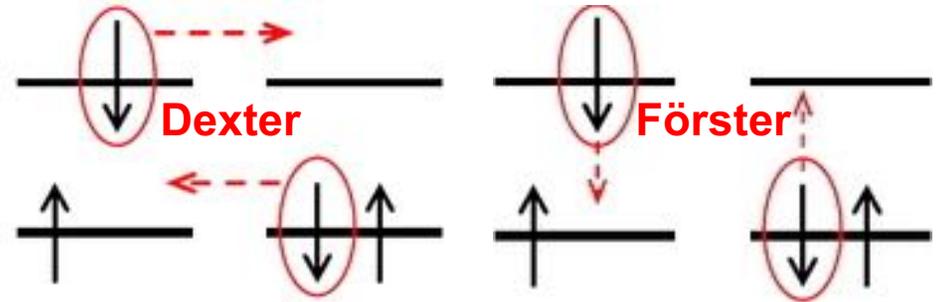
$$k_{\text{Dexter}}^{-1} = \boxed{40\text{fs}}$$

$$<< k_{\text{Forster}}^{-1} = \left[\frac{2\pi}{\hbar} \sum_{b \notin \{occ\}; j \in \{occ\}} \left| K_{ia\sigma, jb\sigma} \right|^2 \times \frac{1}{\sqrt{2\pi}\alpha} \exp\left(-\frac{(\omega_{ia\sigma} - \omega_{jb\sigma})^2}{2\alpha^2} \right) \right]^{-1} = \boxed{1\text{ps}}$$

Effect of Temperature

Adiabatic MD simulation of a dendrimer at temperature 300 & 100 K

300 K

100 K
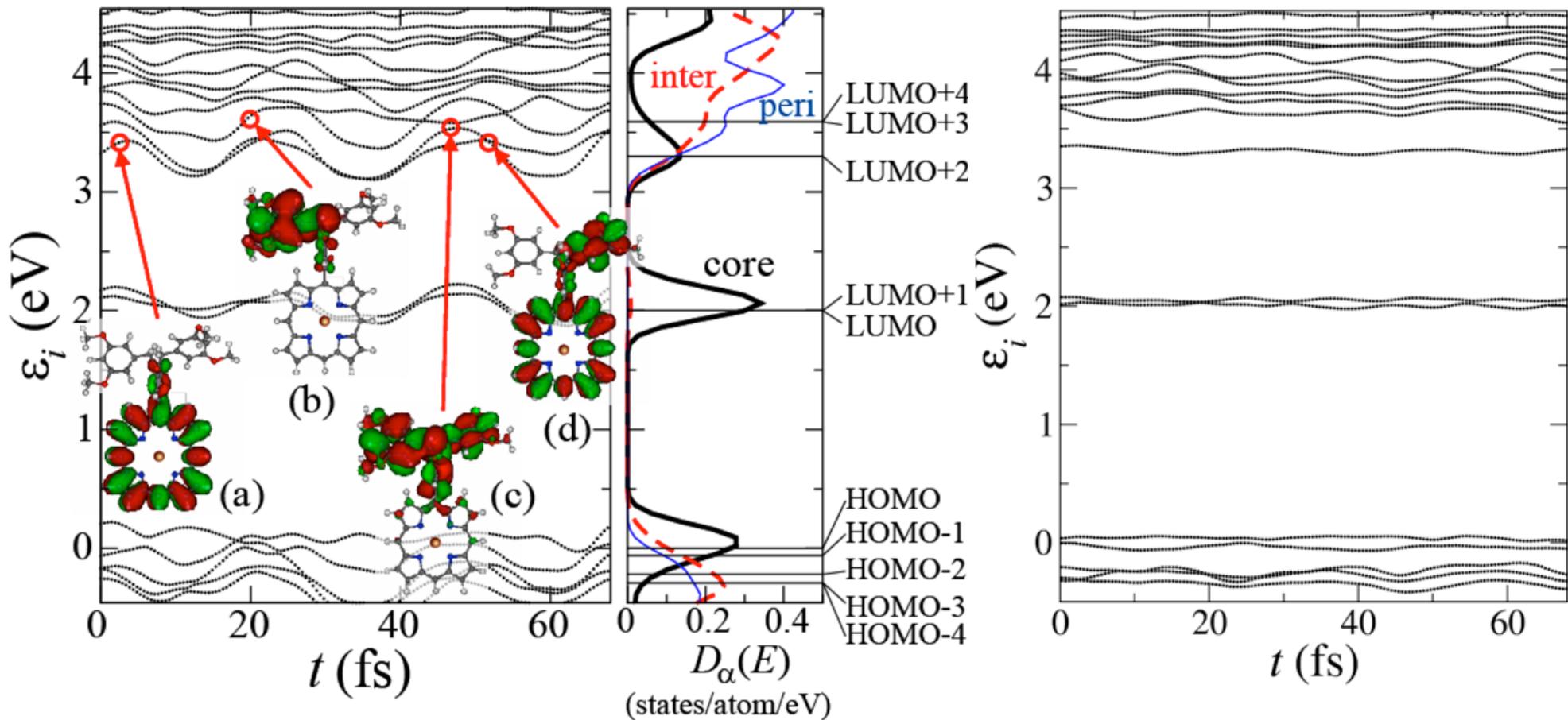
Electron transfer is suppressed at low temperatures

Effect of Solvent

Adiabatic QMD simulation of a dendrimer in solvent, tetrahydrofuran (THF), $(CH_2)_4O$, at temperature 300 K used in experiments [Akai *et al.*, '06, '08]
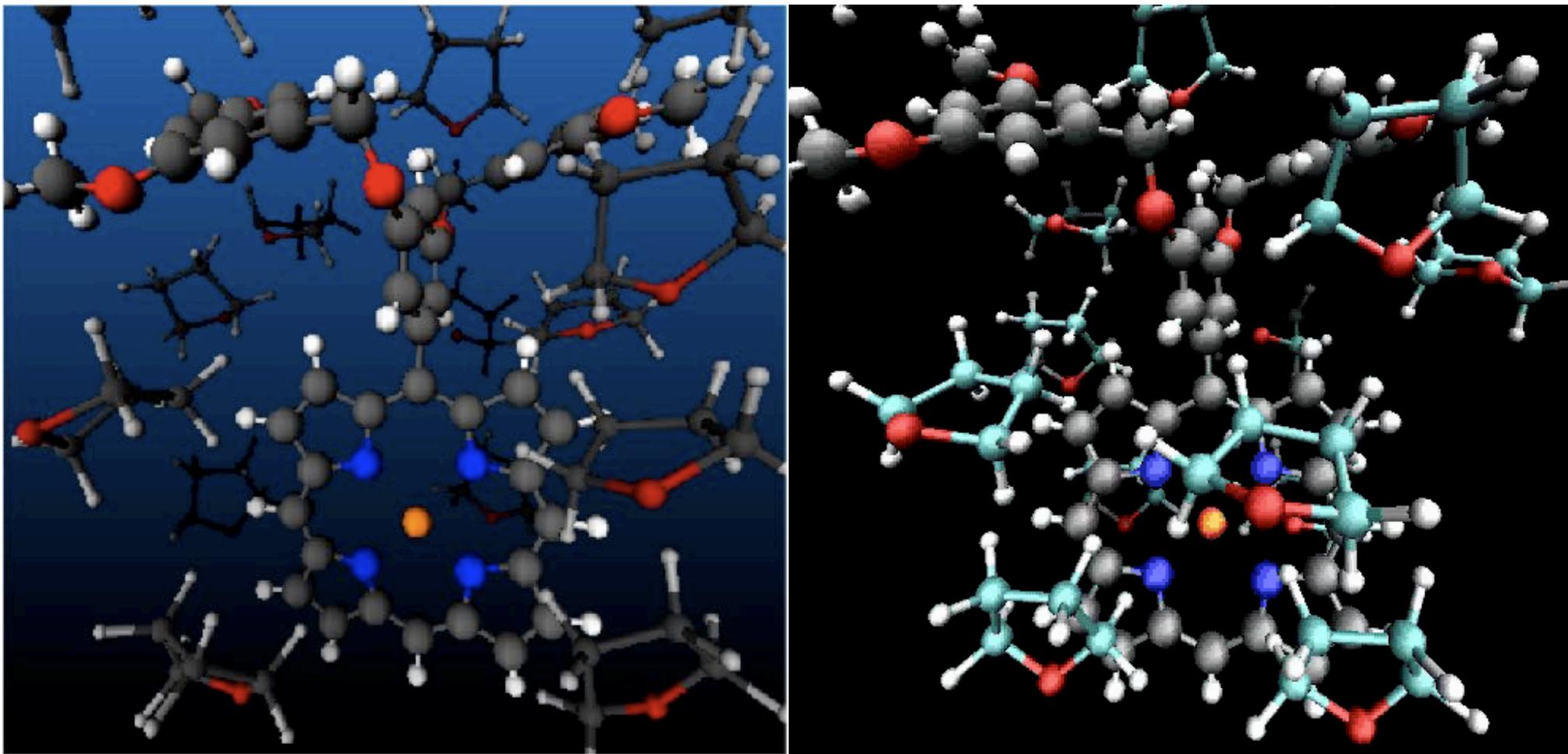
Solvent suppresses orbital energy-crossing & consequently electron transfer

Key Molecular Mechanism

Without solvent
With solvent
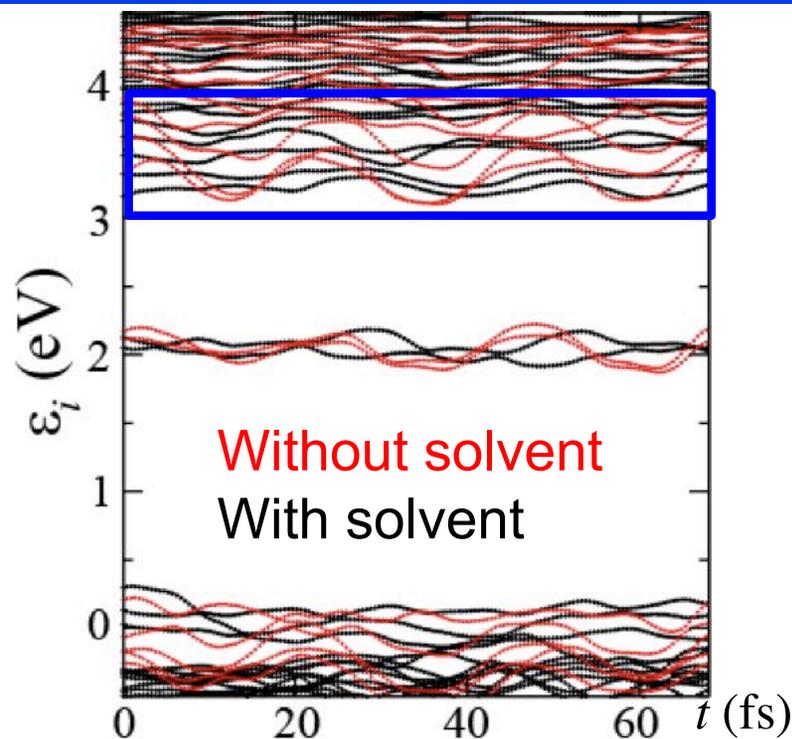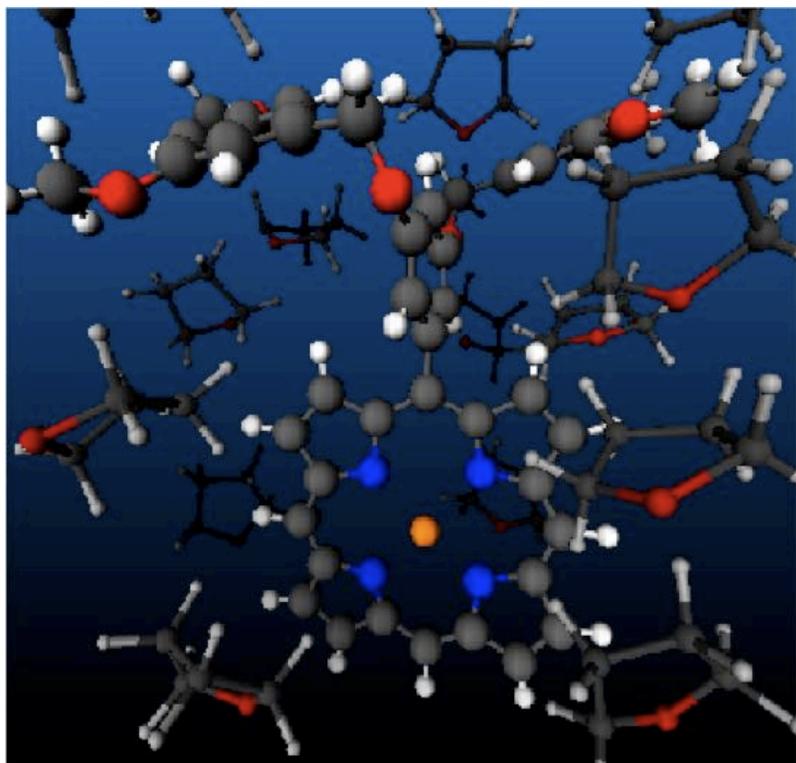
- **Solvent (tetrahydrofuran) suppresses orbital energy-crossing & electron transfer**

$$\sigma = \langle \varepsilon_i^2 \rangle - \langle \varepsilon_i \rangle^2 = 0.13\text{eV (vacuum)} \rightarrow 0.04\text{eV (THF)}$$

- **Aromatic ring motion in the periphery is the key mechanism for rapid electron transfer**

Velocity autocorrelation
in the aromatic rings in the periphery

Without solvent
With solvent
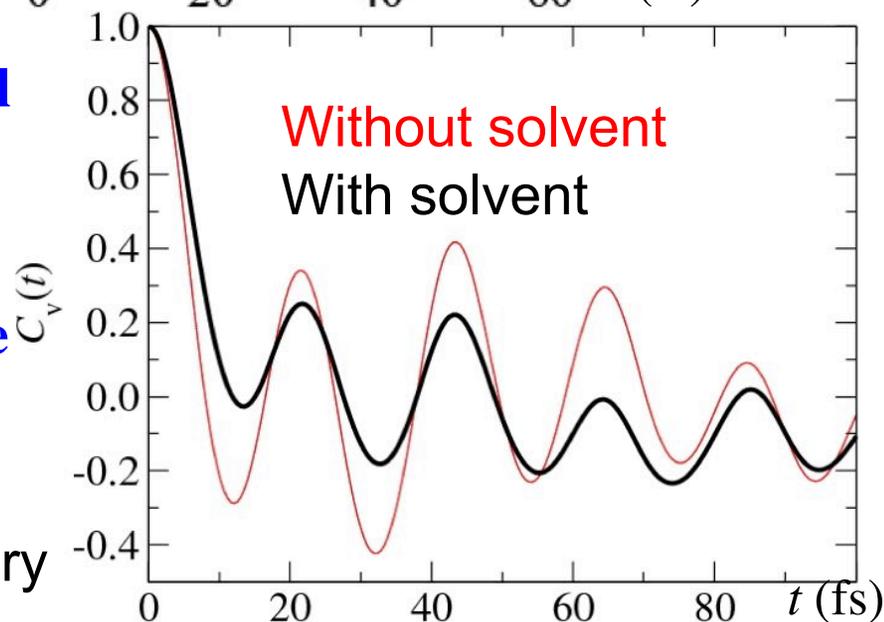
Organic Photovoltaics (OPV)

- **Exciton dynamics**

1. exciton generation

2. exciton diffusion

3. charge transfer k_{CT}

4. charge recombination k_{CR}

e^- h^+ hv D^* D^*

Acceptor Cathode Anode Donor
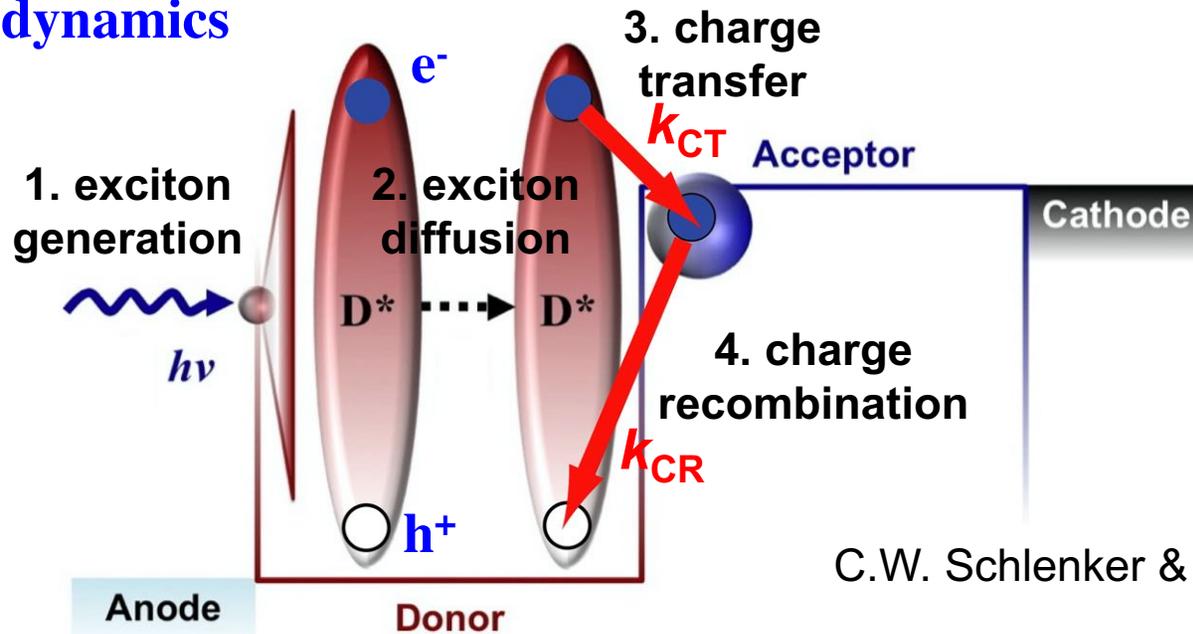
C.W. Schlenker & M. E. Thompson ('11)

- **Open-circuit voltage is sensitive to the interfacial structure**

Tetracene
Rubrene

0.55 V
0.92 V

Top Side

Tetracene

Rubrene

Donor

Acceptor
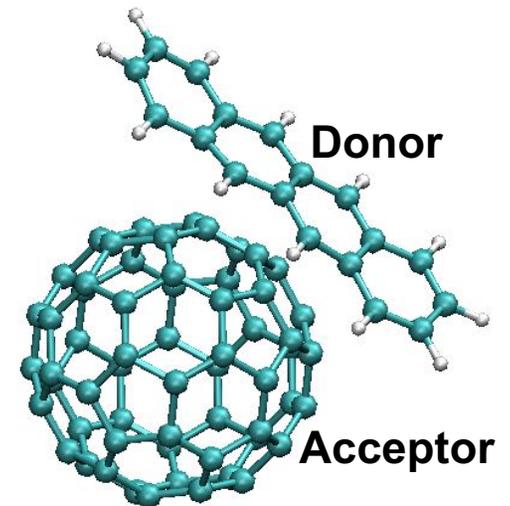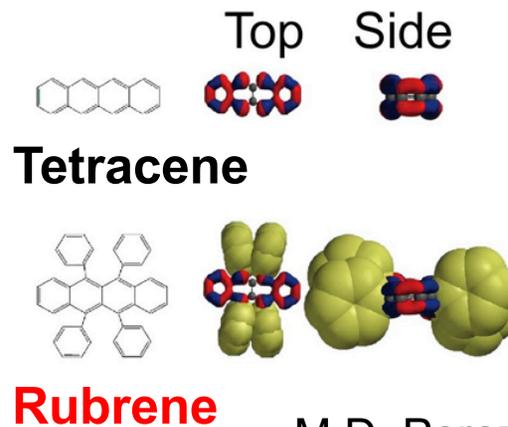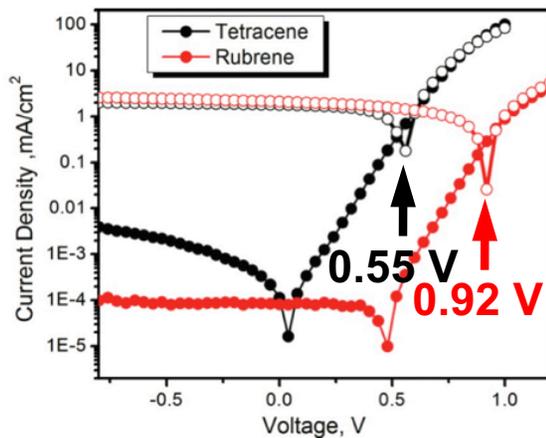
M.D. Perez *et al.*, *JACS* **131**, 9281 ('09)

Tetracene or Rubrene/Fullerene

LUMO: Tetracene/C_{60}
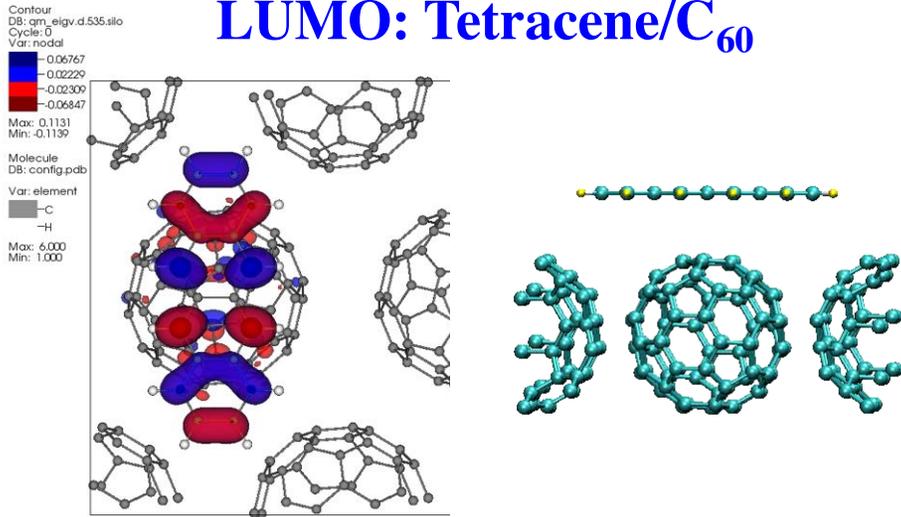
LUMO: Rubrene/C_{60}
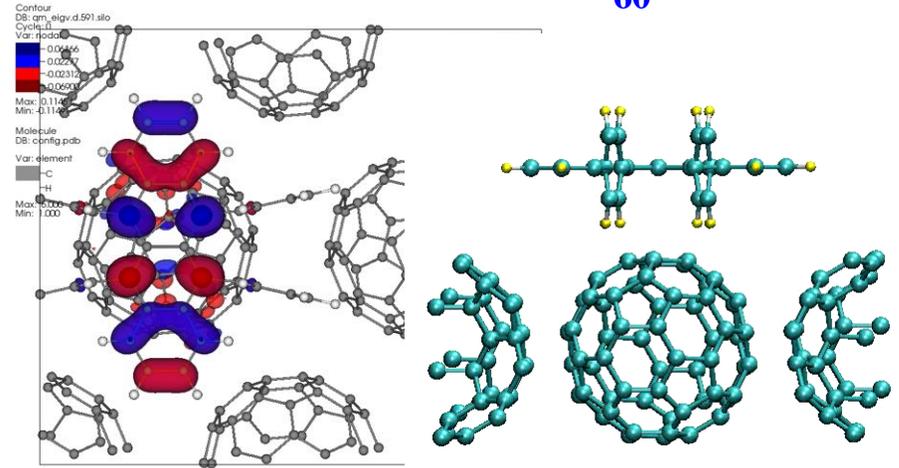
Small level fluctuation $\rightarrow$ small charge transfer
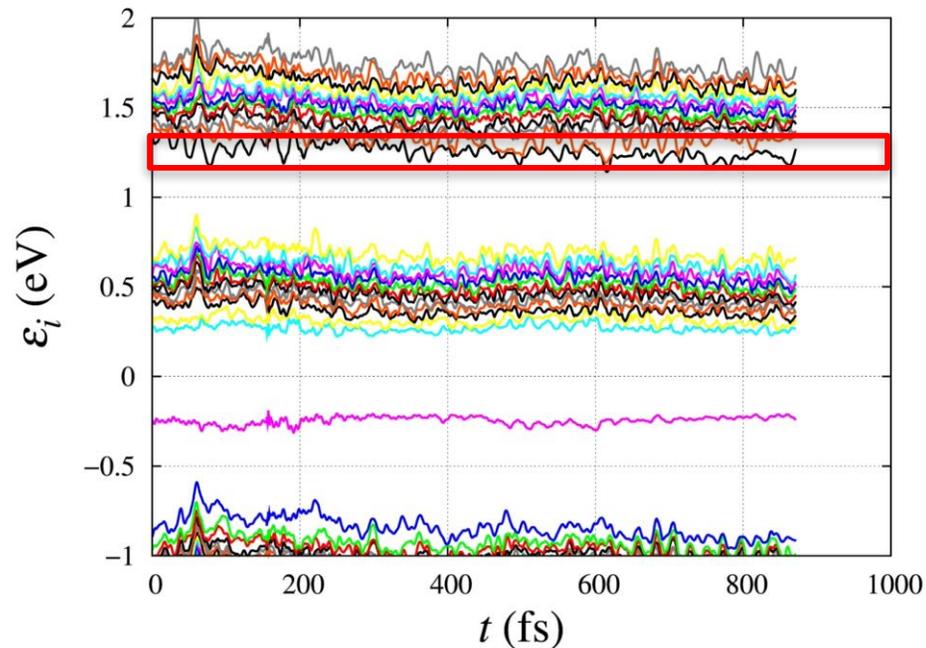
Large level fluctuation $\rightarrow$ large charge transfer
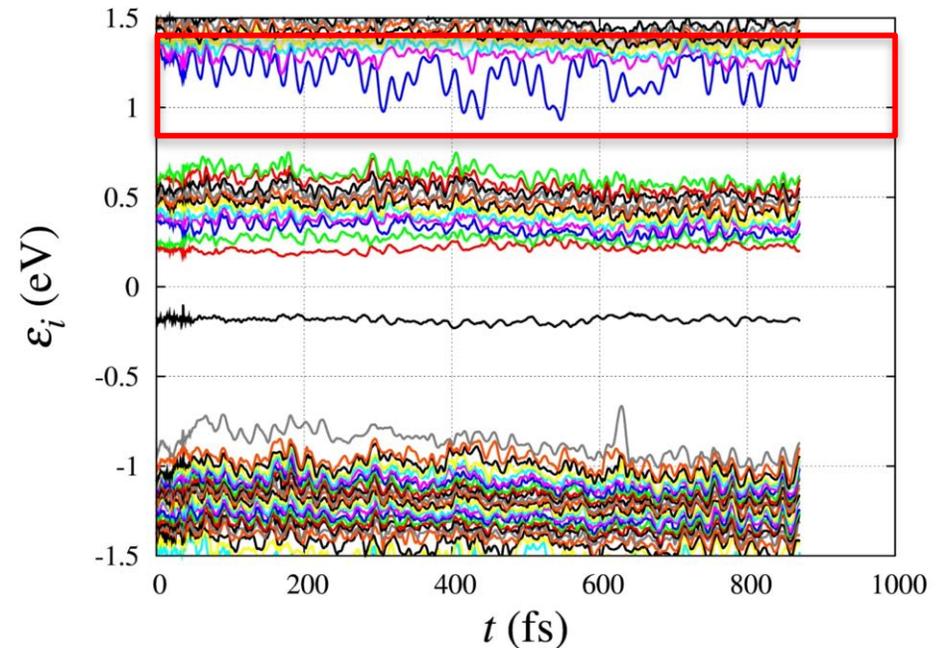
Mou *et al.*, *J. Chem. Phys.* **136**, 184705 ('12)

Ring Breathing Modes

ε^R_{avg}

$\varepsilon^R_{fluctuation}$

ε^T_{avg}

C-C stretch: 22.7 fs

$C_{Rubrene}$
$C_{Tetracene}$
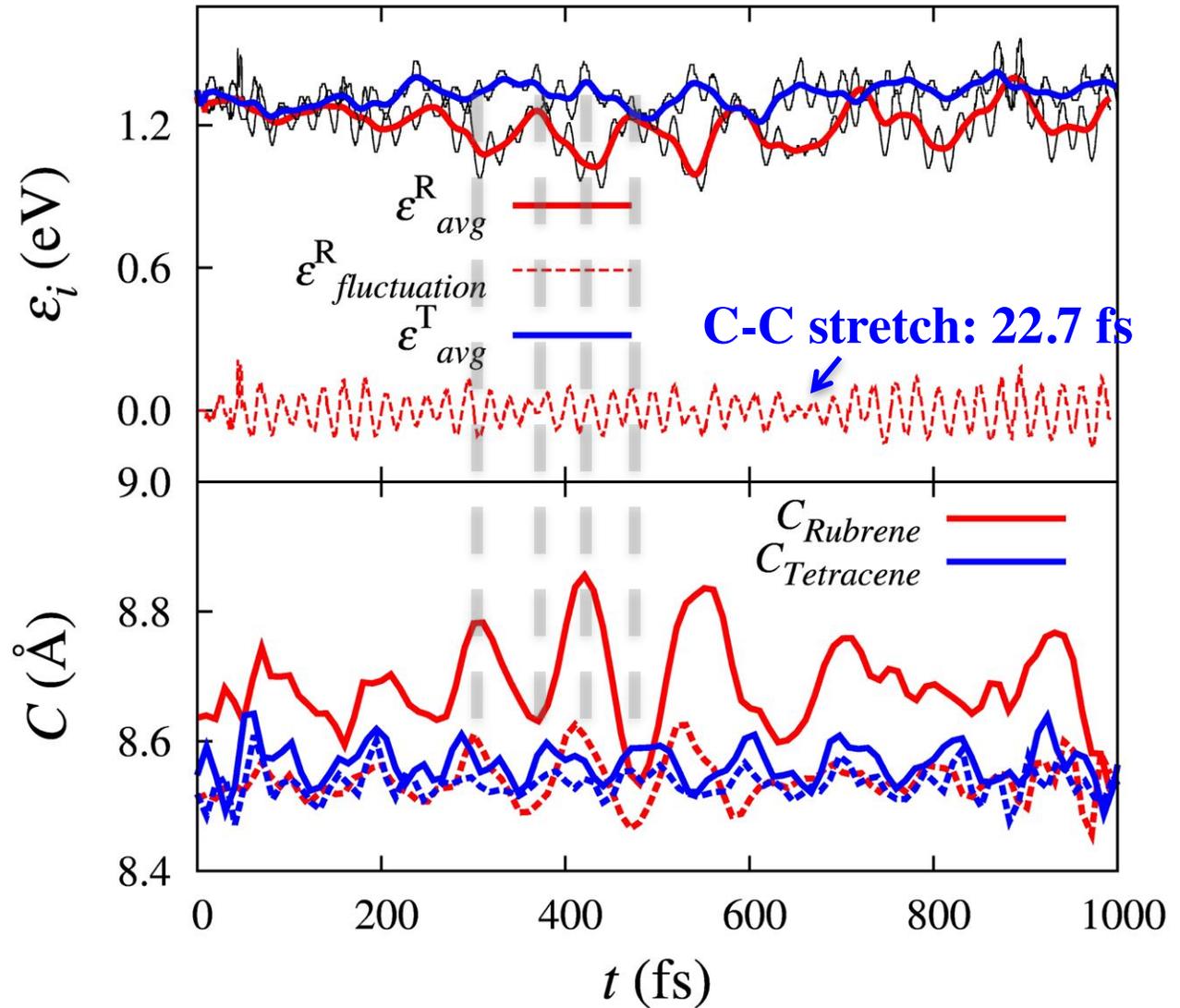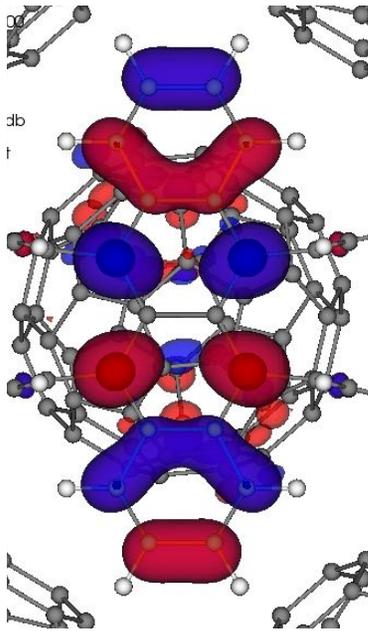
- **The phenyl rings expand the inner rings of the backbone & enhances their breathing modes → Increased charge transfer**

Inorganic Nanowire Photovoltaics (NWPV)

GaAs nanowires under electronic microscopy
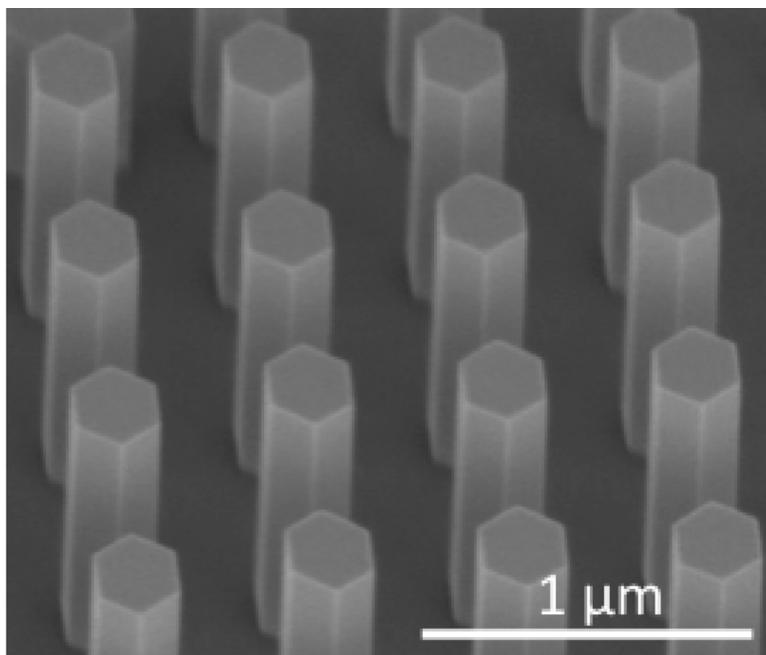
GaAs Nanowire with perfect {110} surfaces

[111]

{110} Planes

1 µm
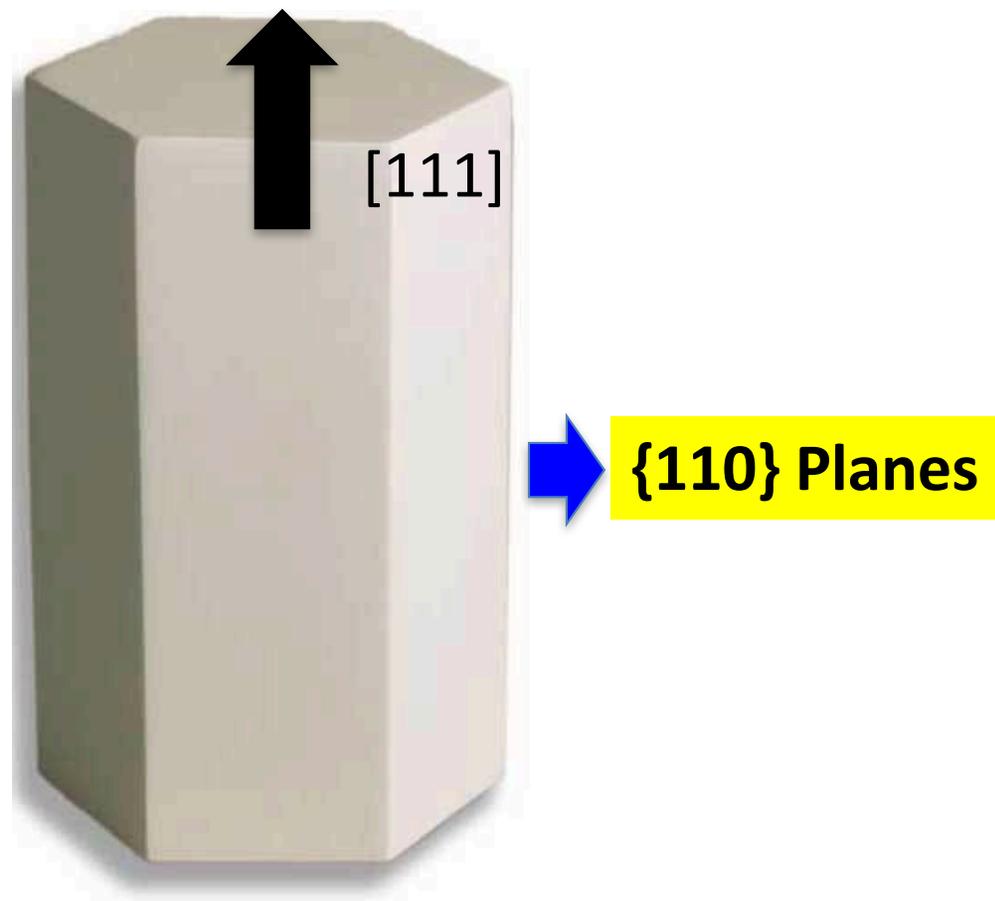
Yao. *et al.*, *ACS Nano* **10**, 2424 ('16)

NAQMD Simulation of GaAs (110) Surface

Simulation Setup for GaAs (110)
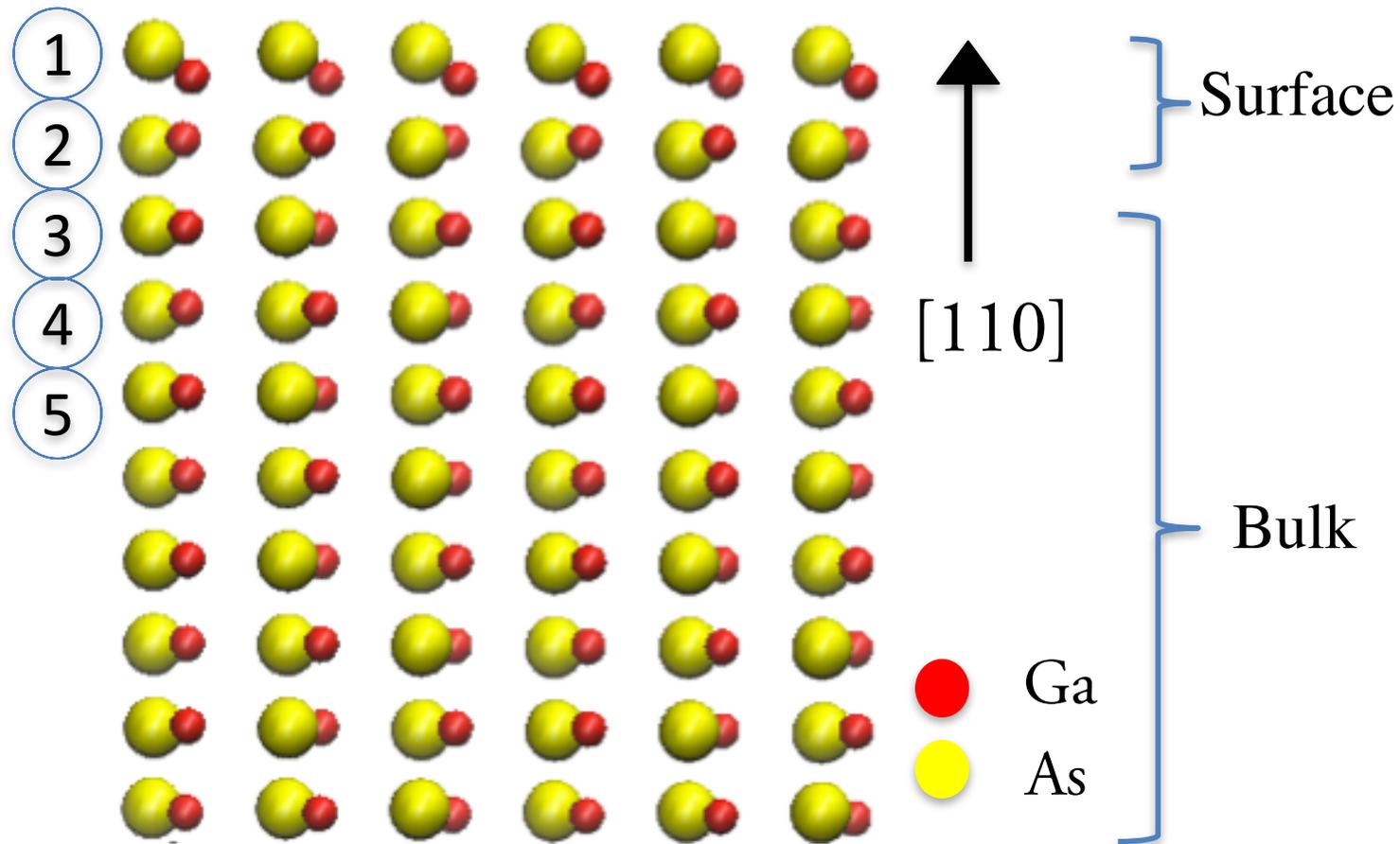
- **Definition of surface and bulk**
- **Atomic bilayers are numbered sequentially**

Brown *et al., J. Appl. Phys.*
117, 054307 ('15)

Electronic Structure at (110) Surface

- **Electronic partial density of states projected onto the wave functions of atomic bilayers**
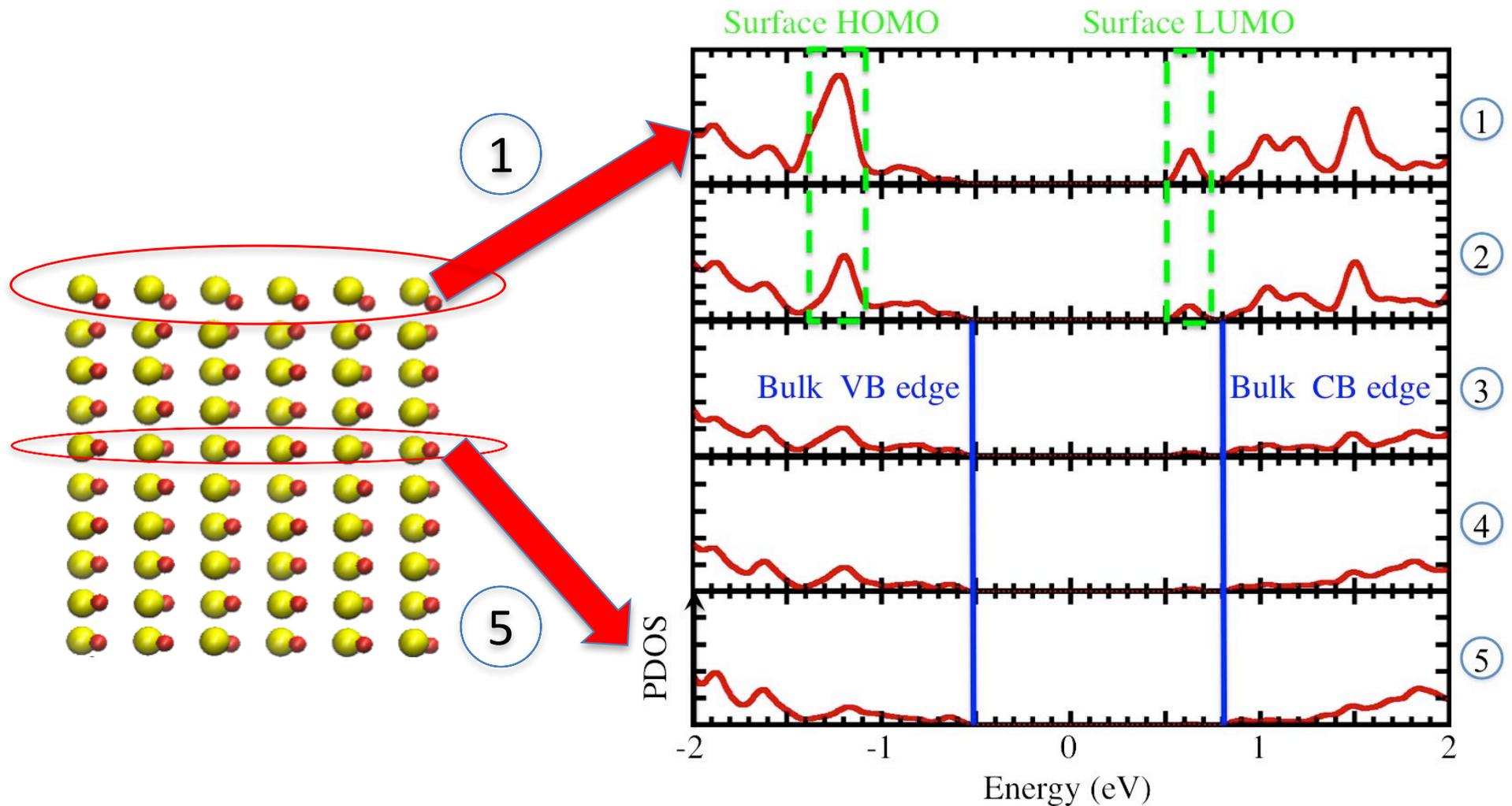
- **Surface relaxation causes spontaneous formation of a type-II (staggered) heterostructure**

Staggered Band Alignment Driven Charge Transfer

Photo excitation & charge recombination in type II heterojunction

- **Bulk CB edge**
- **Photo excitation**
- **Bulk VB edge**
- **Bulk recombination**
- **Charge transfer**
- **Surface LUMO**
- **Surface recombination**
- **Surface HOMO**
- **Type II heterojunction**
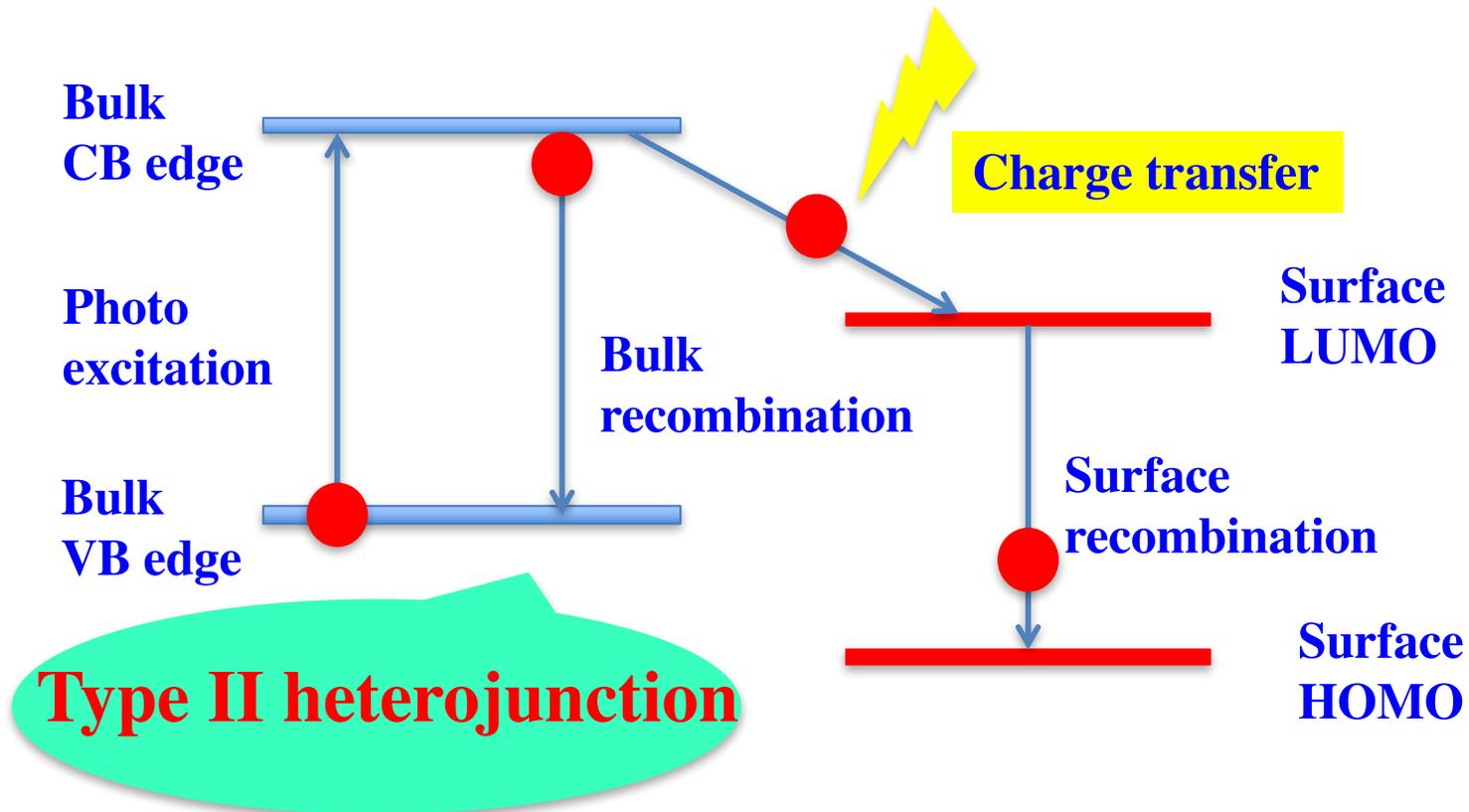
- **Staggered band alignment drives a photoexcited electron in the bulk to lower energy surface states, whereas holes remain near the valence-band (VB) edge (which is a bulk state)**

Bulk *vs*. Surface Excitations

- **Existence probability of KS wave functions at the surface as a function of the KS energy.**
- **Two types of excitations by exciting one electron from an occupied orbital to an unoccupied orbital**

Existence probability at surface

$$P_i^{\text{surface}} = \int\limits_{\mathbf{r}\in\text{surface}}^{\text{electron}} |\Psi_i(\mathbf{r})|^2 d\mathbf{r}$$

Existence probability at bulk

$$P_i^{\text{bulk}} = \int\limits_{\mathbf{r}\in\text{bulk}}^{\text{electron}} |\Psi_i(\mathbf{r})|^2 d\mathbf{r}$$
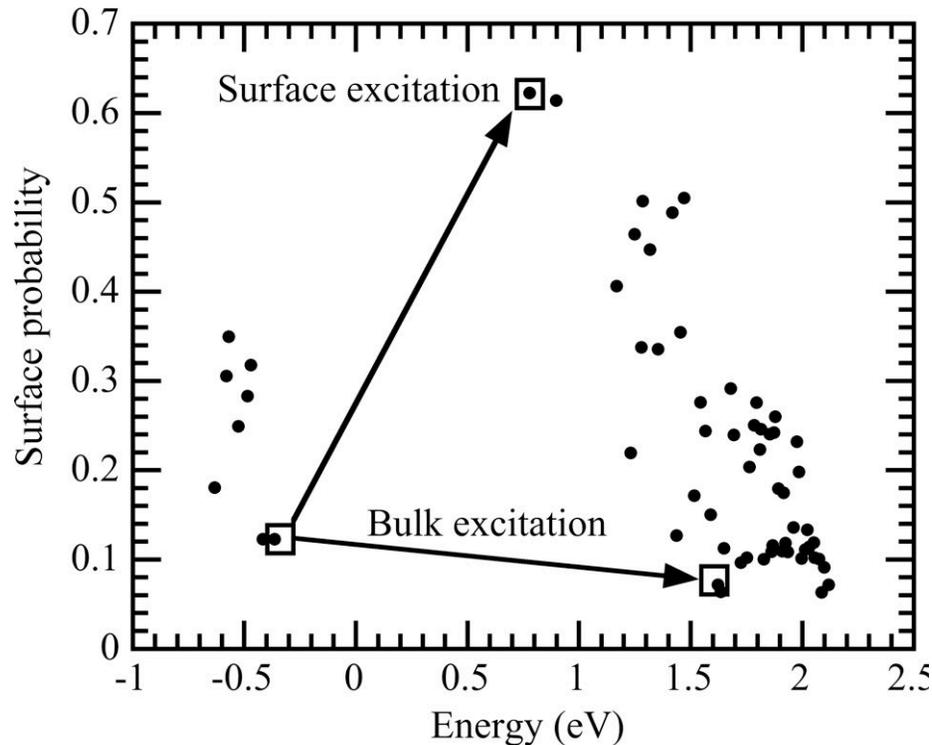
Bulk- & surface-excitations are initiated by the transitions denoted by arrows

Carrier Wave Functions & Charge Transfer Rate

Electron (orange) & hole (green) wave functions of the bulk-excitation simulation from time 0 and 169 fs, exhibits homogeneous distribution to surface localization
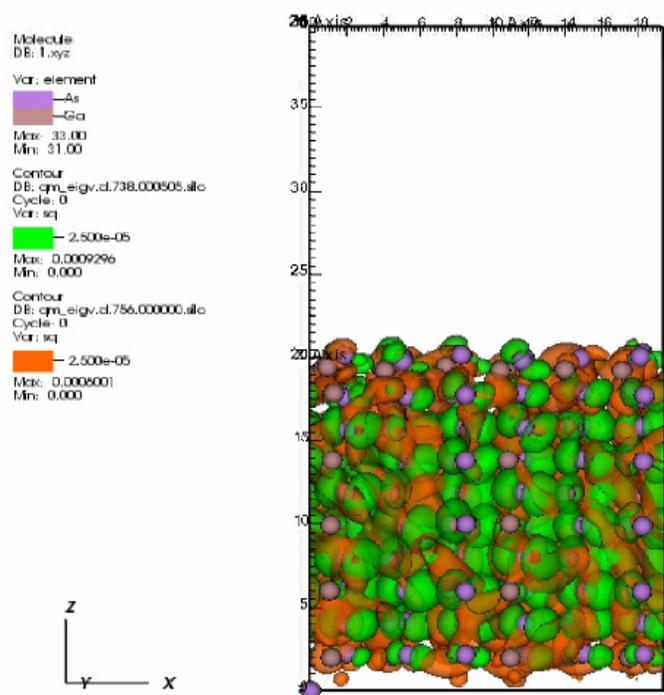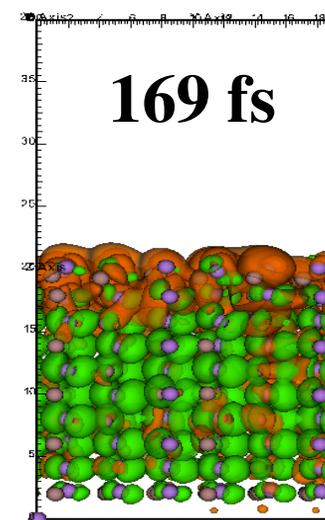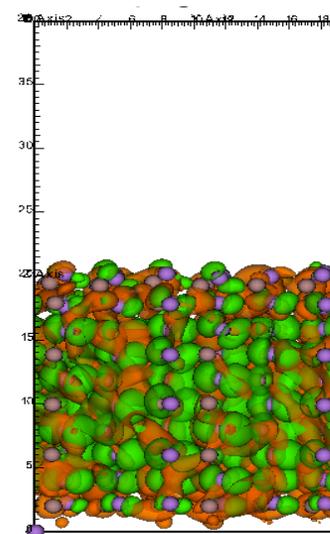
In the NAQMD simulation for bulk excitation, the excited electron quickly transfers to surface

From the time evolution of the surface probability of the excited electron, charge-transfer (CT) rate is estimated to be $k_{CT} = 6.25 \times 10^{12}$ s^{-1}

Phonon-Assisted Charge Recombination in Bulk

Transition probability $\gamma_{ij}(t)$ from the current excited state i to another state j as a function of time t

(a) Bulk excitation

(b) Surface excitation
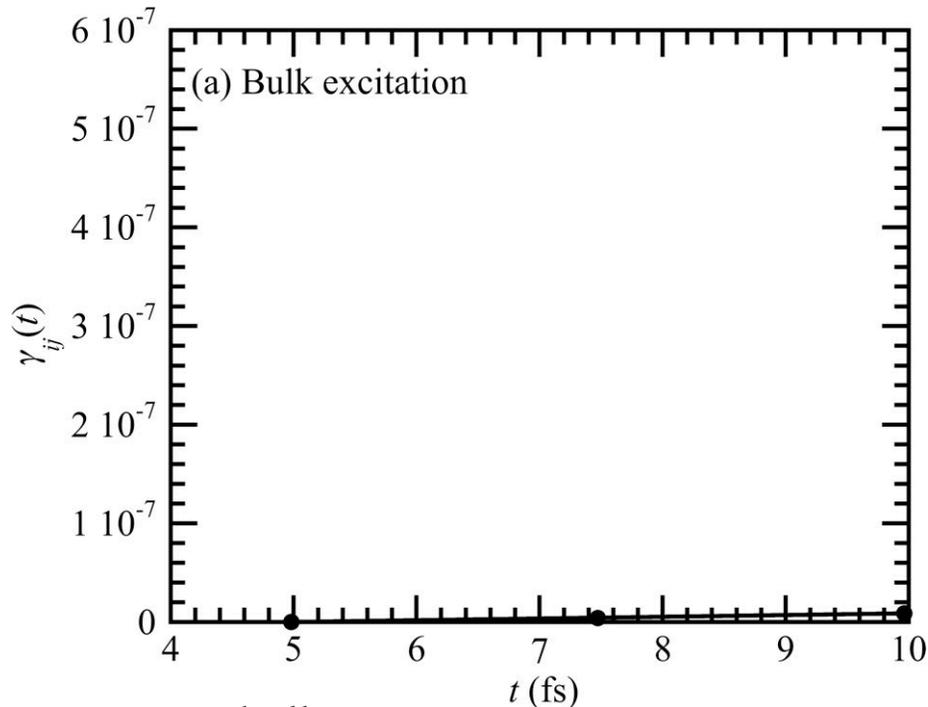
$k^{bulk}_{CR\text{-}phonon} = (1.7\pm0.1)\times10^{6}\ s^{-1}$
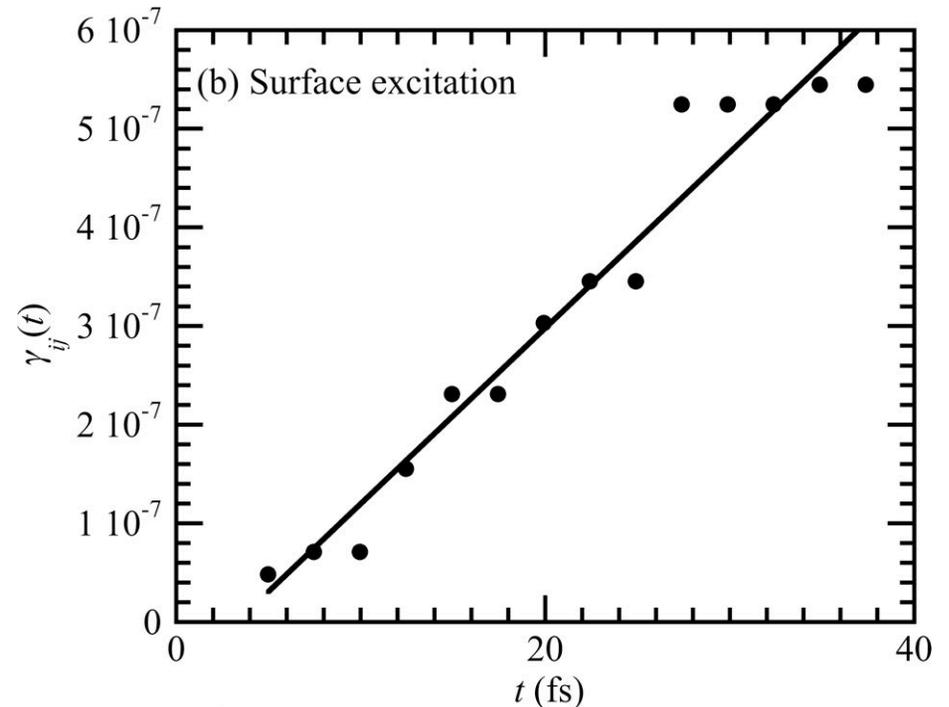
$k^{surface}_{CR\text{-}phonon} = (1.8\pm0.1)\times10^{7}\ s^{-1}$

Charge-recombination (CR) rate is enhanced by an order-of-magnitude near surface

Spontaneous-Emission CR Rate

$$\gamma_{I,J}^{\text{Dipole}} = \frac{4n(\omega_I - \omega_J)^3 \left|\langle\Phi_I|\hat{\mathbf{r}}|\Phi_J\rangle\right|^2}{3c^3}$$

X. Zhang *et al.*,
PRB **84**, 235208 ('11)

- Bulk
$R_{\text{CR\_SE}} = 2.8\times10^2 \ (s^{-1})$

- Surface
$R_{\text{CR-SE}} = 9.3\times10^3 \ (s^{-1})$

Comparison with phonon assisted CR rates

	Bulk	Surface
Phonon assisted R_{CR}	$1.7\times10^6 \ (s^{-1})$	$1.8\times10^7 \ (s^{-1})$
SE R_{CR}	$2.8\times10^2 \ (s^{-1})$	$9.3\times10^3 \ (s^{-1})$

Phonon assisted charge recombination is the dominant CR channel

Modelling Carrier-Population Kinetics

- **Core-shell structure GaAs nanowire with diameter *D***
- **Carrier populations at the core & shell**

- CR at surface: 1.8×10^7 (s^{-1})
- CR in bulk : 1.7×10^6 (s^{-1})
- CT rate : 6.25×10^{12} (s-1)

Electron in the bulk

$k_{CT}(D)$

k_{CR}

$k_{CR}^{surface}$

D
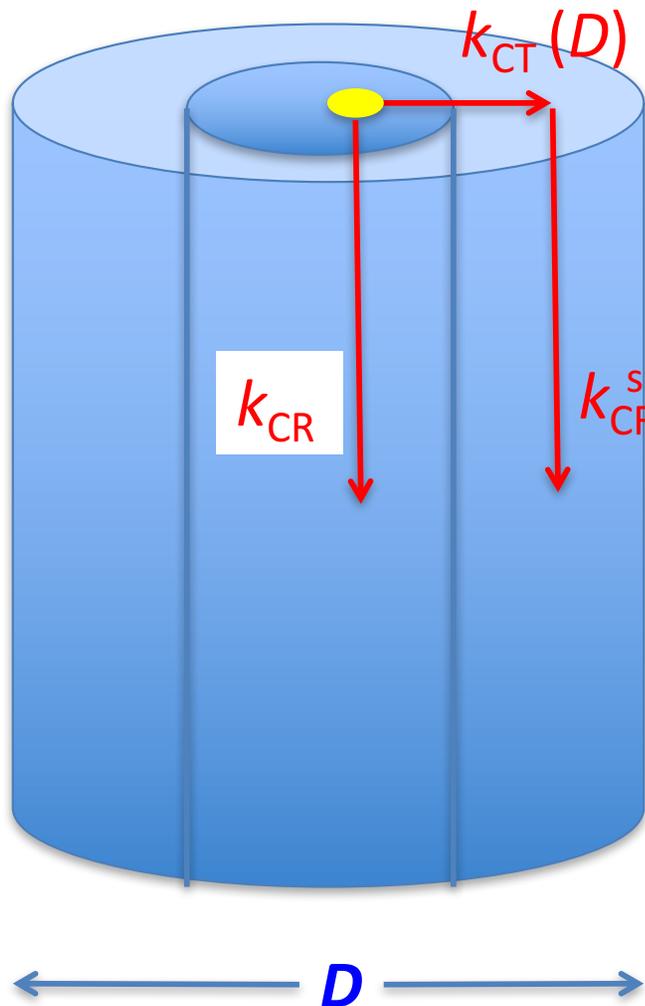
kinetic equation for carrier populations:

$$\frac{d}{dt}\begin{bmatrix} P_{core} \\ P_{shell} \end{bmatrix} = -\begin{bmatrix} k_{CT}(D) + k_{CR}^{bulk} & 0 \\ -k_{CT}(D) & k_{CR}^{surface} \end{bmatrix}\begin{bmatrix} P_{core} \\ P_{shell} \end{bmatrix}$$

Carrier population vs Time (ps), curves for 30 nm and 3 nm.

$$P(t) = P_{core}(t) + P_{shell}(t)$$

$\Delta E/E$ (arbitrary units) vs Pump-probe delay (ps) for 80 nm, 50 nm, 30 nm.

H. Joyce *et al.*, *Nanotech.* **24**, 214006 ('13)
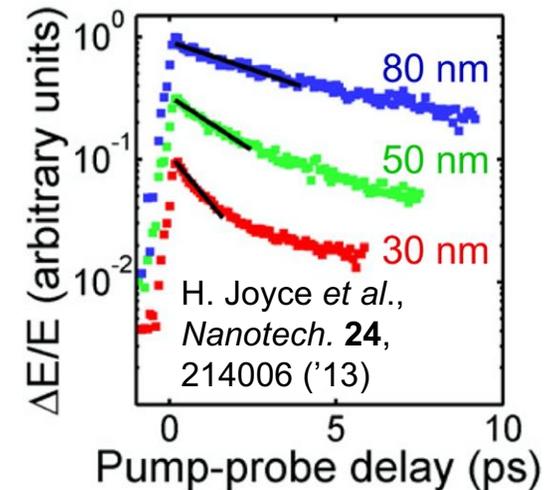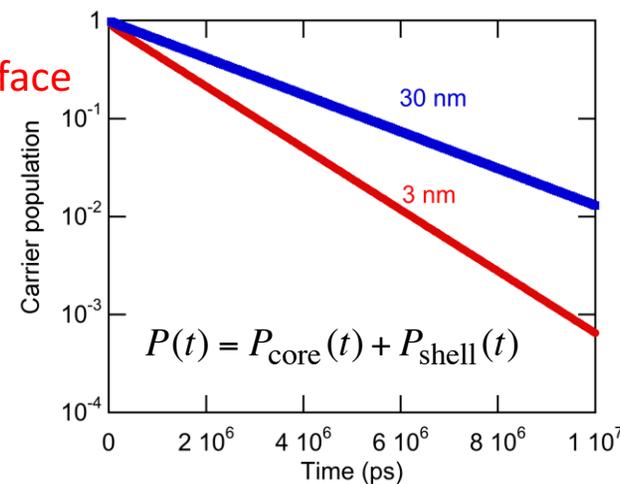
1. **Faster decay with decreasing diameter in agreement with experiments**
2. **Decay time with ideal (110) sidewalls too large → more realistic sidewalls?**

Charge Recombination in Twinned NW

SEM image of twinned nanowire
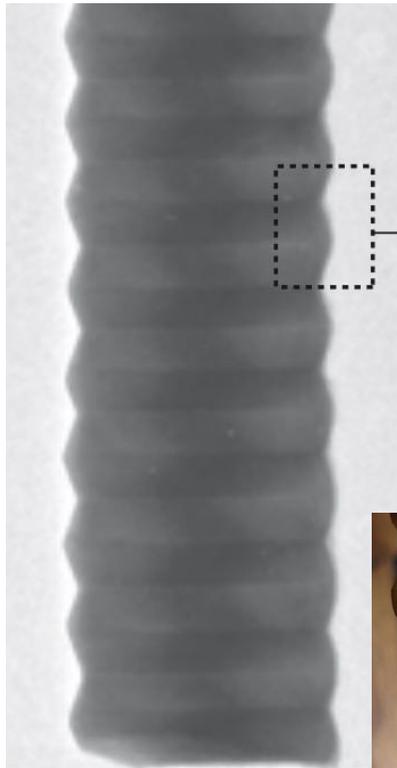
TEM image of twinned nanowire

100 nm
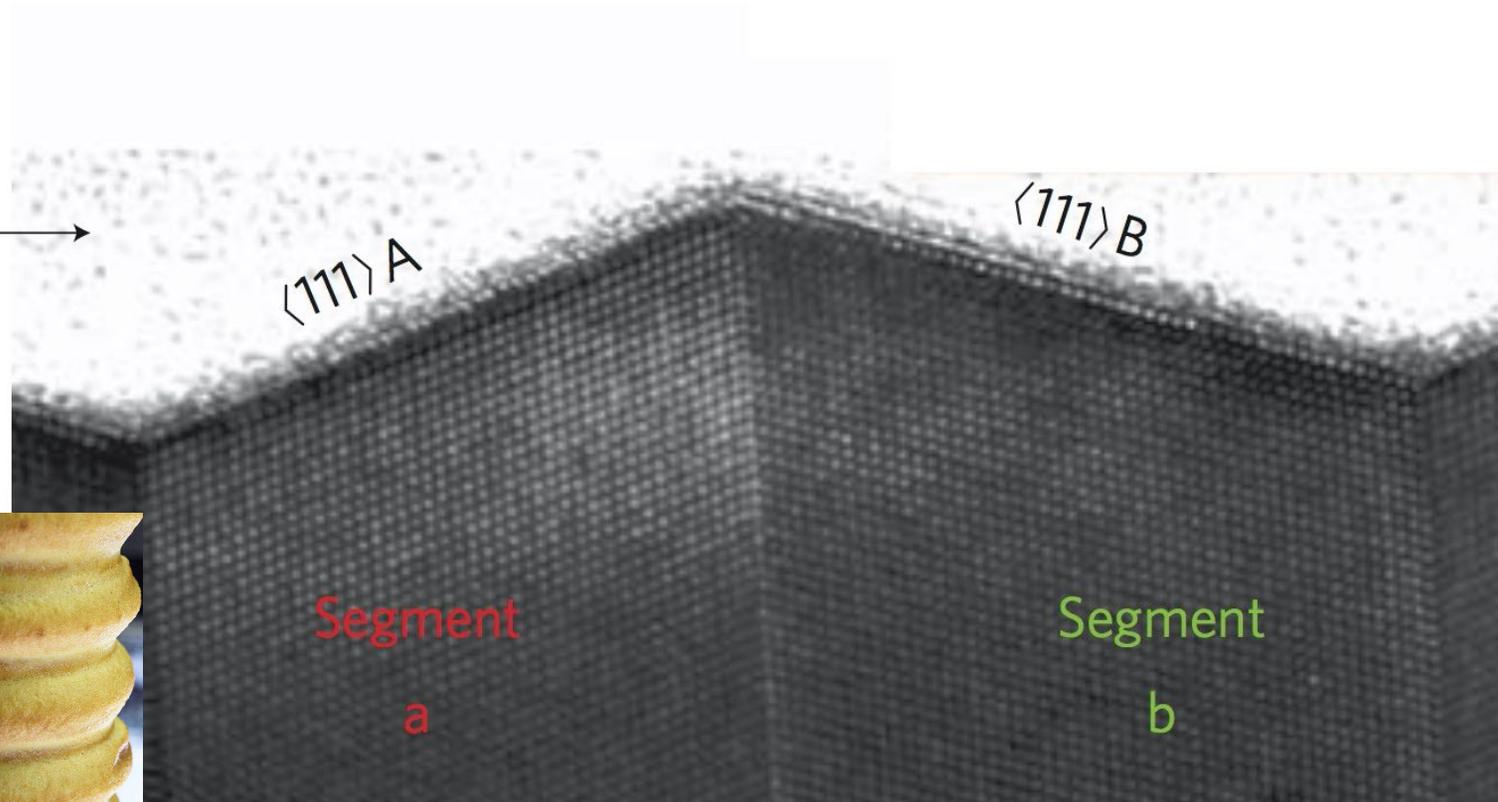
Real GaAs {110} facets contain high density of twin defects

Caroff *et al*. *Nat. Nanotechnol.* **4**, 50 ('09)

Twin-Twin Attraction
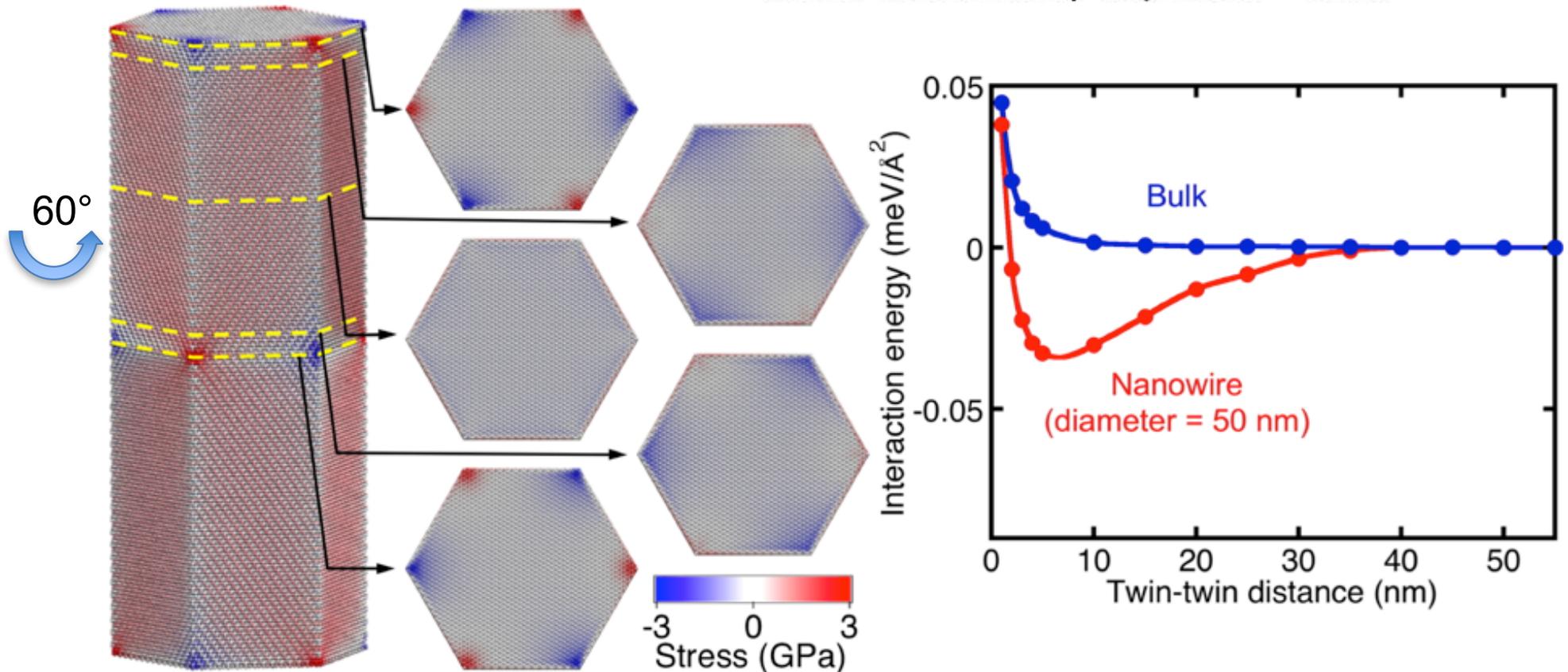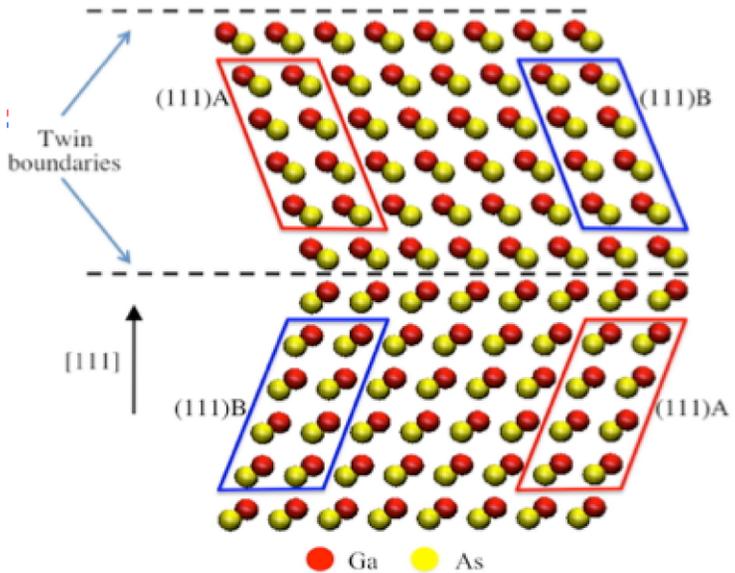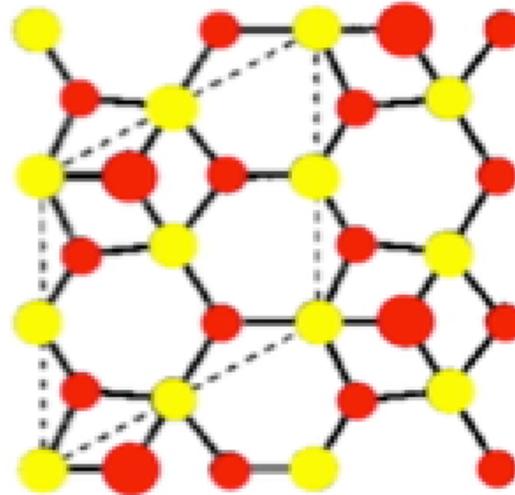
- **Twin planes in a [111] GaAs nanowire attain attractive interaction mediated by surface strain → self-replicating generation of a twin superlattice**
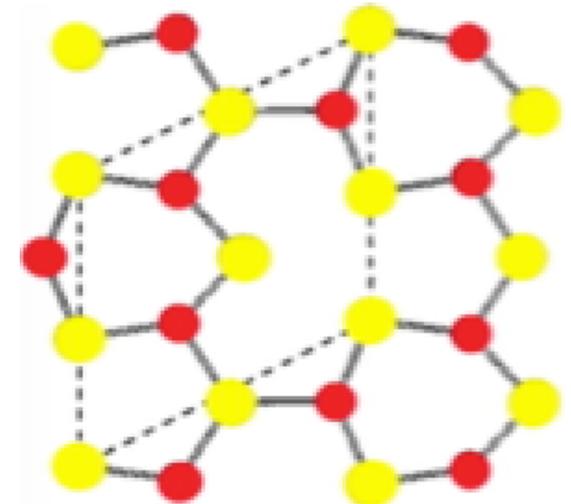
Twinned GaAs Nanosheet (NS)

Relaxed GaAs crystal viewed from the [112] direction

Top view of the Ga-adatom reconstruction of GaAs (111)B surface

Top view of the Ga-vacancy reconstruction of (111)A surface

- These energetically lower reconstructed surfaces are charge-neutral
- NS with these reconstructed sidewall surfaces remains stable during quasi-Newton energy minimization

Sheng *et al.*, *Appl. Phys. Lett.* **105**, 231602 ('14)

KS Energy Projection: Band Alignment

Electronic partial densities-of-states (PDOS) projected onto the (111)A and (111)B sidewall
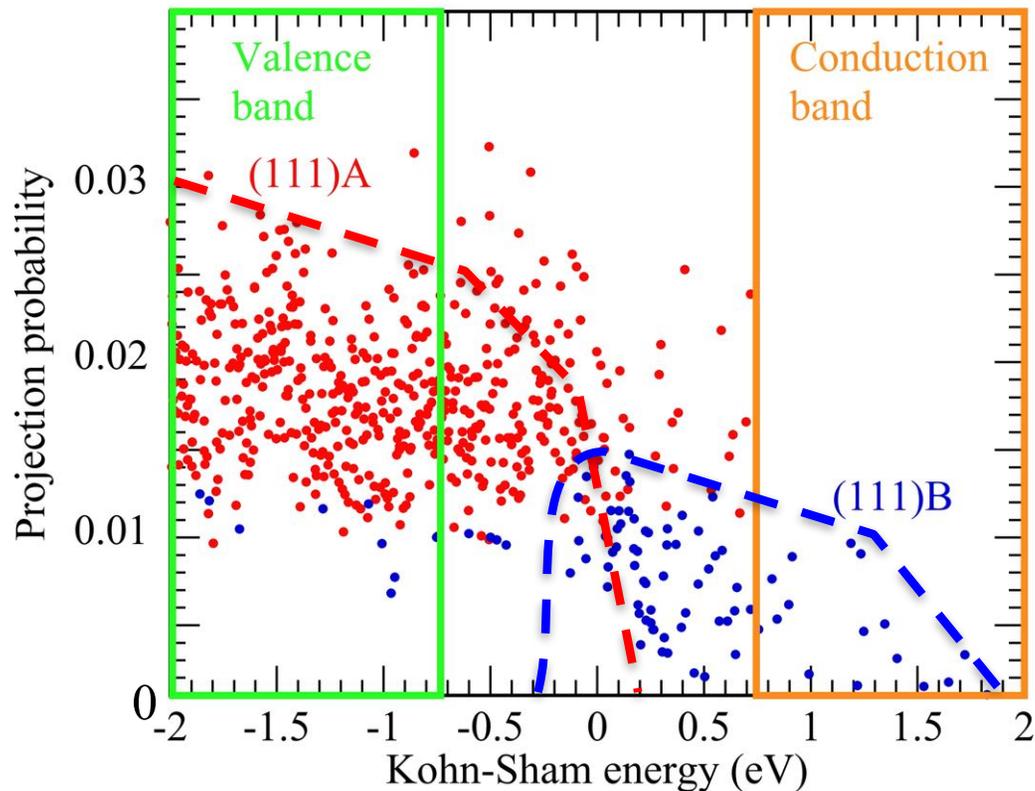
Schematic of the bulk CB (orange) and VB (green) along with (111)A (red) and (111)B (blue) surface-state energies
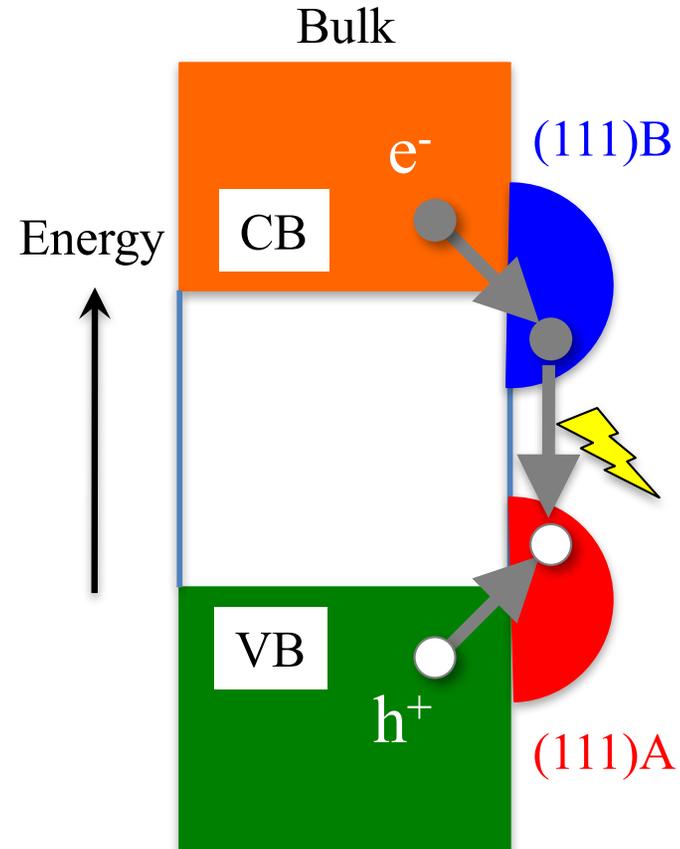
- **Gap states derived from (111)A surfaces are located just above bulk valence band (VB) top**

- **Gap states derived from (111)B surfaces are located just below bulk conduction band (CB) bottom**

Bulk-State Photoexcitation

- **NAQMD simulation for electron excitation: bulk VB top → bulk CB bottom**
- **Energy relaxation of photoexcited electron-hole pairs**
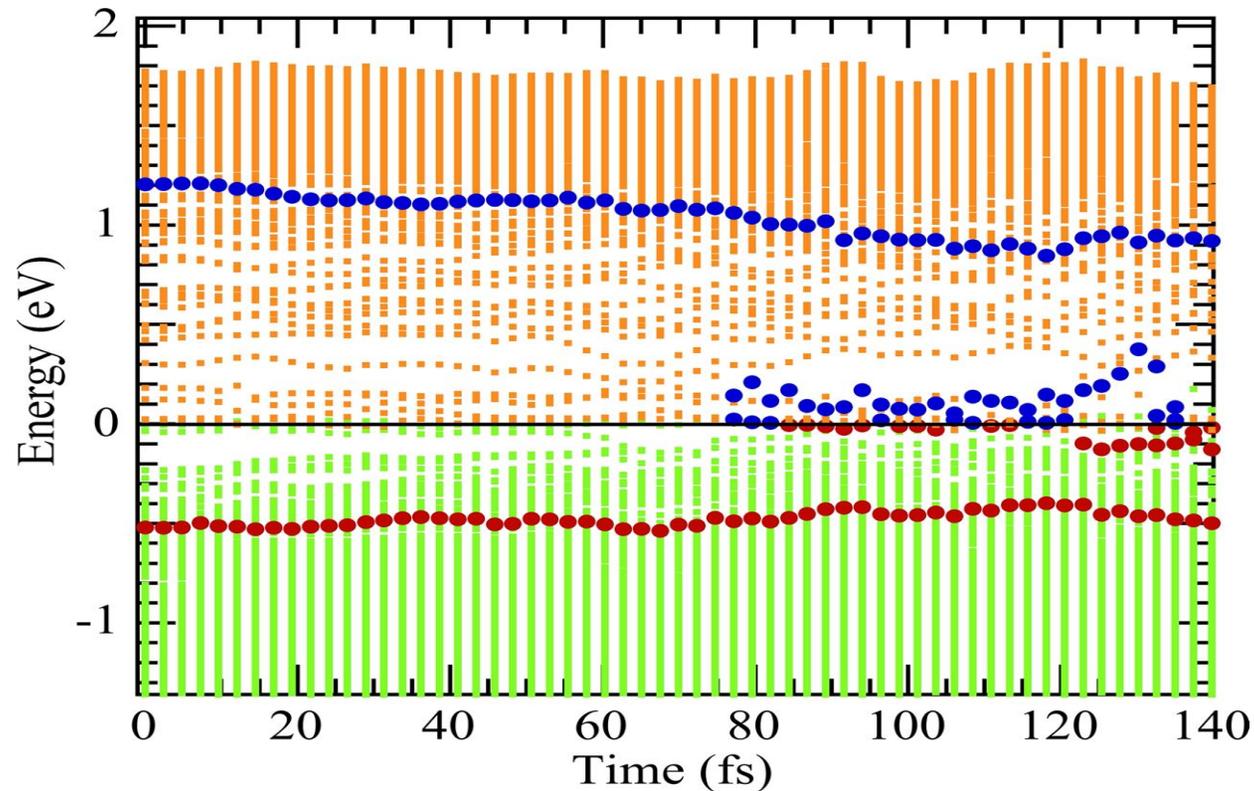
- **Initially, only one electron-hole pair exists**
- **More electron-hole pairs are created starting at ~80 fs near the Fermi energy**

Energy Relaxation on Surface

Logarithm of average excitation energy as a function of time
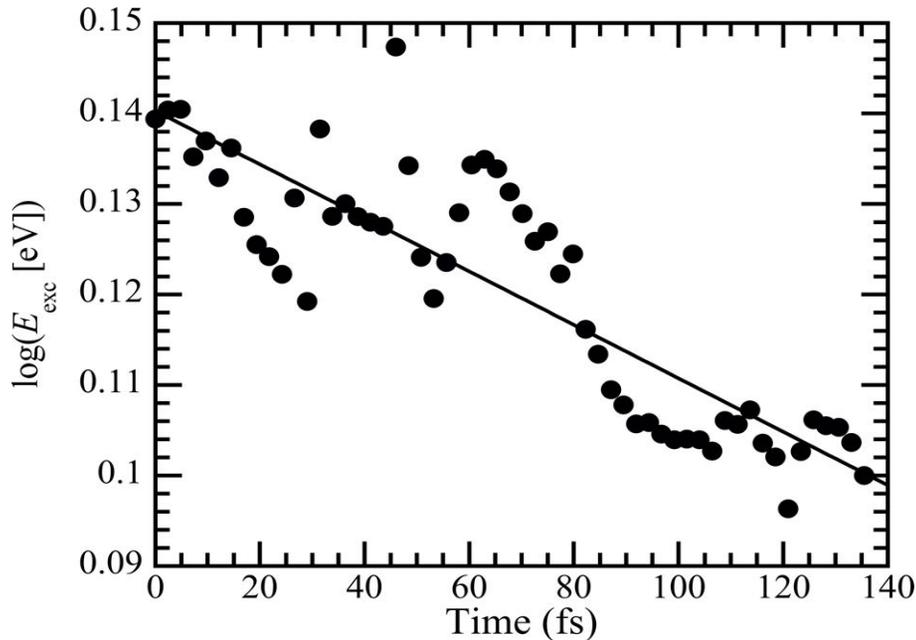
Average electronic excitation energy as a function of time
$k_{CR} = (3.0 \pm 0.2) \times 10^{11} \ (s^{-1})$

Average electronic excitation energy

$$\bar{E}(t) = \dfrac{\sum\limits_{i=1}^{iF}(2 - n_i(t))(\varepsilon_F(t) - \varepsilon_i(t)) + \sum\limits_{i=iF+1}^{\infty} n_i(t)(\varepsilon_i(t) - \varepsilon_F(t))}{\dfrac{\sum\limits_{i=1}^{iF}(2 - n_i(t)) + \sum\limits_{i=iF+1}^{\infty} n_i(t)}{2}}$$

$\varepsilon_i(t)$ is the i*th* KS energy

Charge recombination rates
$k_{CR} = (3.0 \pm 0.2) \times 10^{11} \ (s^{-1})$ **(111)**
$k_{CR} = (1.8 \pm 0.1) \times 10^{7} \ (s^{-1})$ **(110)**

- **Calculated CR rate at (110) surface is orders-of-magnitude smaller**
- **Much larger CR rate (~10^{11} s^{-1}) is likely due to the twin superlattice-related surface geometry**

# Modelling Carrier-Population Kinetics

- **Core-shell structure GaAs nanowire with diameter *D***
- **Aiming at estimating the surface recombination velocity**
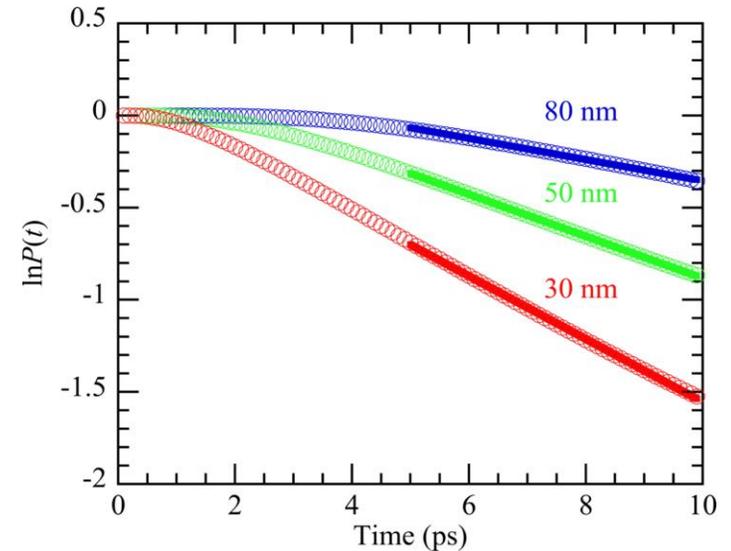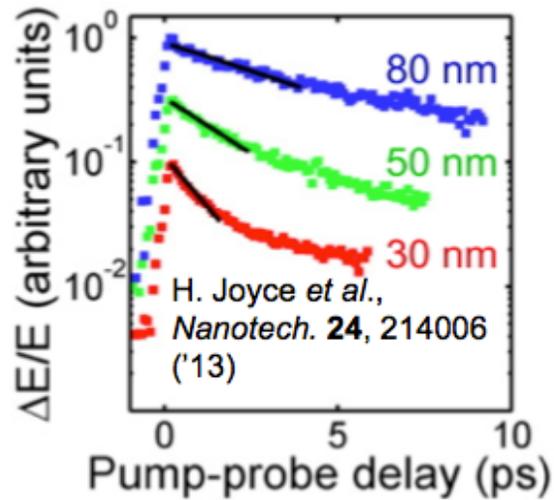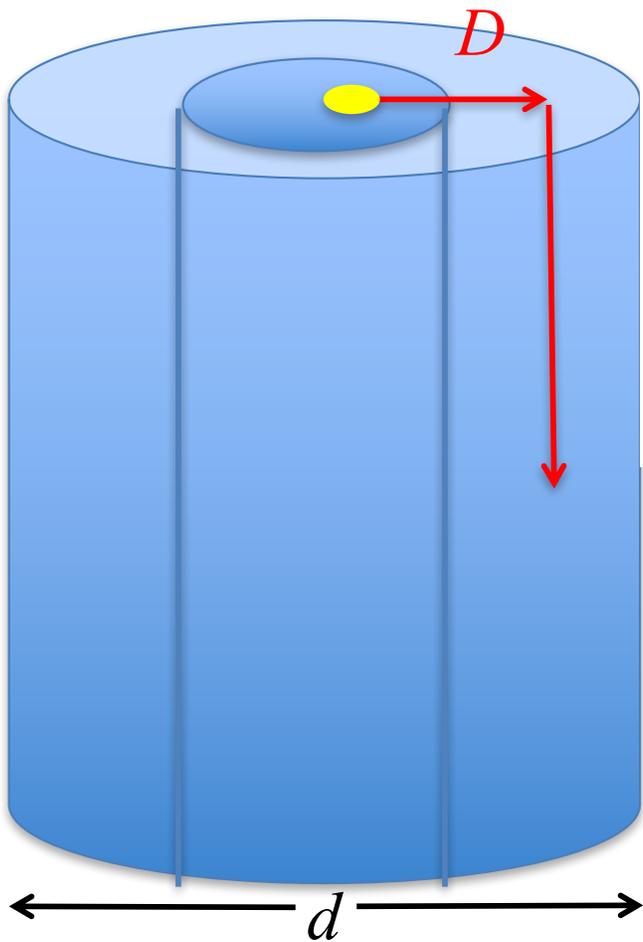
1. **Faster decay with decreasing diameter in agreement with experiments;**
2. **Decay time with realistic [111] sidewalls is consistent with experimental data**

# Surface Recombination Velocity

CR rate as a function of the NW diameter
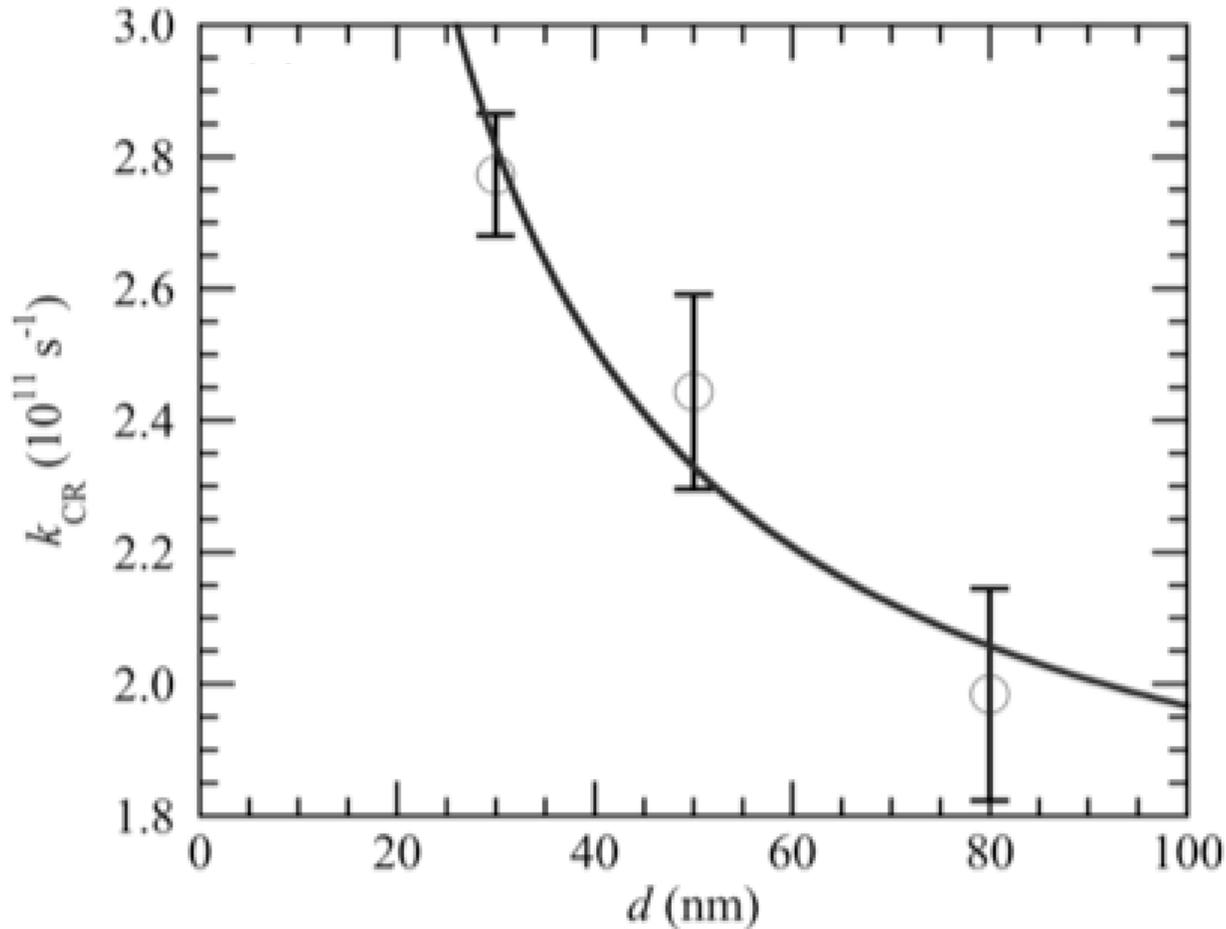
Surface recombination velocity (SRV) in NW

$$k_{CR}(D) = k_{CR}^{\infty} + \frac{4S}{D}$$

- **Calculated SRV = $(3.6 \pm 0.9) \times 10^3$ m/s** [Sheng *et al.*, *Appl. Phys. Lett.* **105**, 231602 ('14)]

- **Good agreement with the experimental value (5.4×10^3 m/s)** [Joyce *et al.*, *Nanotechnol* **24**, 214006 ('13)]

Hybrid Organic/Inorganic Photovoltaics

- **Hybrid P3HT (poly[3-hexylthiophene])/ZnO-nanowire photovoltaics for scalable manufacturing**
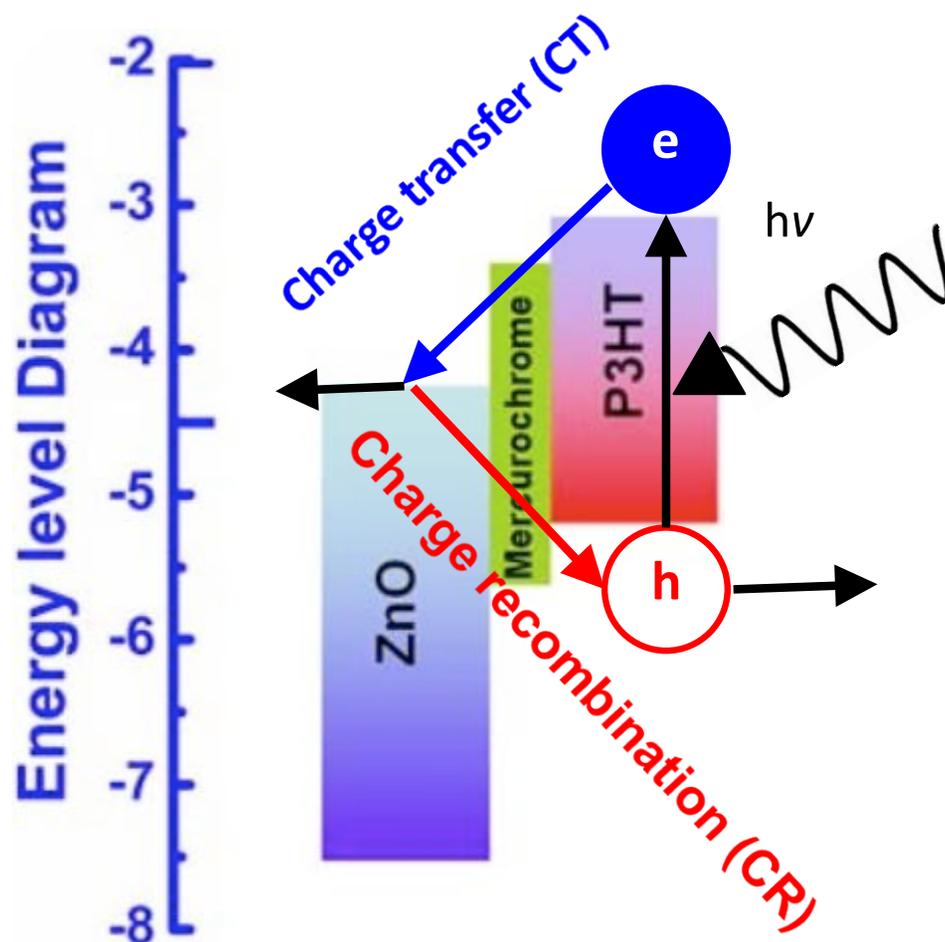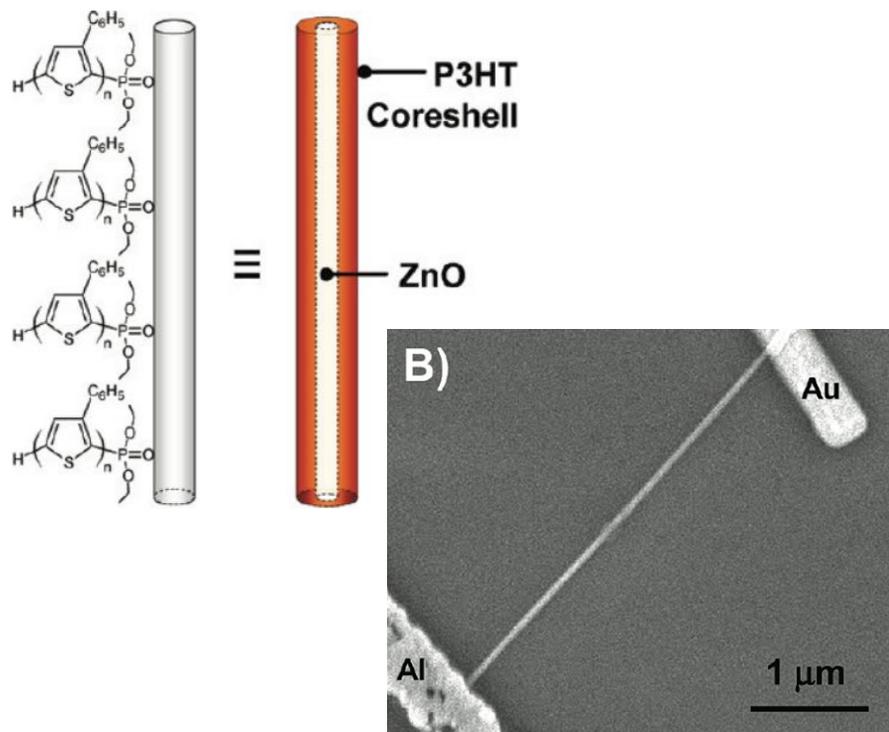
Briseno *et al.*, *Nano Lett.* **10**, 334 ('10)

Lin *et al.*, *Appl. Phys. Lett.* **94**, 064308 ('09)

- **Problem: Interfacial molecular design principles for enhancing charge transfer (CT) & suppressing charge recombination (CR)?**
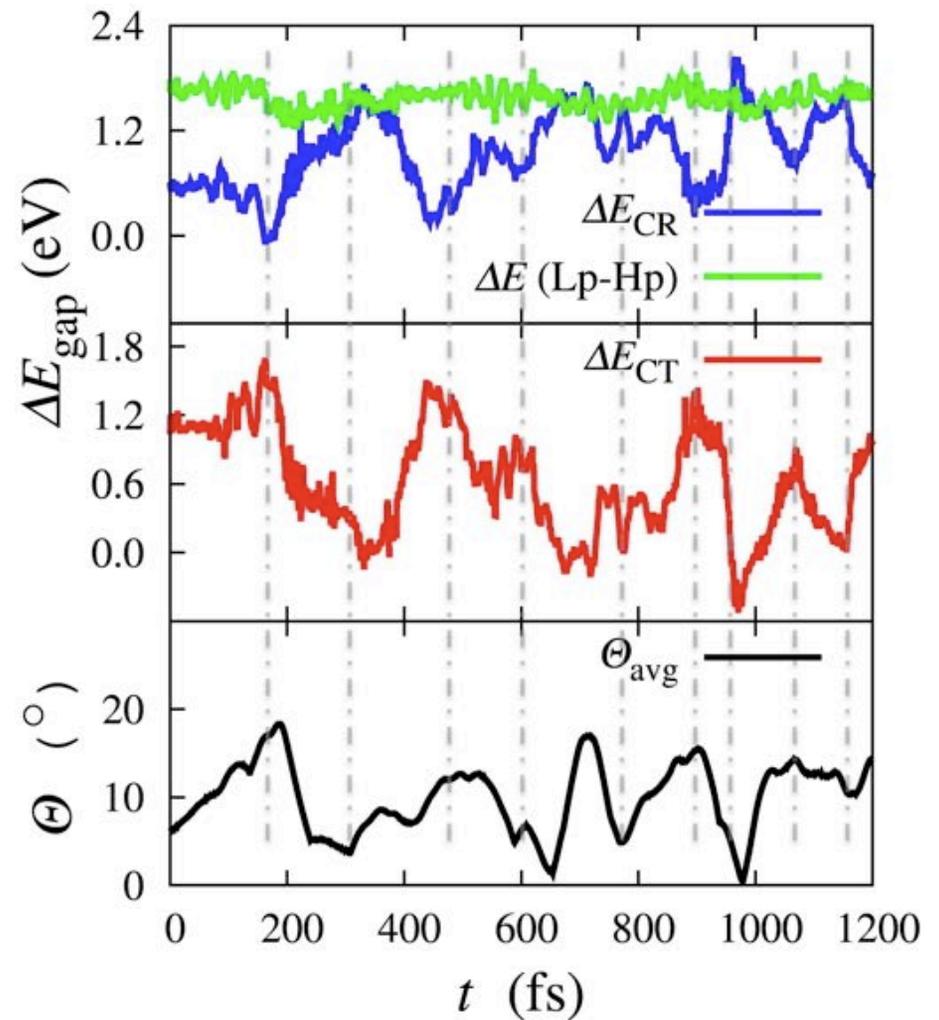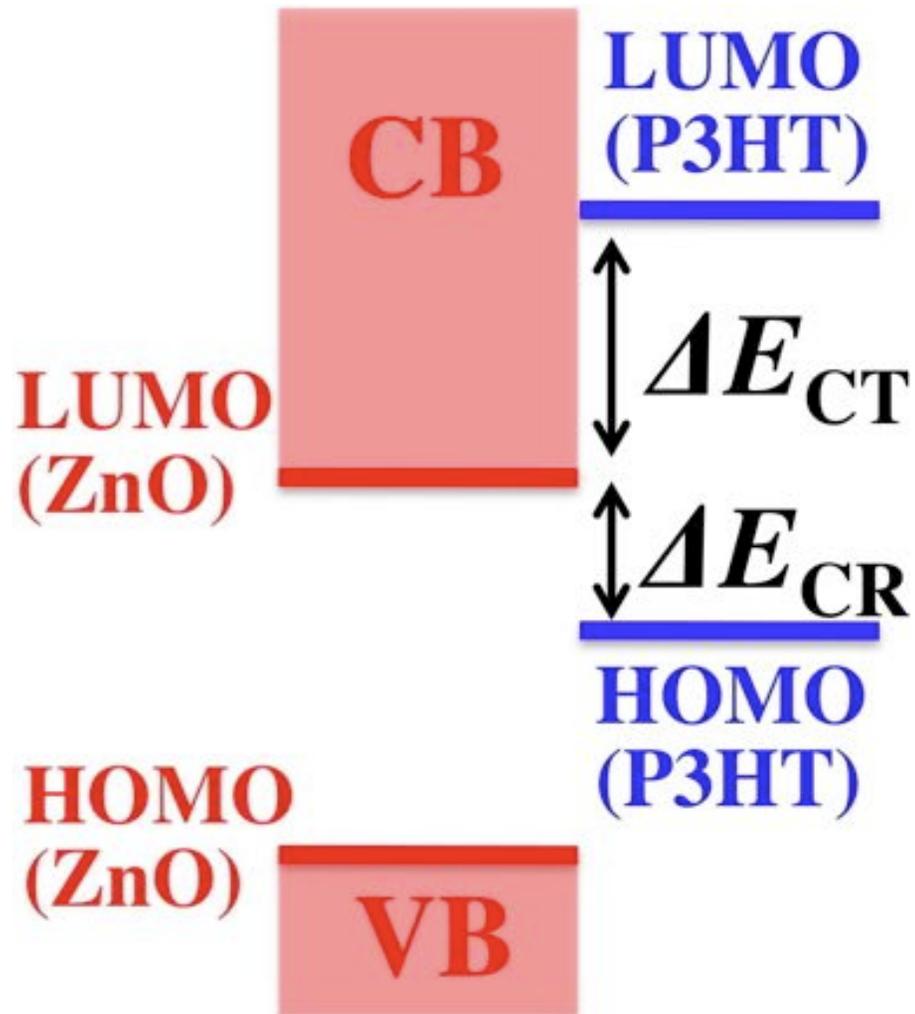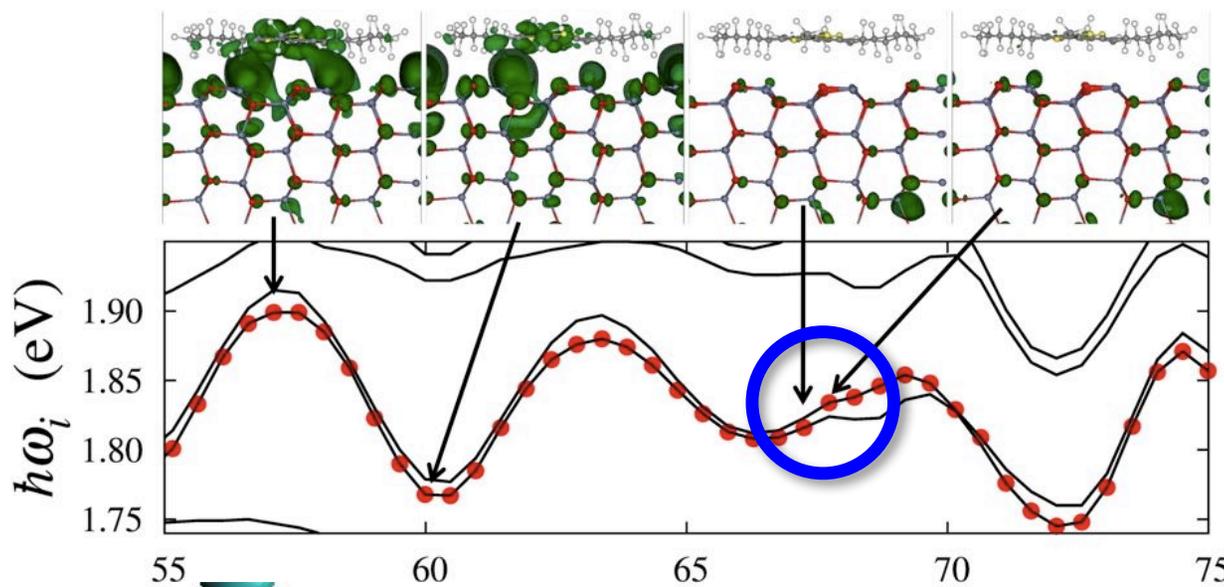
Effects of Molecular Disorder on CT/CR
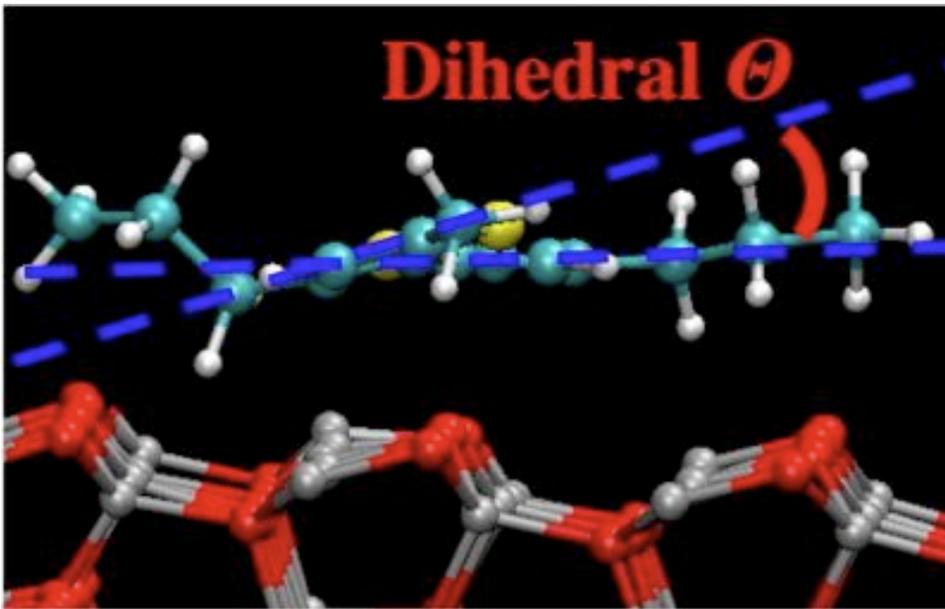
- **552-atom nonadiabatic quantum molecular dynamics simulation of P3HT on ZnO ($10\bar{1}0$)**

- **Twisting of P3HT (static disorder) increases charge-recombination (CR) rate, but not affects charge-transfer (CT) rate**
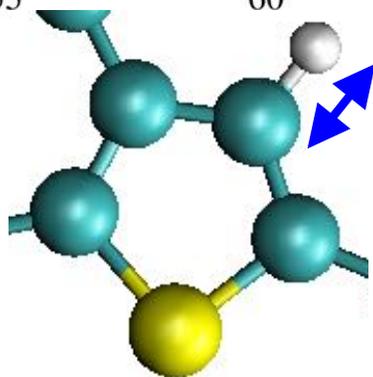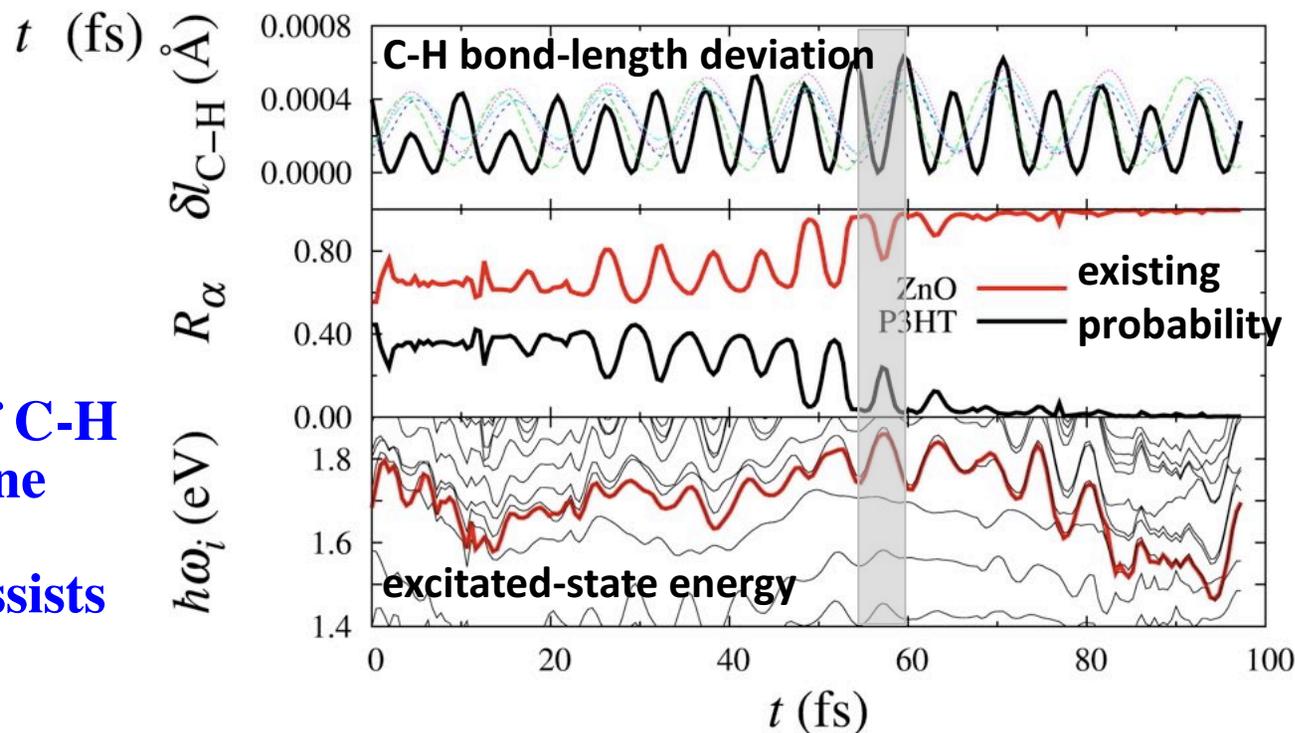

Mou *et al.*, *Appl. Phys. Lett.* **100**, 203306 ('12)
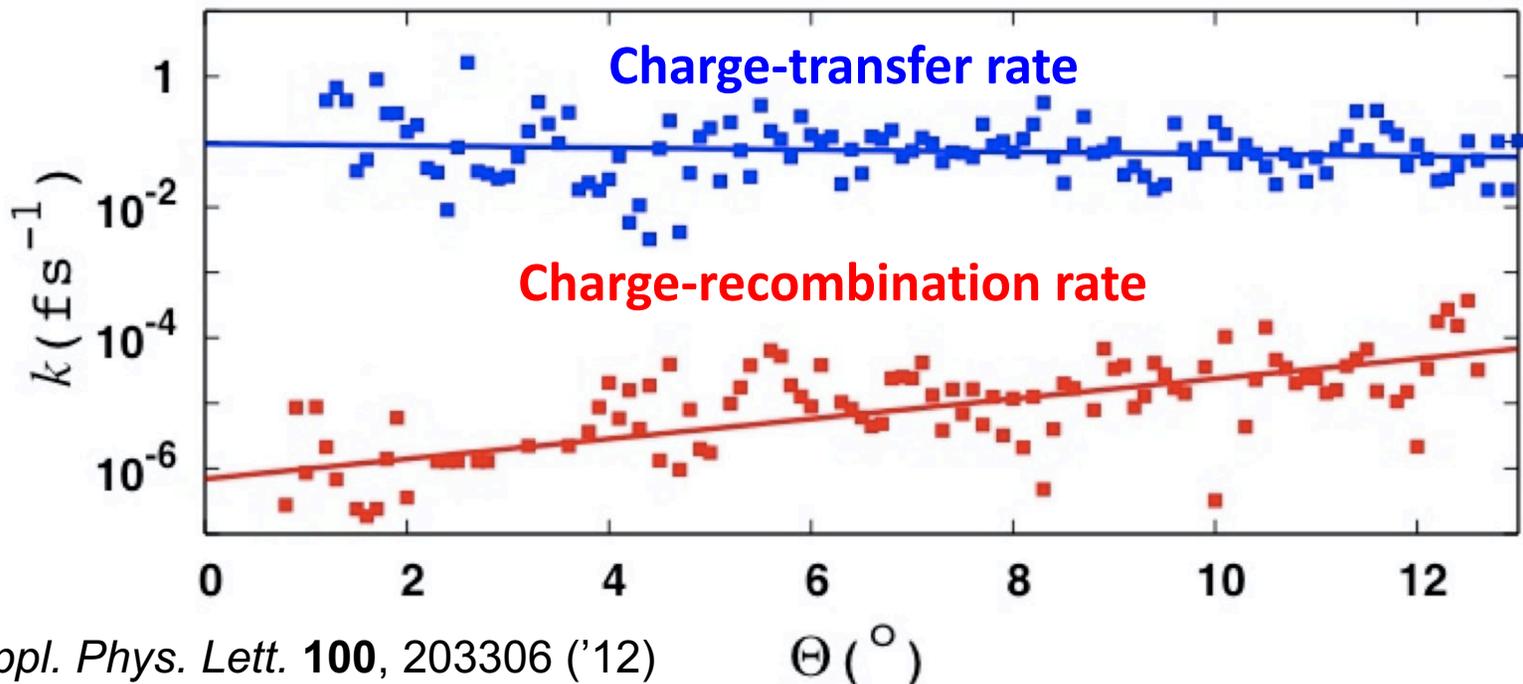
Molecular Mechanism

Effect of Dynamic Disorder

- **Energy-level fluctuation of period ~6 fs assists electronic transition**

- **Thermal vibration of C-H bonds on the backbone chain around their equilibrium length assists charge transfer**

Interfacial Molecular-Design Principle

- *Static disorder* of P3HT conformation is *detrimental* to the efficiency of hybrid P3HT/ZnO photovoltaics by increasing the charge-recombination rate

- *Dynamic disorder* (*i.e.* thermal fluctuation of C-H bonds in P3HT) is *essential* for high efficiency by assisting charge transfer

- A design principle for efficient photovoltaics—weak interfacial bonding: (1) avoid *static disorder*; (2) promote *dynamic disorder*

- **Example: Grazing incidence x-ray diffraction & photocurrent measurements show increase of photocurrent with improved P3HT crystallinity near P3HT/ZnO interfaces due to the insertion of an alkane-thiol self-assembled monolayer**

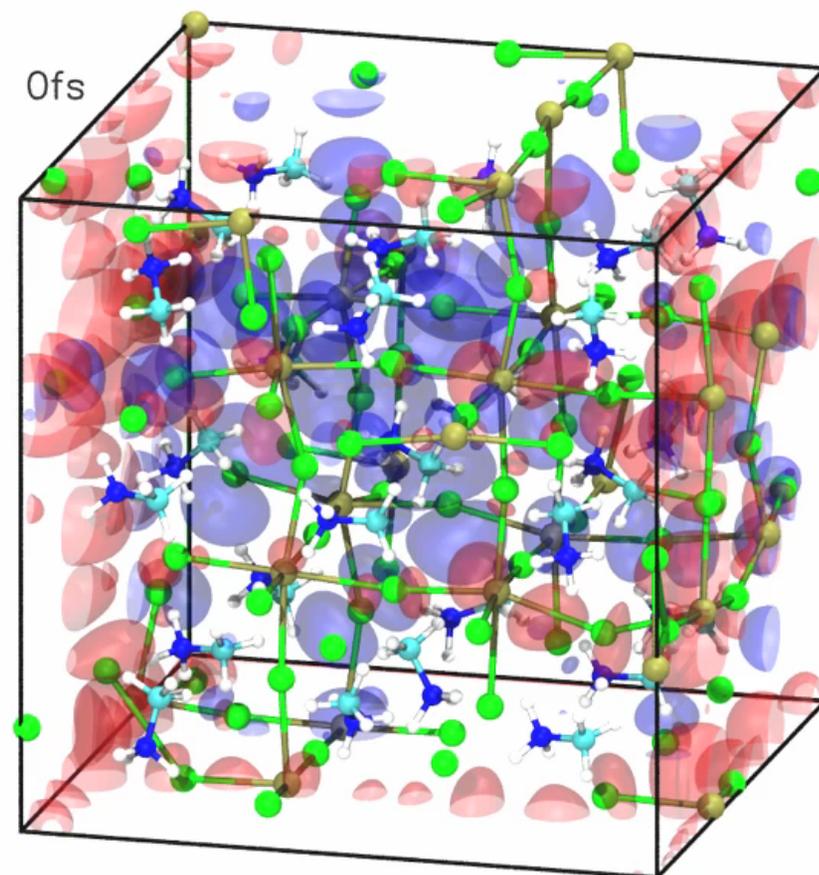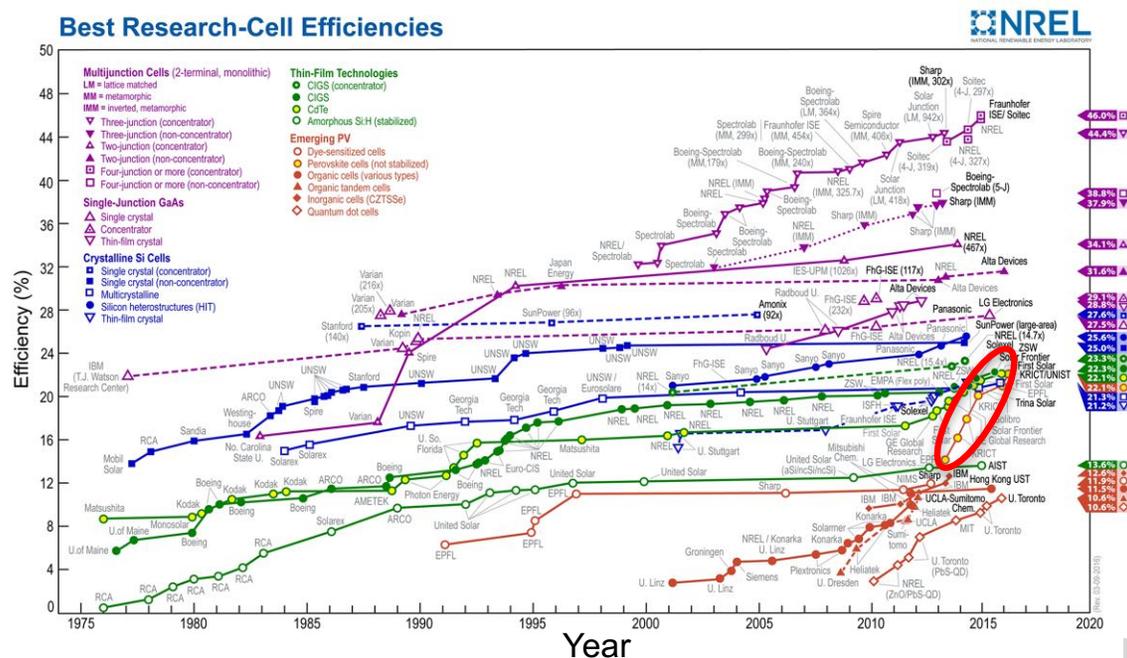| Sample	J_{sc} (mA/cm^2)
Unmodified	0.28 ± 0.011
C$_{18}$SH	0.42 ± 0.020
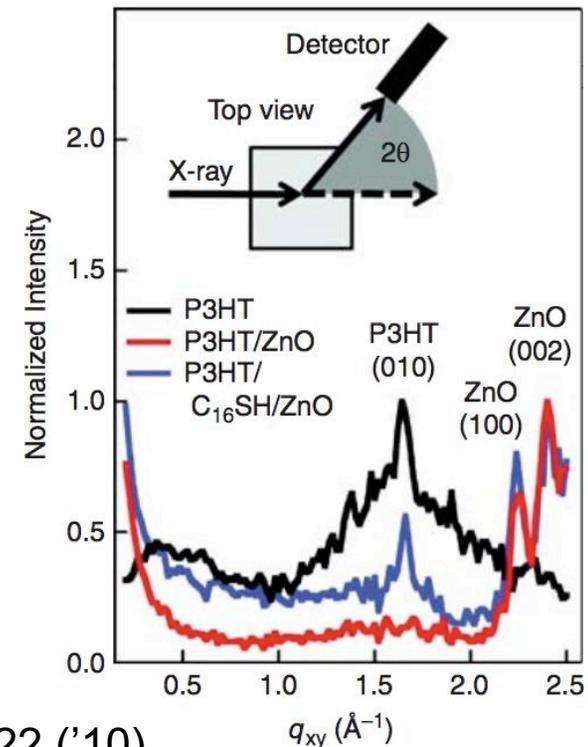
Hsu & Lloyd, *MRS Bulletin* **35**, 422 ('10)

Photoexcited Carriers in MAPbI$_3$

- **Organometal halide perovskites (*e.g.* methylammonium lead iodide, CH$_3$NH$_3$PbI$_3$ or MAPbI$_3$) for solar cells with high power conversion efficiency > 20%**

  [Stranks & Snaith, *Nat. Nanotechnol.* **10**, 391 ('15)]

Quasi-electron   Quasi-hole   H, C, N, I, Pb

- **Nonabiabatic QMD simulation**
  Pb & I sublattices act as disjunct pathways for rapid & balanced transport of free electrons & holes—electron (63% Pb-6p) & hole (90% I-5p);
  diffusion coefficients $D_e = (1.16\pm0.31)\times10^{-2}$ cm^2/s & $D_h = (1.01\pm0.42)\times10^{-2}$ cm^2/s

  Expt: $D_e = (1.7\pm1.1)\times10^{-2}$ cm^2/s & $D_h = (1.1\pm0.7)\times10^{-2}$ cm^2/s [Stranks *et al.*, *Science* **342**, 341 ('13)]
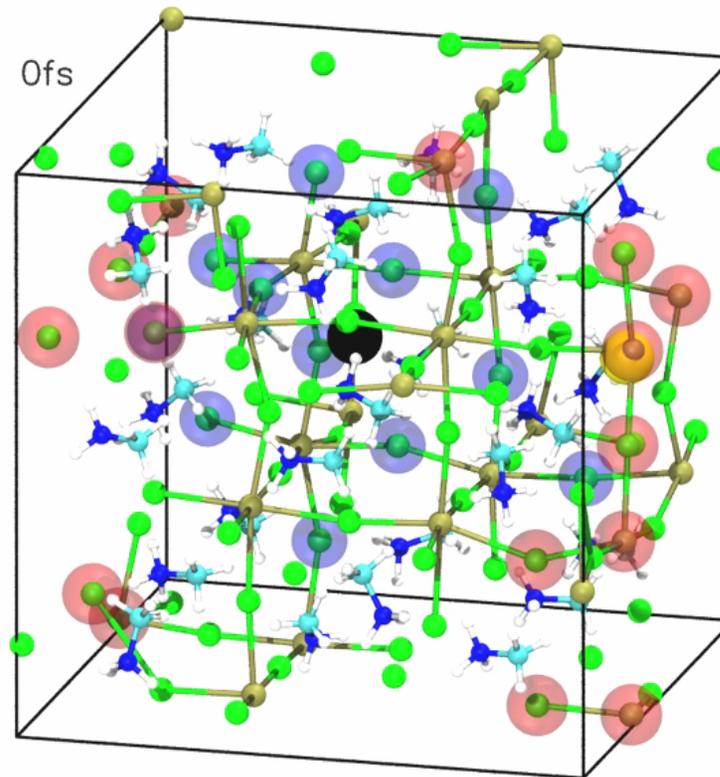
Rapid & Balanced Carrier Transport

- **Separate electron & hole express lanes are the key nanostructural feature for rapid & balanced carrier transport: $D_e = (1.16 \pm 0.31) \times 10^{-2}$ cm²/s & $D_h = (1.01 \pm 0.42) \times 10^{-2}$ cm²/s**

  Expt: $D_e = (1.7 \pm 1.1) \times 10^{-2}$ cm²/s & $D_h = (1.1 \pm 0.7) \times 10^{-2}$ cm²/s [Stranks *et al.*, *Science* '13]

Mean-square displacements
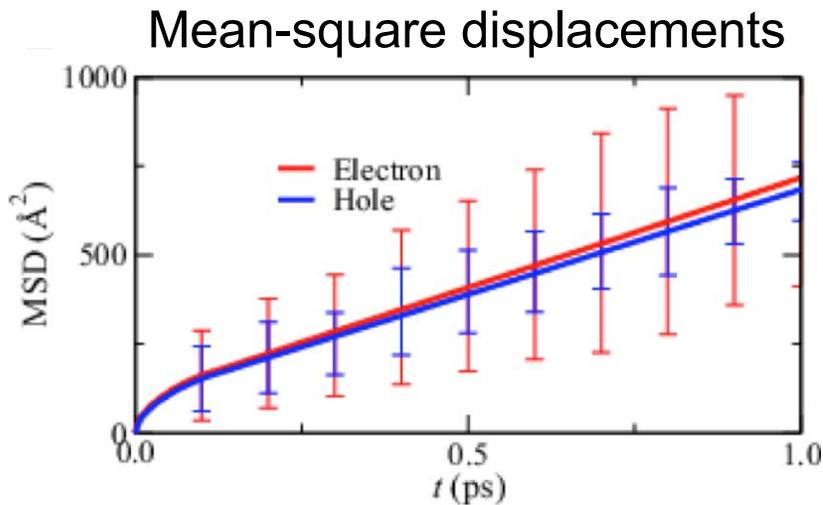
$$x_{\text{COM-PBC}} = \frac{L}{2\pi} \, \text{Im} \ln \int d\mathbf{r} \, |\psi(\mathbf{r})|^2 \exp(i\frac{2\pi}{L}x)$$

Electron
Electron COM
Hole
Hole COM
H, C, N, I, Pb

- **Small radiative recombination rate: $\tau^{-1}/\rho = (1.99 \pm 0.43) \times 10^{-12}$ cm³/s**

Hakamata *et al.*, *Sci. Rep.* **5**, 19599 ('16)

Screening Role of Methylammonium Sublattice

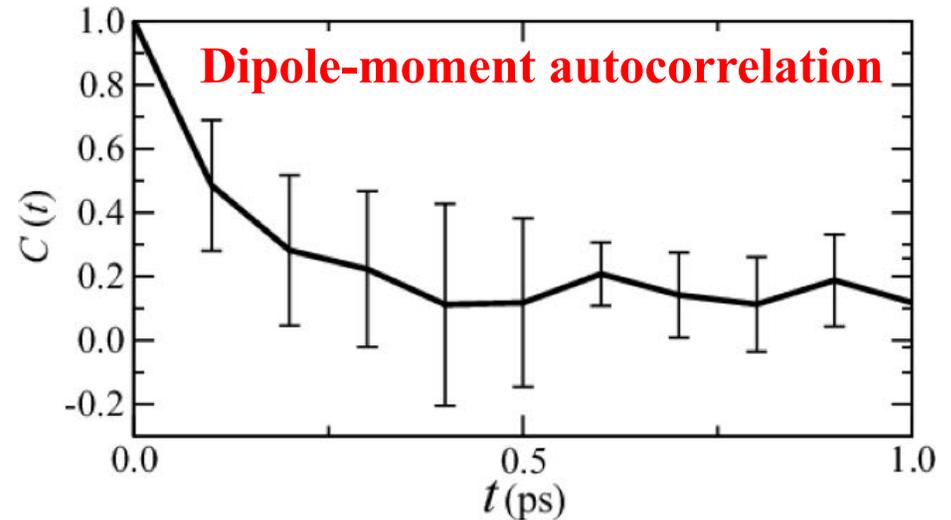**Dielectric constant**

Dipole-moment autocorrelation
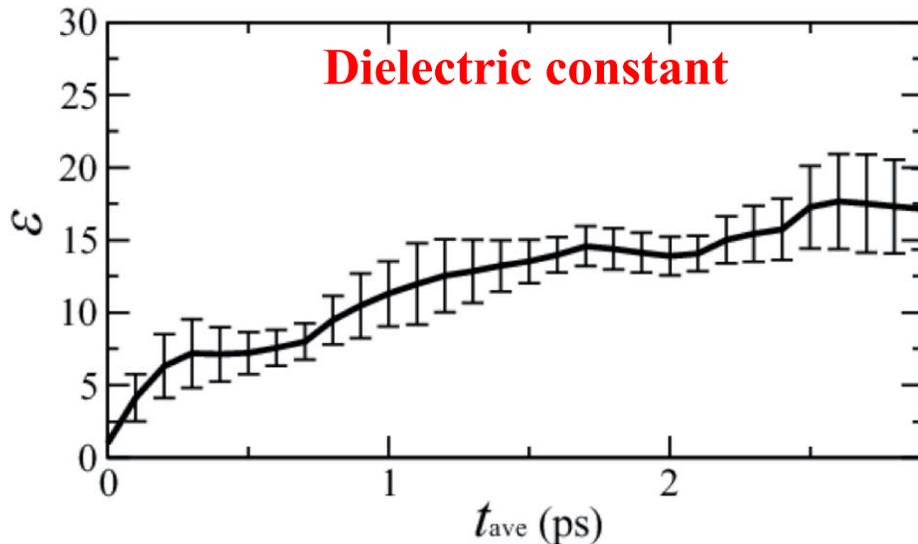
$$\varepsilon = 1 + \frac{4\pi}{3k_B TV}\left(\langle \mathbf{M}^2 \rangle - \langle \mathbf{M} \rangle^2\right)$$

time average

dipole moment

$$C(t) = \frac{\langle \mathbf{M}(t + t_0) \cdot \mathbf{M}(t_0) \rangle}{\langle \mathbf{M}(t_0) \cdot \mathbf{M}(t_0) \rangle}$$

Rapid response time ~ 1 ps

cf. $\varepsilon_{\text{expt}}$ (10^{12} Hz) = 7-10

cf. τ_{expt} = 2 ps

Lin *et al., Nat. Photonics* **9**, 106 ('15)

Deschler *et al., JPCL* **5**, 1421 ('15)

- **Large dielectric constant of MA sublattice causes small exciton binding energy, 0.012 ± 0.009 eV (experimental upper bound = 0.05 eV** [D'Innocenzo *et al., Nat. Commun.* **5**, 3586 ('14)]**)**

- **MA sublattice quickly screens out electrostatic electron-hole attraction to unbind an exciton & generate free carriers within 1 ps** [*cf.* Zhu *et al., Science* **353**, 1409 ('16)]

Hakamata *et al., Sci. Rep.* **5**, 19599 ('16)

MAterials Genome Innovation for Computational Software

Basic Energy Sciences

**Priya Vashishta-PI, Malancha Gupta, Rajiv K. Kalia, Aiichiro Nakano,
Oleg Prezhdo** *University of Southern California*
Uwe Bergmann and David Fritz *Linac Coherent Light Source, SLAC*
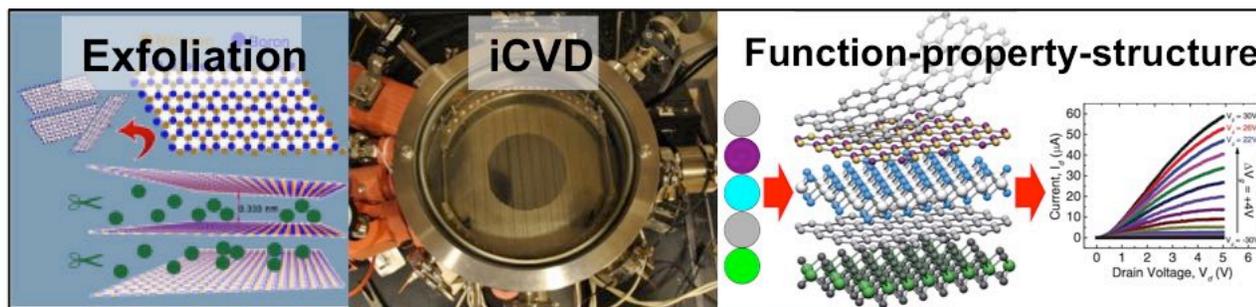**William A. Goddard, III** *California Institute of Technology*
Kristin A. Persson *Lawrence Berkeley National Laboratory*
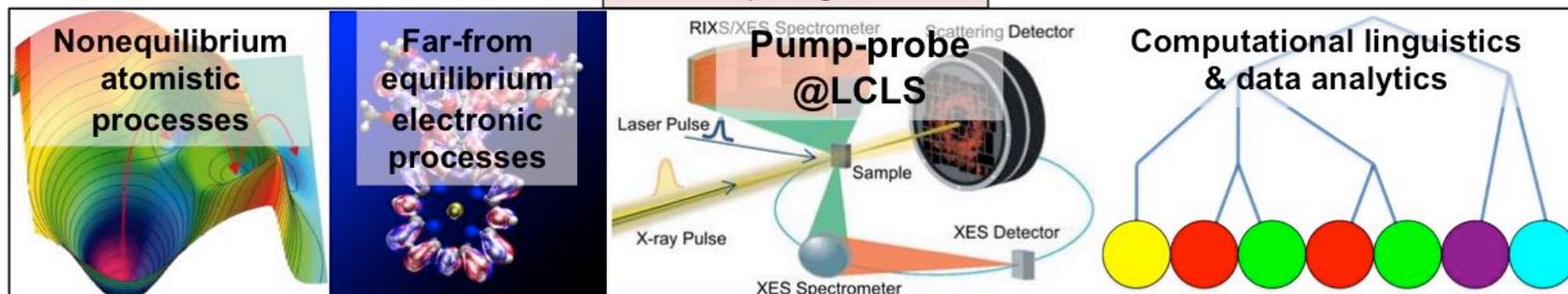**David J. Singh** *University of Missouri*
Pulickel M. Ajayan *Rice University*

Computational Synthesis of Functional Layered Materials: MAGICS Software Stack
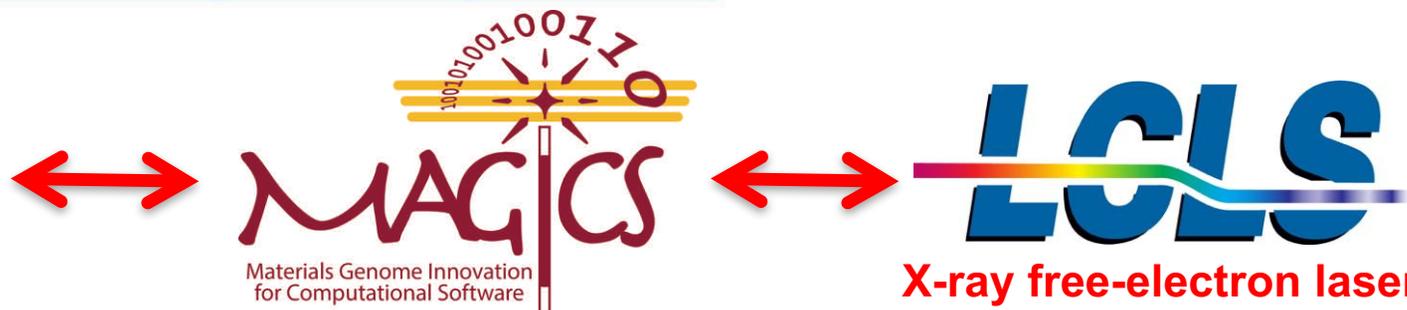
INCITE|AURORA–MAGICS–LCLS Synergy

Linac Coherent Light Source

World's first free-electron X-ray laser
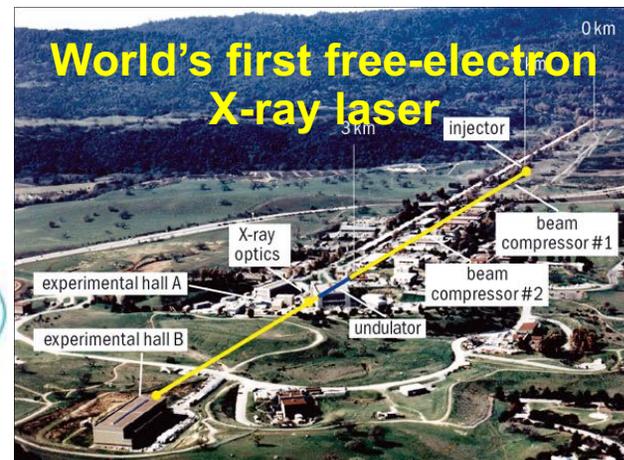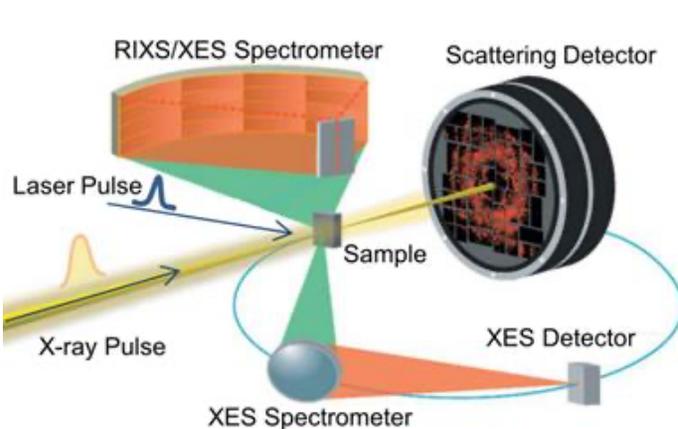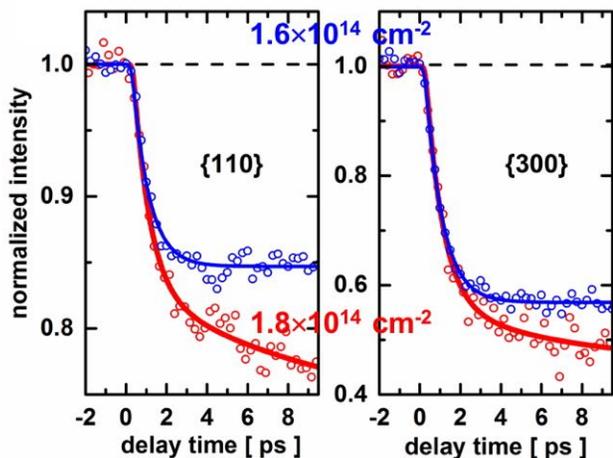
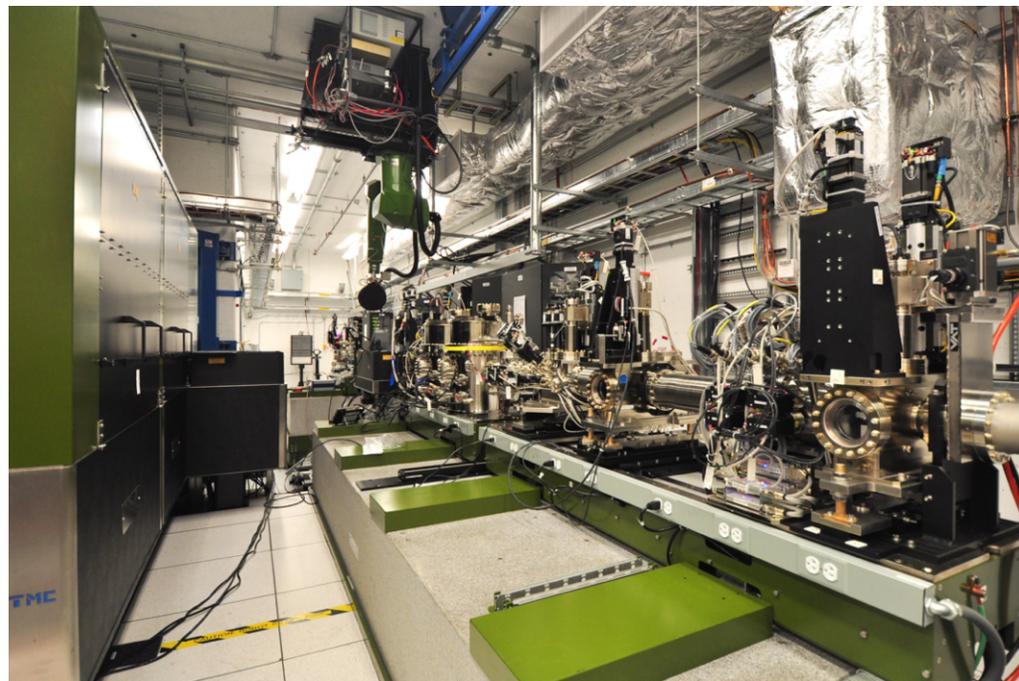**DOE INCITE & Aurora ESP Awards**
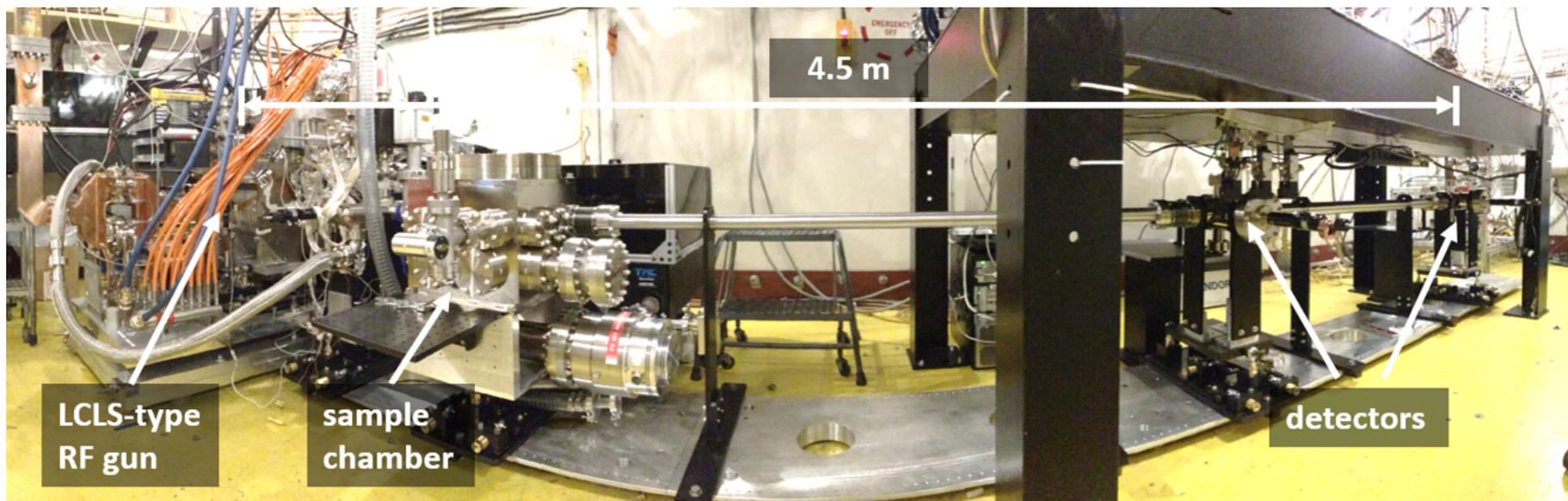
HOMO

LUMO
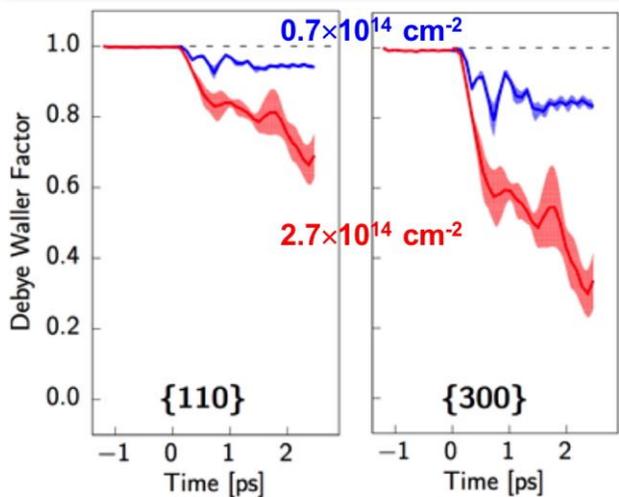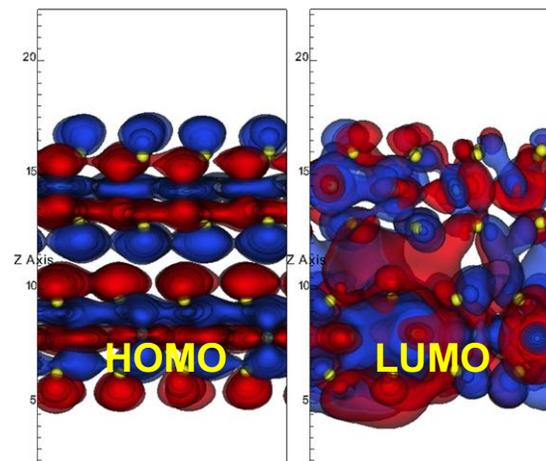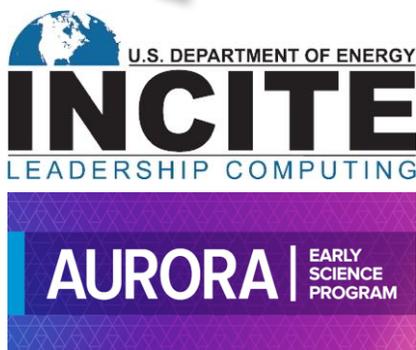
SLAC Ultrafast Pump-Probe Experiments

X-ray pump-probe (XPP)
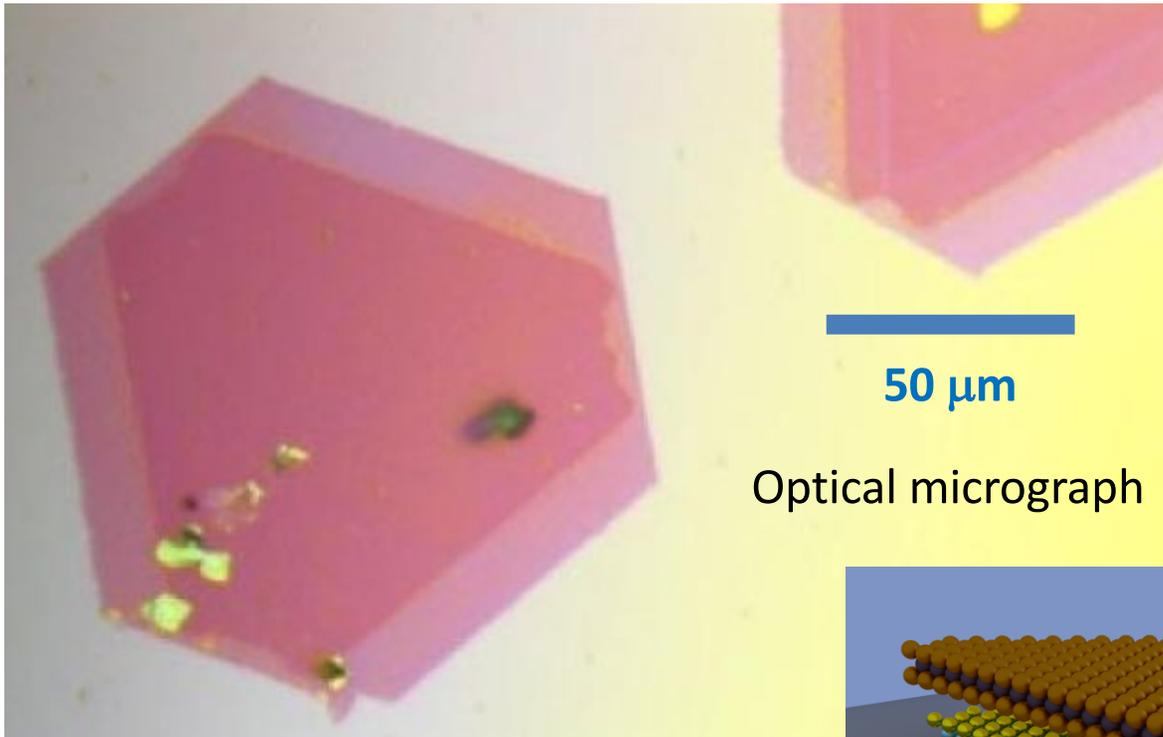**instrument: 4-25 KeV**

Ultrafast electron diffraction
(UED) instrument: 3-5 MeV

2D Transition Metal Dichalcogenide (TMDC)

- **Mono- and bi-layer MoSe$_2$ synthesized by the Rice group (P. Ajayan)**


50 μm

Optical micrograph

- **Question: What is the nature of optically induced lattice dynamics for photo-patterning (*e.g.*, semiconducting 2H to metallic 1T phases) of TMDC?**
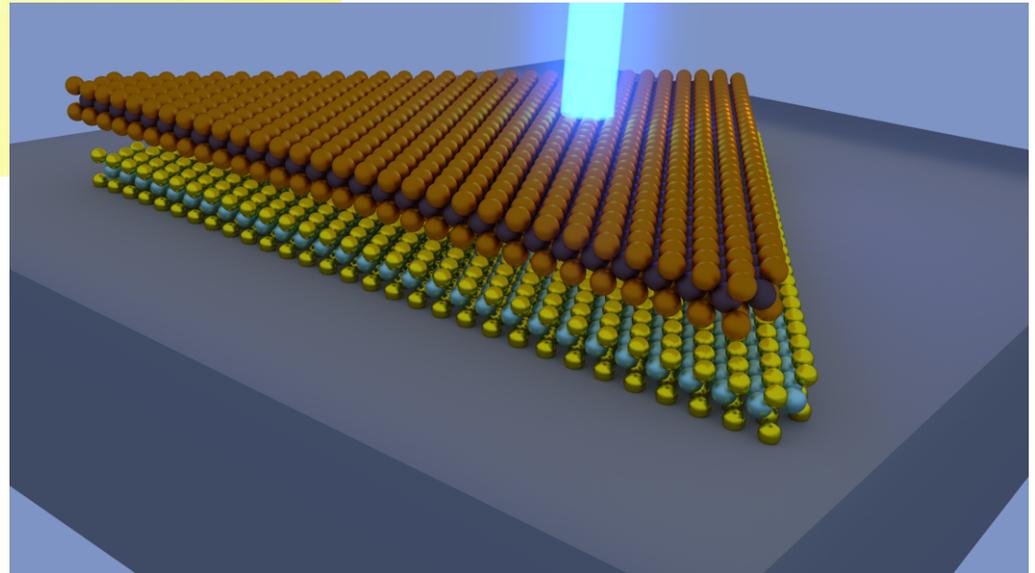
Ultrafast Coupled Electron-Lattice Dynamics

- **Ultrafast electron diffraction experiment shows nearly perfect energy conversion from electronic excitation to lattice motions within ps**

$$\exp(-\langle(\mathbf{q}\cdot\mathbf{u}(t))^2\rangle)$$
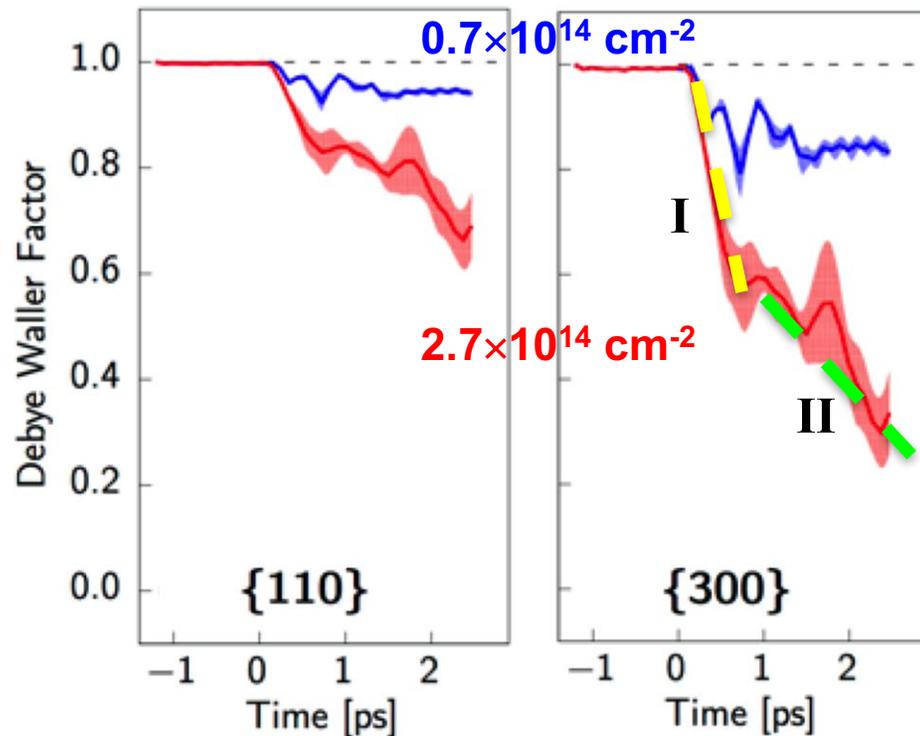
atomic displacement
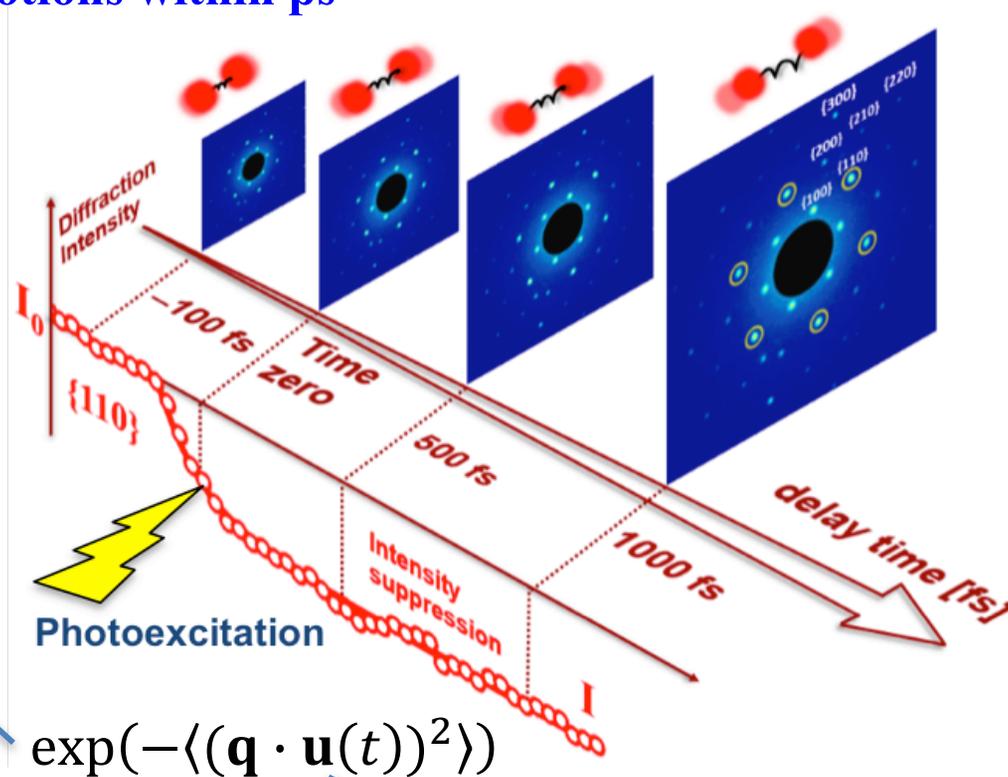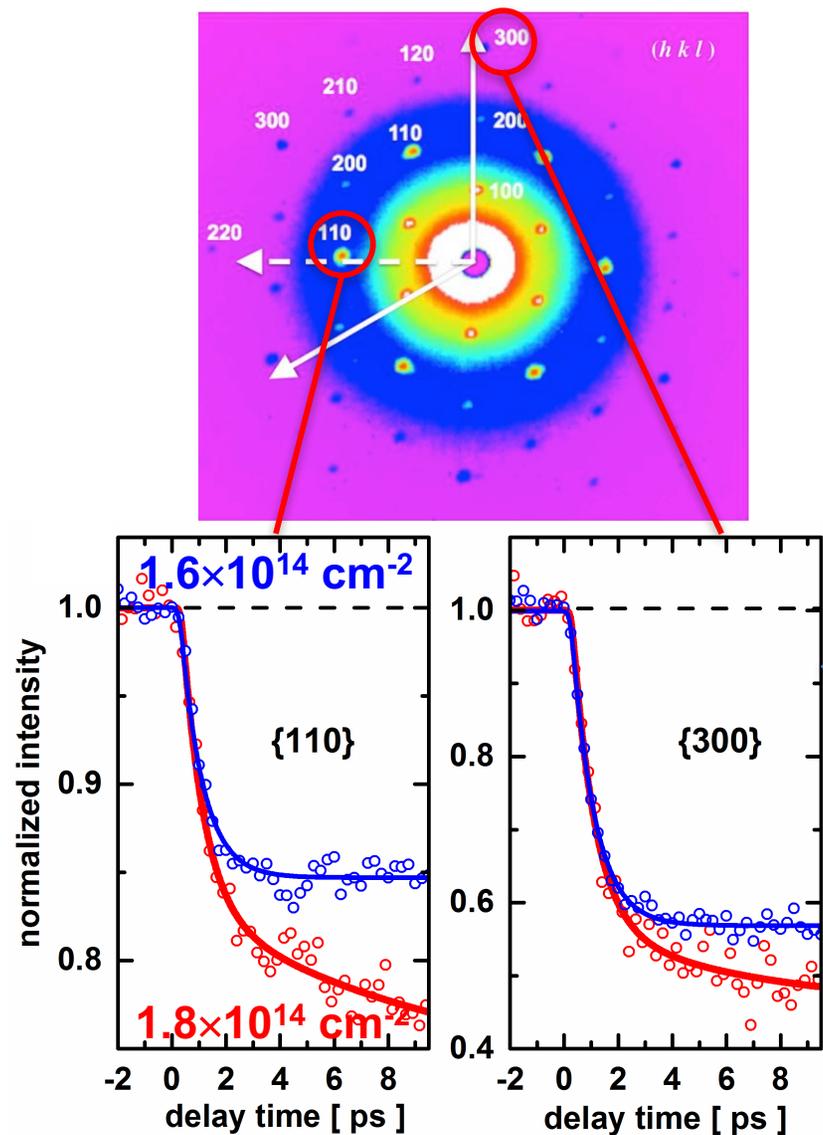
- **Dynamics of Debye-Waller factor reveals rapid disordering for both {300} & {110} peaks**

- **Transition from mono- to bi-exponential decay at higher electron-hole density**

M.F. Lin *et al.*, *Nature Commun.* **8**, 1745 ('17)

Strong Electron-Lattice Coupling

- **NAQMD simulations reproduce (1) rapid photo-induced lattice dynamics & (2) mono- to bi-exponential transition at higher electron-hole density**


Mo Se

0.7×10^{14} cm^{-2}

2.7×10^{14} cm^{-2}

I

II

{110}   {300}

Debye Waller Factor

Time [ps]   Time [ps]

0 cm^{-2} 0.6×10^{14} cm^{-2}

1.8×10^{14} cm^{-2} 3.0×10^{14} cm^{-2}

ω [cm^{-1}]

- **Rapid lattice dynamics is explained by the softening of M-point (1/2 0 0) phonon**
- **Bi-exponential transition is explained by the softening of additional phonon modes at higher electron-hole densities**

  M.F. Lin *et al.*, *Nature Commun.* **8**, 1745 ('17)
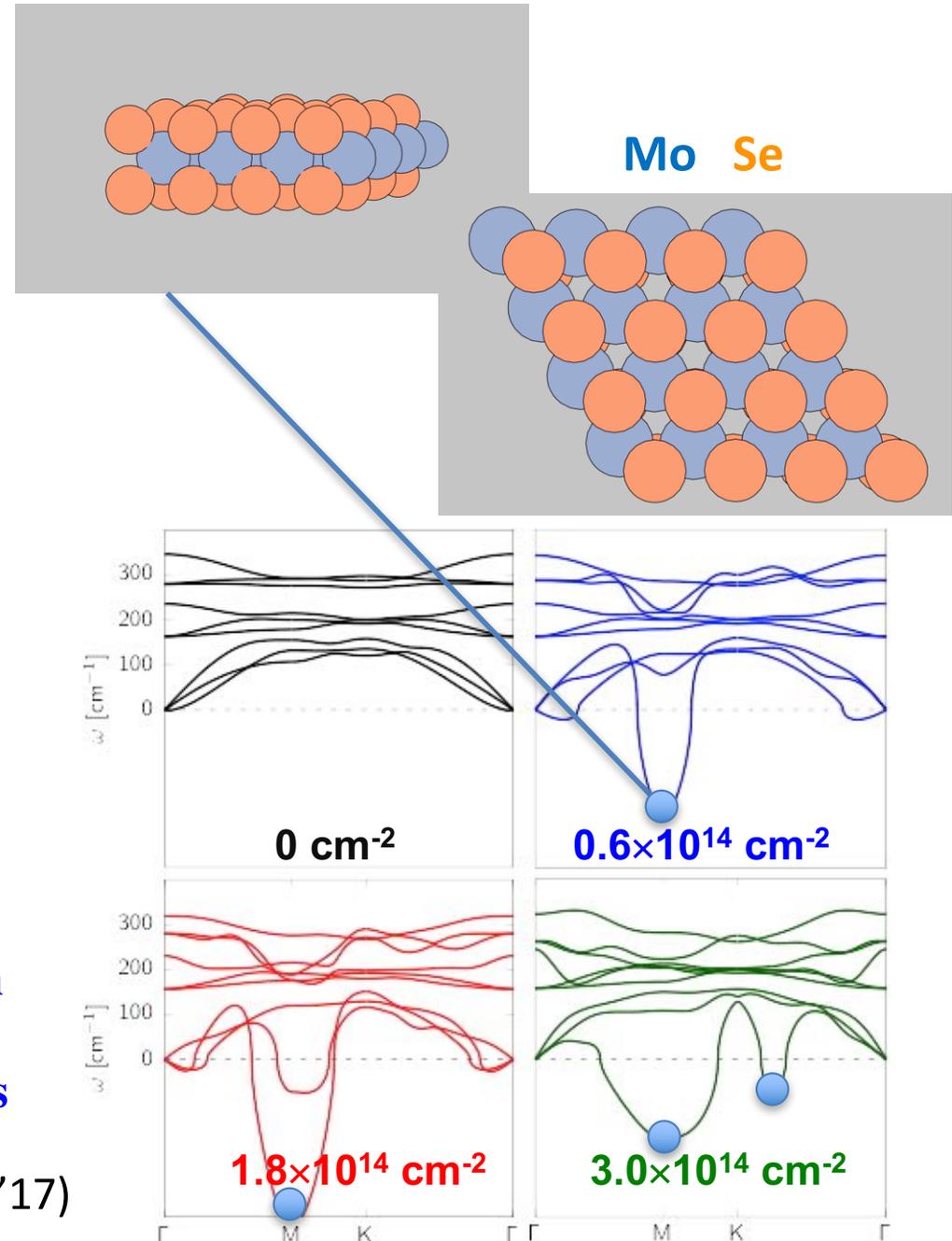
Electronic Origin of Phonon Softening

- **Electronic Fermi surface for the electron-hole density n(e-h) ranging from 0.2 to 2×10^{14} cm^{-2}**
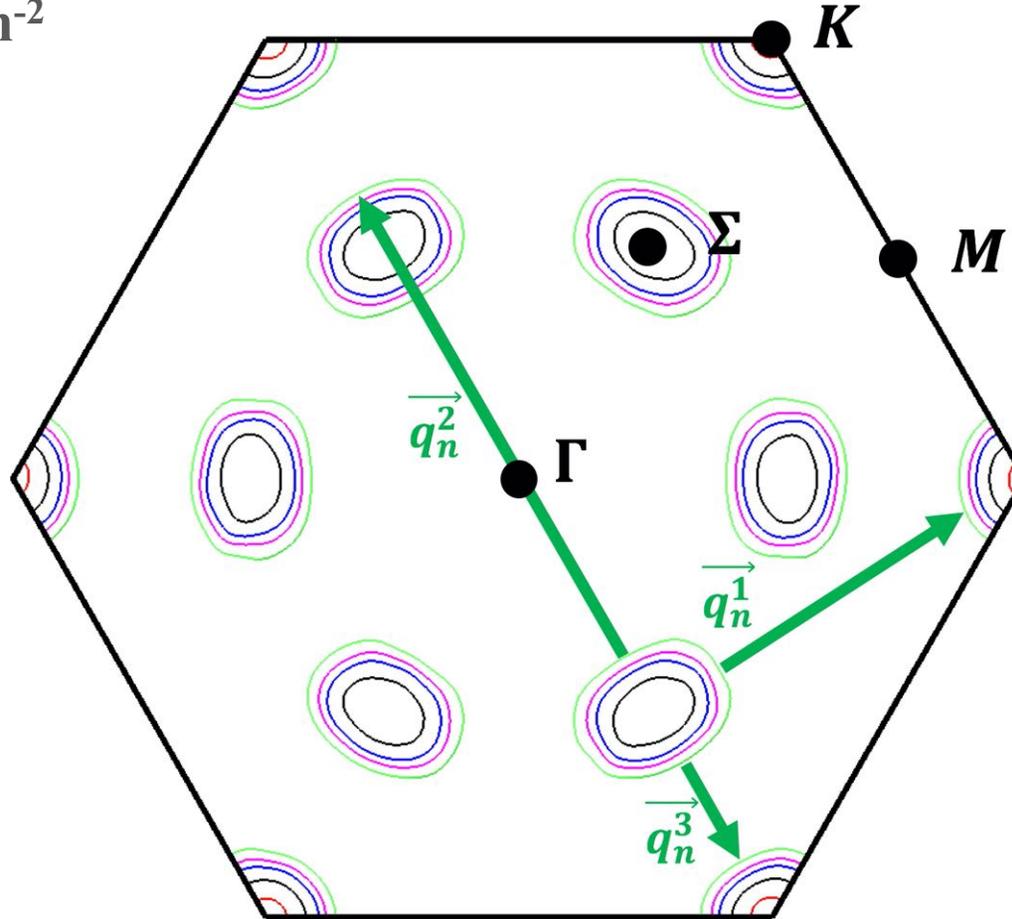
n(e-h) = 0.22, 1, 2, 3, 4 $\times10^{14}$ cm^{-2}

- **While the Fermi surface is localized at K-points at minimal excitation (red), it occupies Σ-pockets at larger n(e-h) (black & blue), enabling electron scattering by emitting $\vec{q}_n^1$ (M), $\vec{q}_n^2$ (Σ) and $\vec{q}_n^3$ (K) phonons**
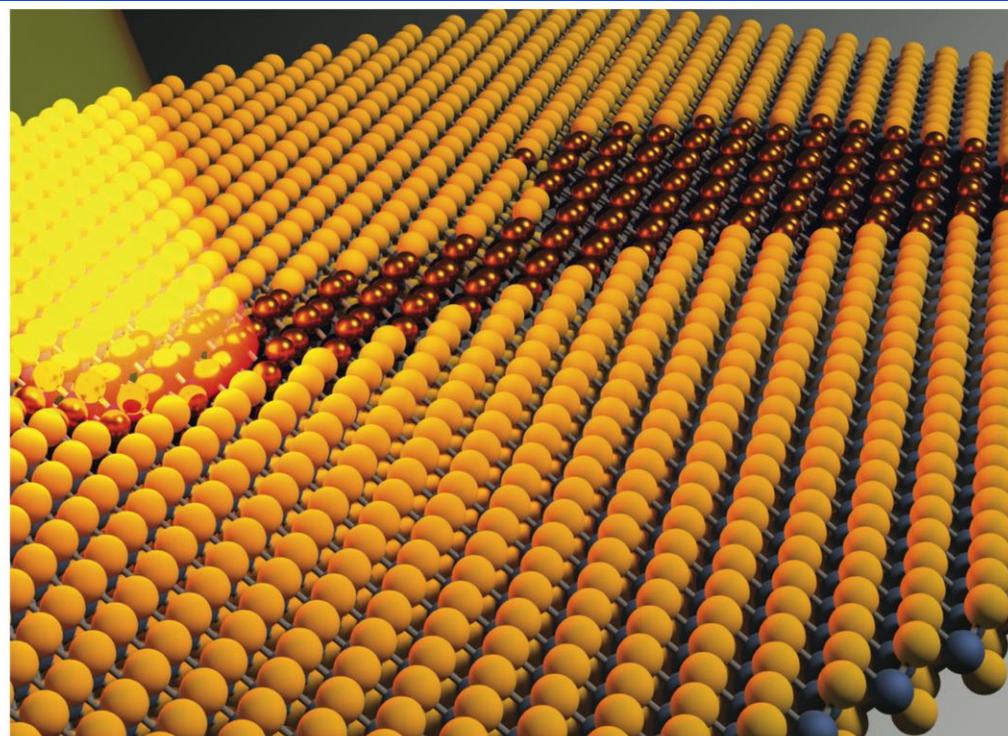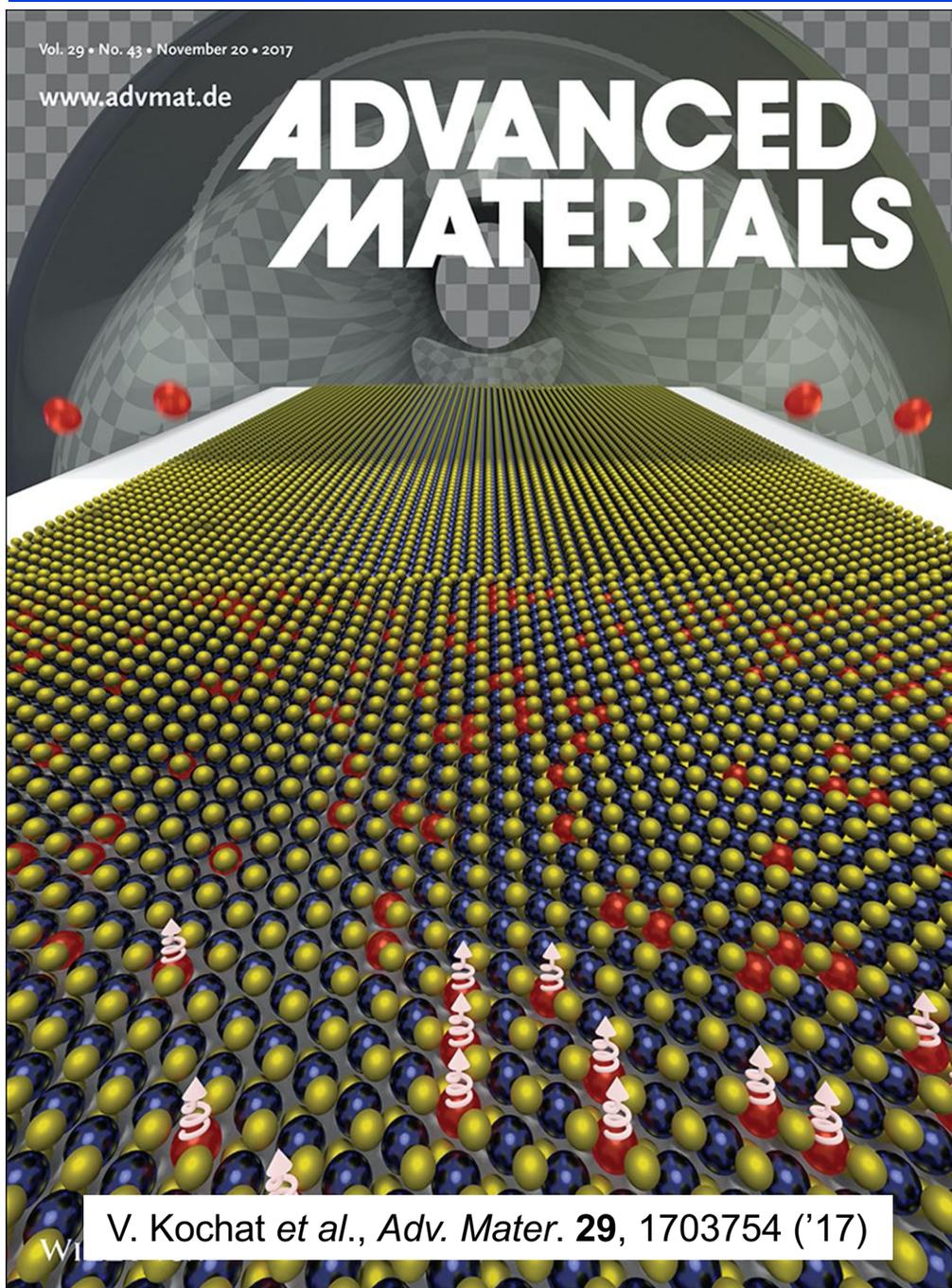
Simulation-Experiment Synergy
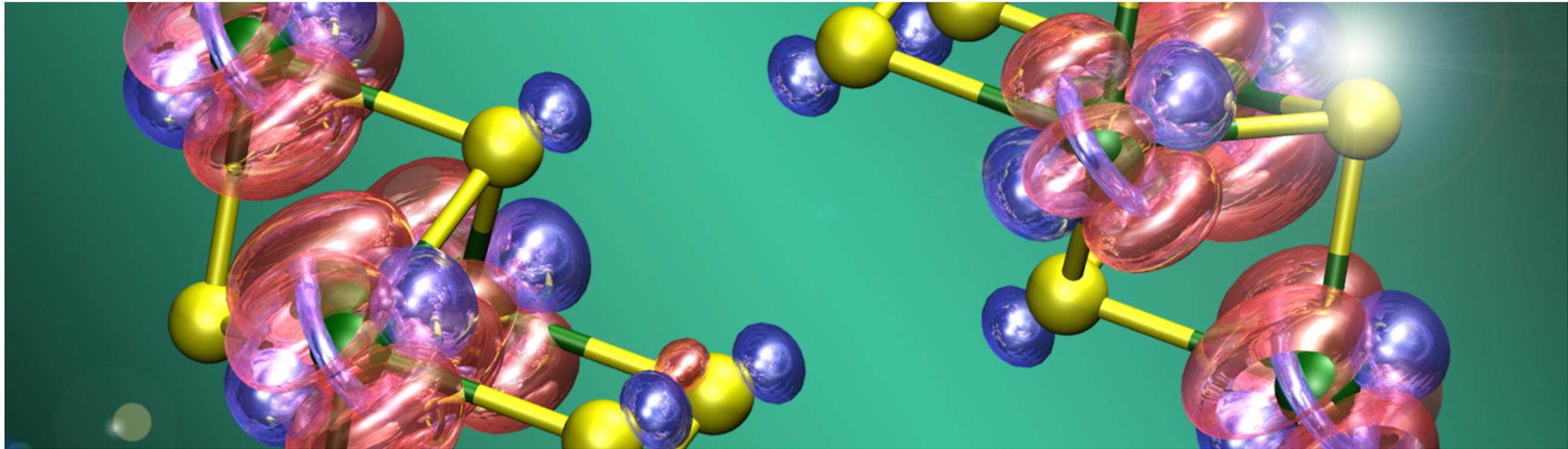
- **In the ultrafast 'electron camera,' laser light hitting a material is almost completely converted into nuclear vibrations — key to switching material properties on & off at will for future electronics applications**

- **High-end quantum simulations reproduce the ultrafast energy conversion at exactly the same space & time scales, & explain it as a consequence of photo-induced phonon softening**

M.F. Lin *et al., Nature Commun.* **8,** 1745 ('17)
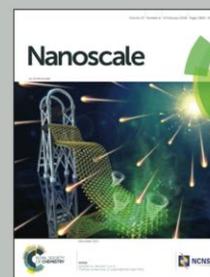
MAGICS QMD Simulations

A. Krishnamoorthy *et al.*, *Nanoscale* **10**, 2742 ('18)

V. Kochat *et al.*, *Adv. Mater.* **29**, 1703754 ('17)

ROYAL SOCIETY OF CHEMISTRY

rsc.li/nanoscale

Registered charity number: 207890

Many-Body Excited States

- **Surface-hopping NAQMD with adiabatic Kohn-Sham basis does not represent many-body excited states such as an exciton (*i.e.*, electron-hole pair bound by electrostatic attraction)**

- **Linear-response time-dependent density-functional theory (LR-TDDFT) obtains many-body electronic excition energies as poles of the frequency-dependent electron-hole-pair response function** [Casida, '95]

Excitonic Effects: LR-TDDFT

- **Excited electron-hole pairs within the linear-response time-dependent density functional theory (LR-TDDFT)**

$$\delta V(t) = \delta v_{kl\tau}(t)\hat{a}^+_{k\tau}\hat{a}_{l\tau} \longrightarrow \delta P_{ij\sigma}(t) = \delta\langle\Phi(t)|\hat{a}^+_{i\sigma}\hat{a}_{j\sigma}|\Phi(t)\rangle$$

$$\chi_{ij\sigma,kl\tau}(t-t') = \delta P_{ij\sigma}(t)/\delta v_{kl\tau}(t')$$

electron   hole

- **Excitation energies from the poles of the response function** $\chi_{ij\tau,kl\sigma}(\omega)$

$2N_{\text{unoccupied}}N_{\text{occupied}} \times 2N_{\text{unoccupied}}N_{\text{occupied}}$ **matrix eigenequation**

$$\begin{pmatrix} \mathbf{A} & \mathbf{B} \\ \mathbf{B}^* & \mathbf{A}^* \end{pmatrix}\begin{pmatrix} \mathbf{X}_I \\ \mathbf{Y}_I \end{pmatrix} = \hbar\omega_I \begin{pmatrix} \mathbf{1} & \mathbf{0} \\ \mathbf{0} & \mathbf{-1} \end{pmatrix}\begin{pmatrix} \mathbf{X}_I \\ \mathbf{Y}_I \end{pmatrix}$$

I-th excitation energy

Kohn-Sham energy

$$A_{ia\sigma,jb\tau} = \delta_{\sigma,\tau}\delta_{i,j}\delta_{a,b}\left(\varepsilon_{a\sigma}-\varepsilon_{i\sigma}\right) + K_{ia\sigma,jb\tau} \qquad B_{ia\sigma,jb\tau} = K_{ia\sigma,bj\tau}$$

$$K_{ia\sigma,i'a'\sigma'} = \iint \psi^*_{i\sigma}(\mathbf{r})\psi_{a\sigma}(\mathbf{r})\left(\frac{e^2}{|\mathbf{r}-\mathbf{r}'|}+\frac{\delta^2 E_{\text{xc}}}{\delta\rho_\sigma(\mathbf{r})\delta\rho_{\sigma'}(\mathbf{r}')}\right)\psi_{i'\sigma'}(\mathbf{r}')\psi^*_{a'\sigma'}(\mathbf{r}')\,d\mathbf{r}\,d\mathbf{r}'$$

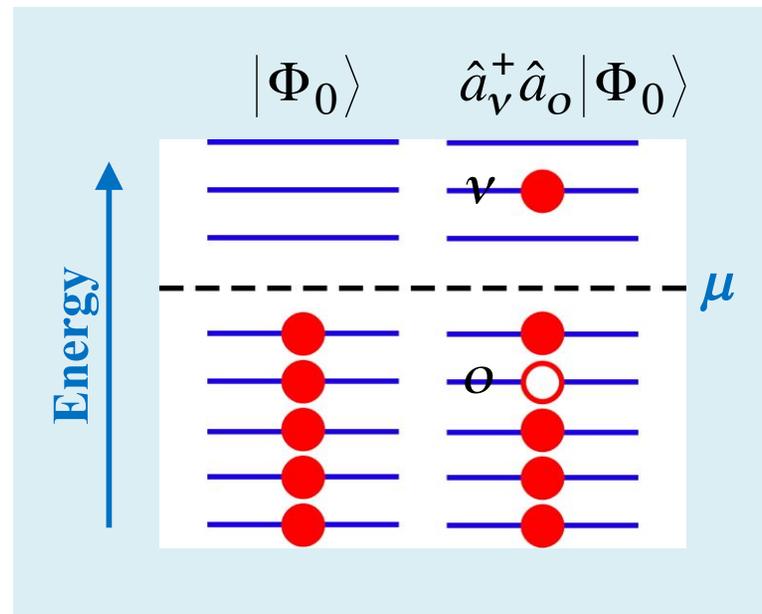**Coulomb & exchange-correlation interaction matrix elements**

Electronic Excited States

- ***I*-th excited state**

$$\left|\Phi_I(\mathbf{r};\mathbf{R})\right\rangle = \sum_{i\in\{\text{occupied}\}} \sum_{a\in\{\text{unoccupied}\}} \sum_{\sigma} \sqrt{\frac{\varepsilon_{a\sigma}-\varepsilon_{i\sigma}}{\hbar\omega_I}}\left(X_{I,ia\sigma}+Y_{I,ia\sigma}\right)\hat{a}_{a\sigma}^+\hat{a}_{i\sigma}\left|\Phi_0(\mathbf{r};\mathbf{R})\right\rangle$$

electron-hole pair   **ground state**

See notes on (1) general time-dependent perturbation, (2) density response with time-dependent Kohn-Sham basis, (3) Fourier transform of step function, (4) excitation energies by LR-TDDFT, (5) many-body wave function

Many-Body Effects: Excitons

- **Incorporating exact-exchange is indispensable for LR-TDDFT to describe $1/R$ binding energy of charge-transfer excitation (where electron moves from a donor to a spatially separated acceptor)**

- **Exchange integral is responsible for the $1/R$ attraction**
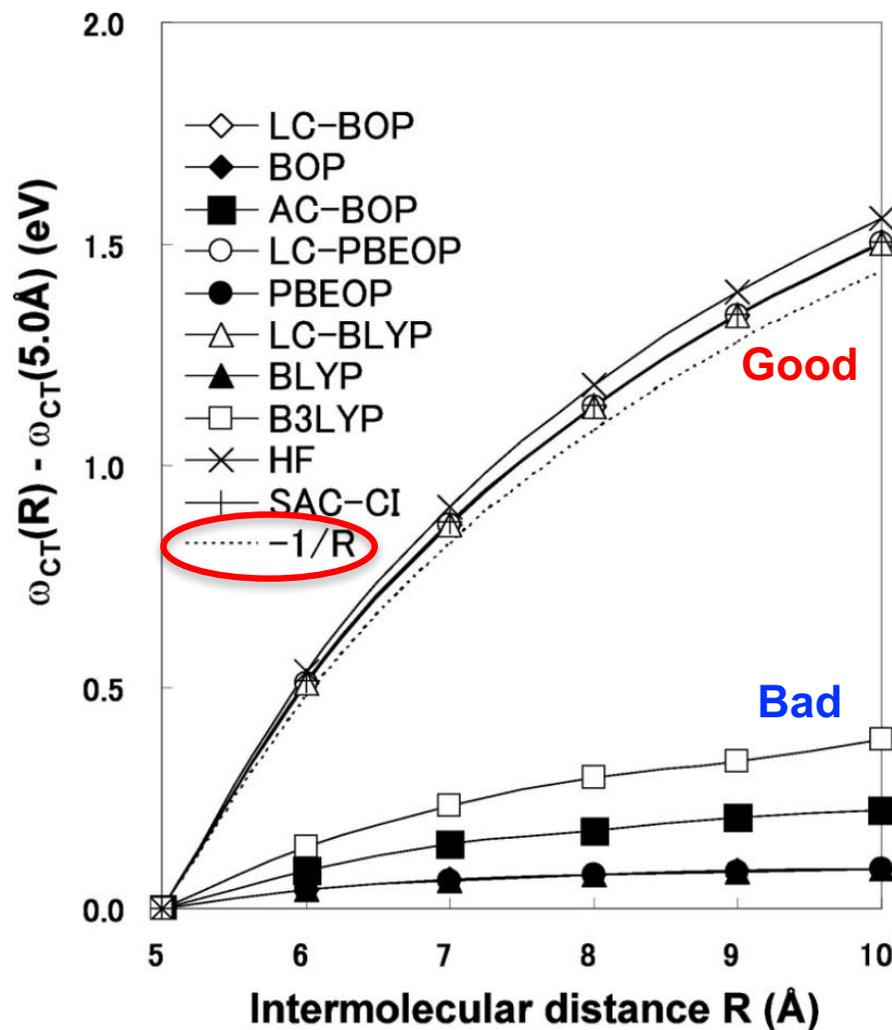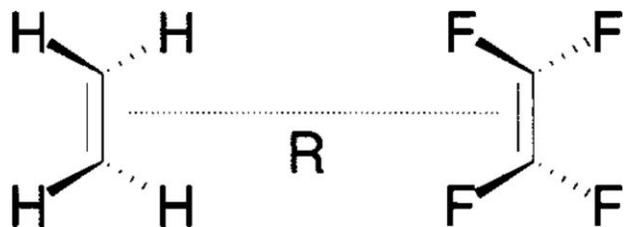
Dreuw *et al.*, *J. Chem. Phys*. **119**, 2943 ('03); Tawada *et al.*, *J. Chem. Phys*. **120**, 8425 ('04)

See notes on (1) range-separated exact-exchange functional,
(2) excited-state forces, (3) excitation-energy balance sheet

Accelerating Exact-Exchange Computation

- **Exact-exchange computation is highly compute-intensive: $O(N^5)$**

$$(si|it) = \int d\mathbf{r}_1 \int d\mathbf{r}_2 \phi_s^*(\mathbf{r}_1)\phi_i(\mathbf{r}_1)|\mathbf{r}_1 - \mathbf{r}_2|^{-1}\phi_i^*(\mathbf{r}_2)\phi_t(\mathbf{r}_2)$$

- **Resolution-of-identity (ROI, closure by projection to a small augmenting basis set) or density-fitting approach reduces its computation to $O(N^4)$**
  Weigend, *Phys. Chem. Chem. Phys.* **4**, 4285 ('02)

$$(si|it) \cong \sum_{P,Q}(si|P)(P|Q)^{-1}(Q|it)$$

- **Adaptive compression (or low-rank tensor product) to reduce the complexity to near GGA-type computation?**
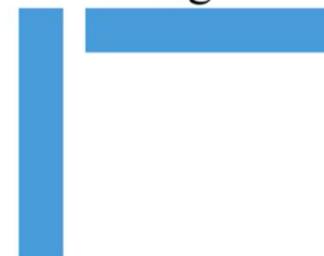 Lin, *J. Chem. Theory Comput.* **12**, 2242 ('16)

Uncompressed Exchange

Same accuracy

Adaptively Compressed Exchange

Full rank
Cost:
Hybrid $\gg$ GGA

Low rank
Cost:
Hybrid $\approx$ GGA

Application: Optical Absorption Spectrum

- **Oscillator strength calculated by the linear-response TDDFT**

Poralizability:
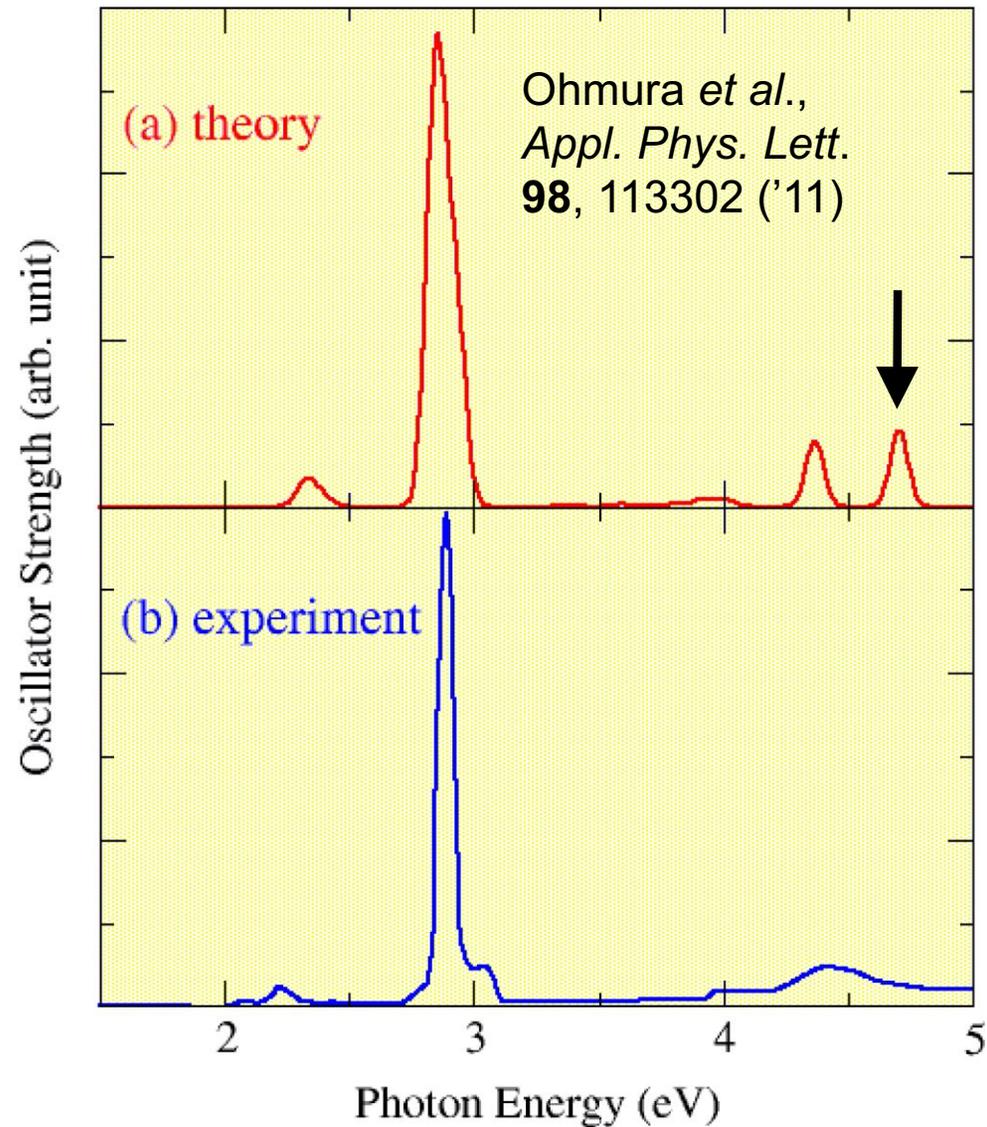
$$\alpha(\omega) = \sum_I \frac{f_I}{\omega - \omega_I}$$

I-th excitation energy

Oscillator strength:

$$f_I = \frac{2\omega_I}{3} \sum_{\alpha = x,y,z} |\langle 0|\hat{\alpha}|I\rangle|^2$$

I-th excited state

(a) theory

Ohmura *et al.*, *Appl. Phys. Lett.* **98**, 113302 ('11)

(b) experiment

Oscillator Strength (arb. unit)

Photon Energy (eV)
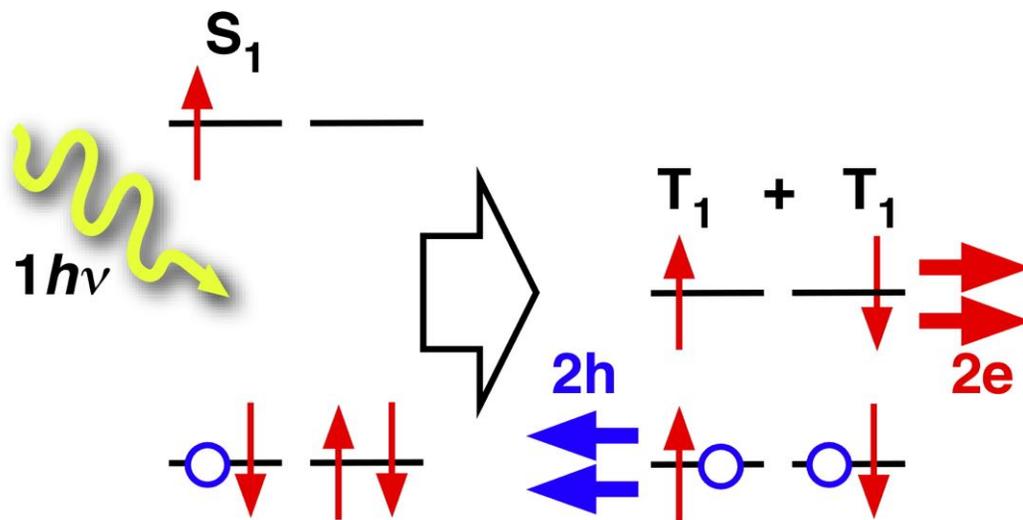
- **Excellent agreement with experimental data** [Akai *et al.*, '06]
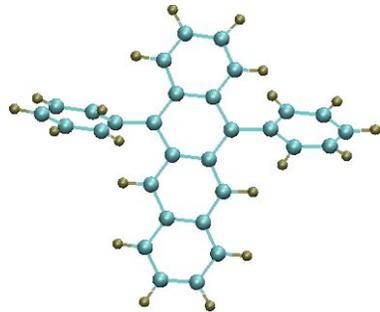
Singlet Fission in Amorphous DPT

- **Photo-current doubling by splitting a singlet exciton into 2 triplet excitons**

- **Singlet fission (SF) in mass-produced disordered organic solid → efficient low-cost solar cells**

- **Exp'l breakthrough: SF found in amorphous diphenyl tetracene (DPT)**

- **Ultrafast transient absorption measurements identified *two time scales* (1 & 100 ps) for exciton population dynamics**

- **Hypothesis: Existence of *SF hot spots* [S. T. Roberts *et al.*, *JACS* 134, 6388 ('12)]**
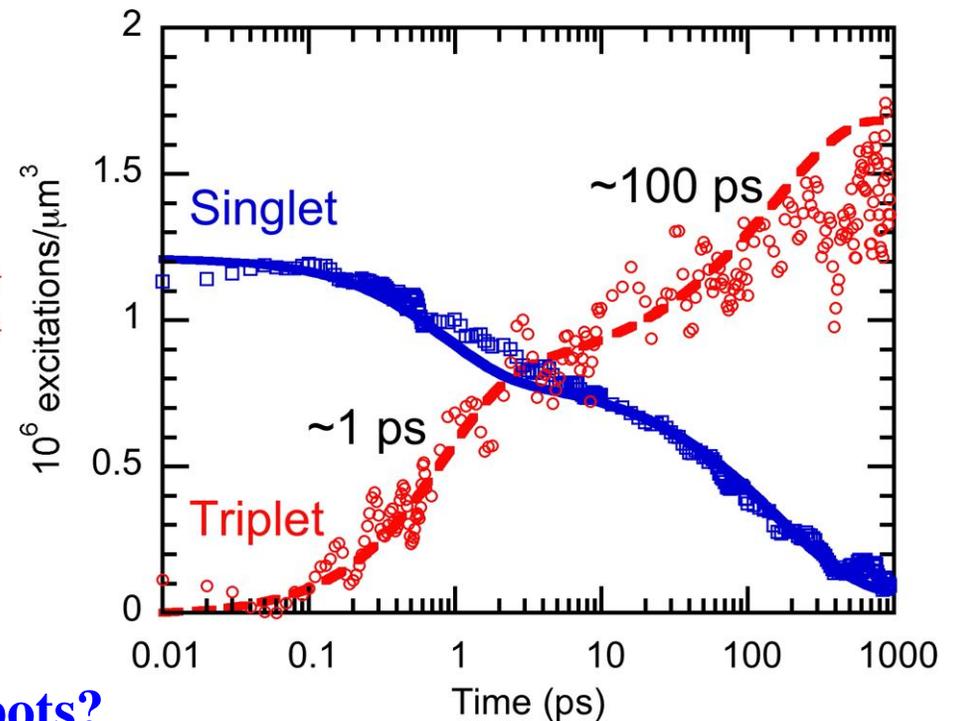
- **Problem: *Molecular origin* of SF hot spots?**
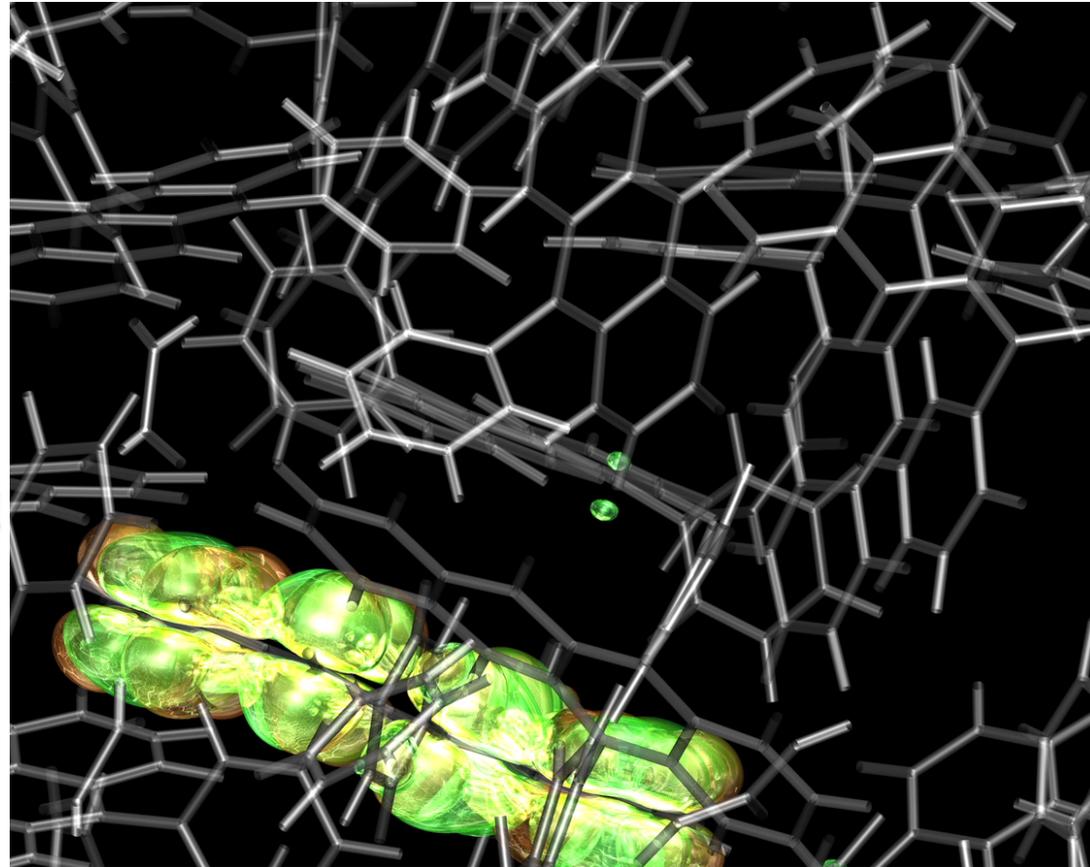
Singlet Fission in Amorphous DPT

- **Photo-current doubling by splitting a singlet exciton into 2 triplet excitons**
- **Singlet fission in mass-produced disordered organic solid → efficient low-cost solar cells**
- **Experimental breakthrough: SF found in amorphous diphenyl tetracene (DPT)**
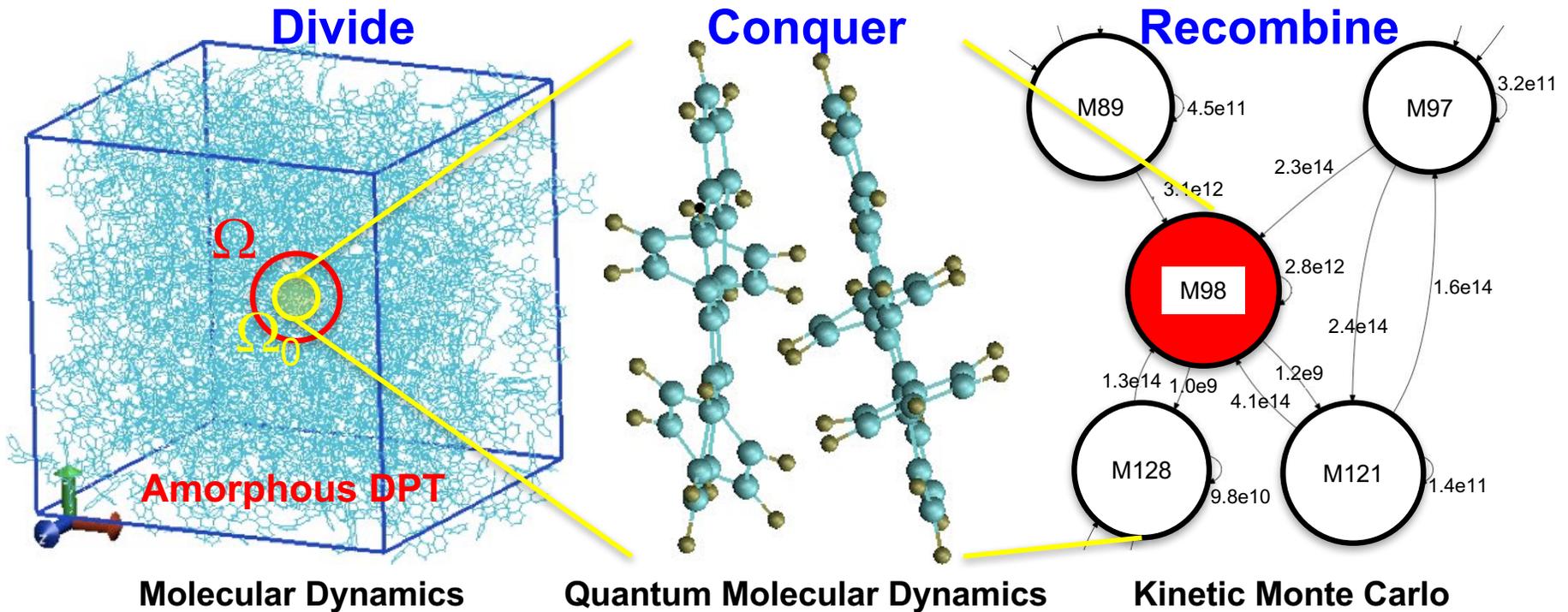

DPT molecule
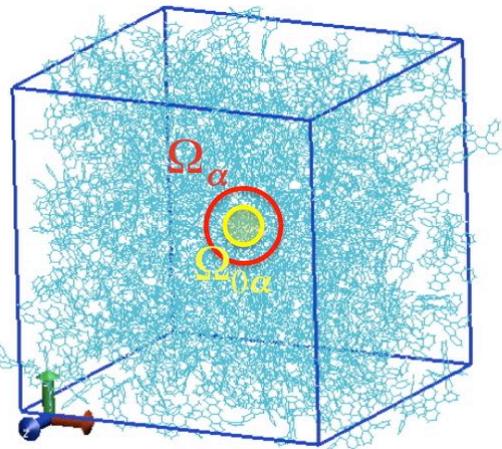
Amorphous DPT
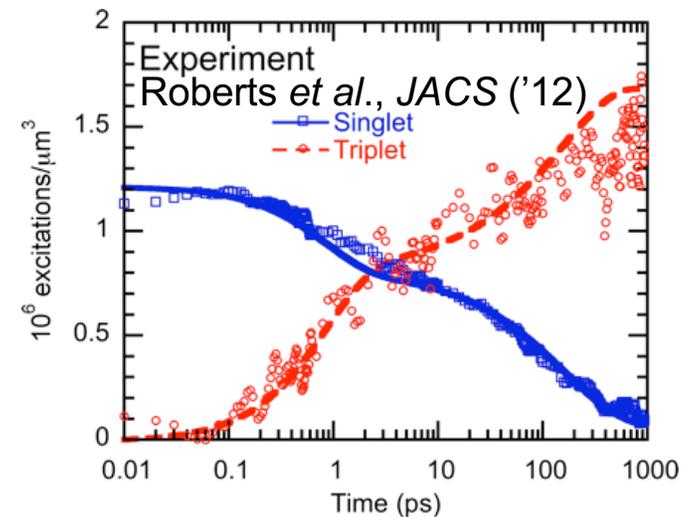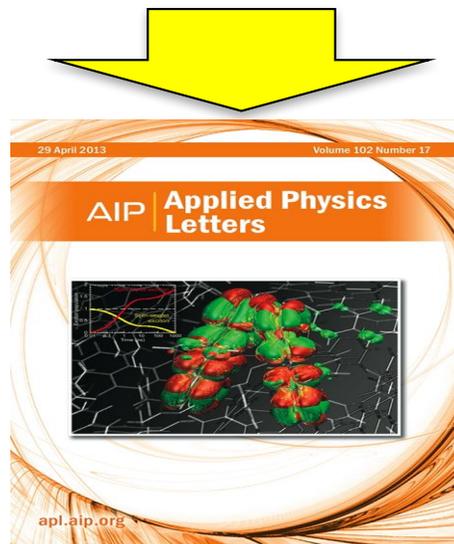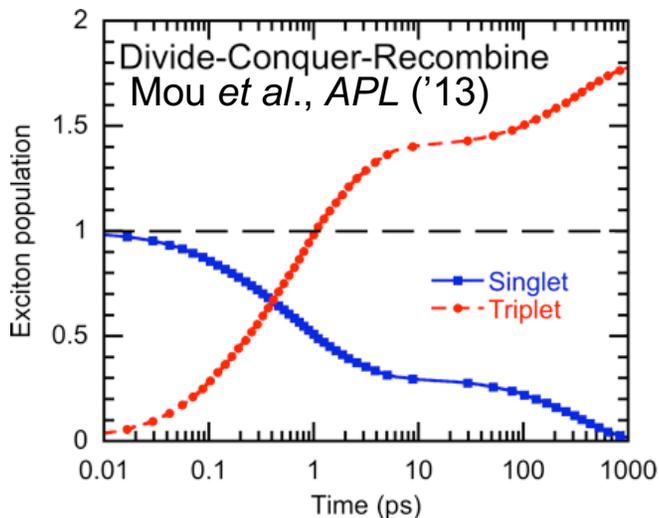
Quasi-electron

Quasi-hole

- **Divide-conquer-recombine nonadiabatic QMD (phonon-assisted exciton dynamics) + time-dependent perturbation theory (singlet-fission rate) + kinetic Monte Carlo calculations of exciton population dynamics in 6,400-atom amorphous DPT**
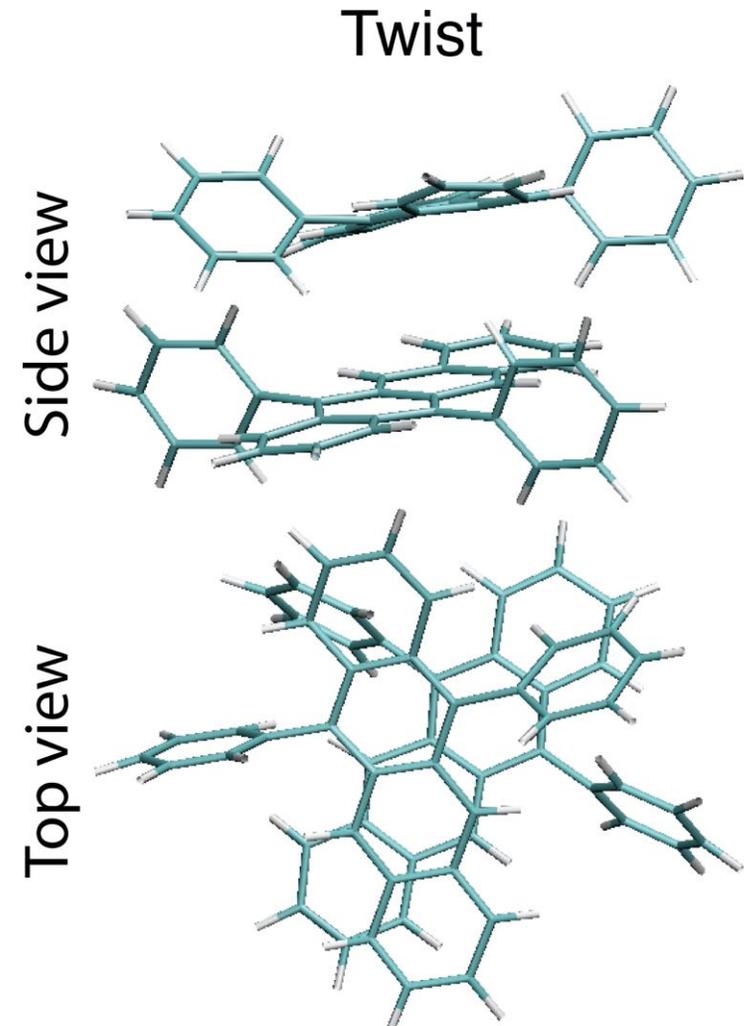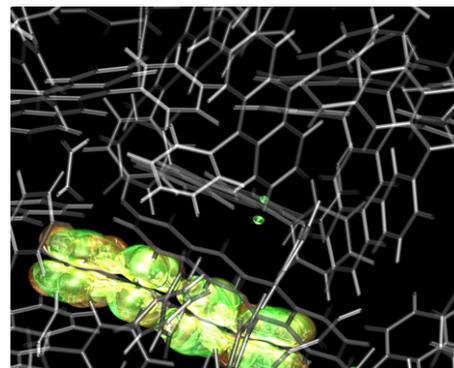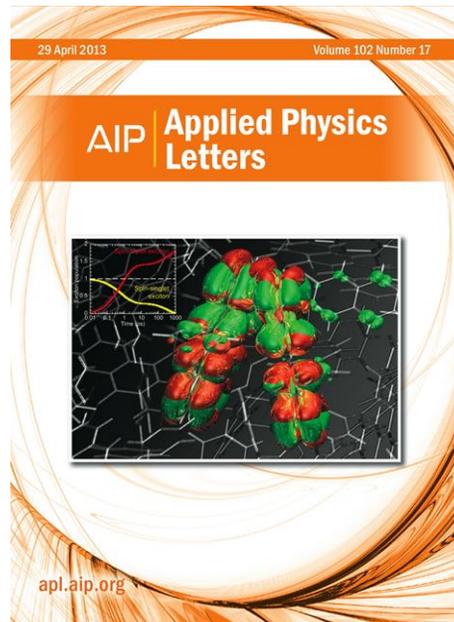
Divide-Conquer-Recombine Electronic Excitation

Divide **Conquer** **Recombine**

Amorphous DPT

Molecular Dynamics **Quantum Molecular Dynamics** **Kinetic Monte Carlo**

Experimental Length & Time Scales

Divide-Conquer-Recombine
Mou *et al.*, APL ('13)

29 April 2013 Volume 102 Number 17

AIP | **Applied Physics Letters**

apl.aip.org

Experiment
Roberts *et al.*, JACS ('12)
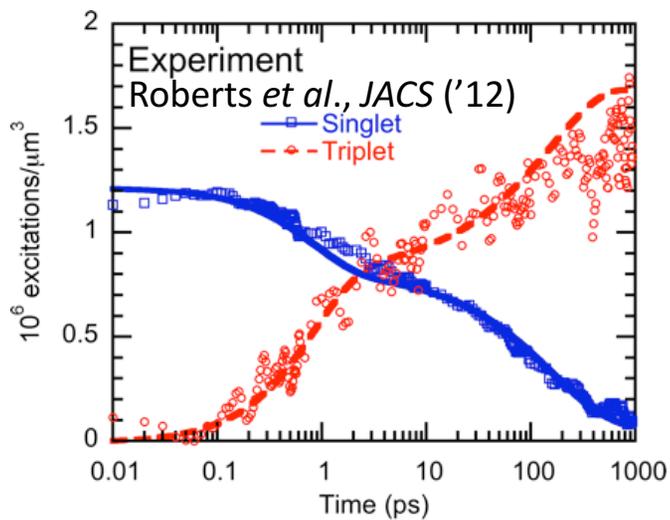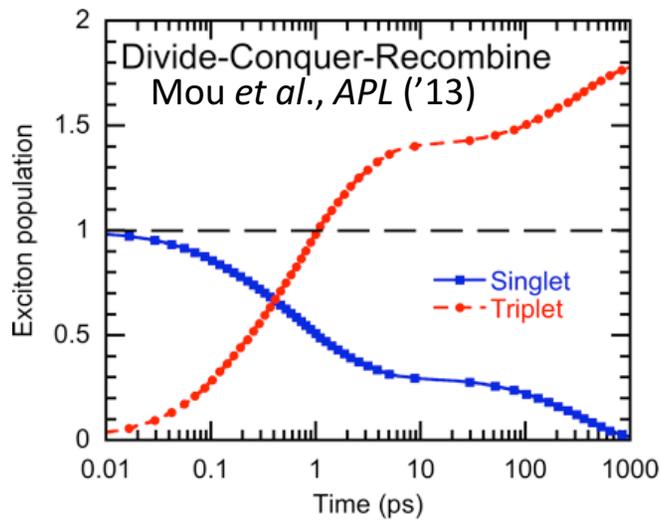
Singlet-Fission Hot Spot

- **Nonadiabatic quantum molecular dynamics simulations not only reproduced experimentally measured exciton population dynamics but also revealed unknown molecular geometry of singlet fission hot spots**

Caveats

- **While the current QXMD code can excite many independent electron-hole pairs, the many-body treatment within LR-TDDFT is restricted to one electron-hole pair (divide-conquer-recombine approach to simulate many interaction electron-hole pairs is under construction)**

- **The current TDDFT xc functionals cannot adequately describe certain phenomena like conical intersection**

Levine *et al.*, *Mol. Phys*. **104**, 1039 ('06); Yang *et al.*, *J. Phys. Chem. Lett*. **7**, 2407 ('16)

Martinez, *Nature* **467**, 412 ('10)